Soil Structure Interaction of Bridges for Seismic Analysis

by

Ignatius Po Lam and Hubert Law

Earth Mechanics, Inc.
17660 Newhope Street, Suite E
Fountain Valley, California 92708

NOTICE

This report was prepared by Earth Mechanics, Inc. as a result of research sponsored by the Multidisciplinary Center for Earthquake Engineering Research (MCEER) through a contract from the Federal Highway Administration. Neither MCEER, associates of MCEER, its sponsors, Earth Mechanics, Inc., nor any person acting on their behalf:

a. makes any warranty, express or implied, with respect to the use of any information, apparatus, method, or process disclosed in this report or that such use may not infringe upon privately owned rights; or

b. assumes any liabilities of whatsoever kind with respect to the use of, or the damage resulting from the use of, any information, apparatus, method, or process disclosed in this report.

Any opinions, findings, and conclusions or recommendations expressed in this publication are those of the author(s) and do not necessarily reflect the views of MCEER or the Federal Highway Administration.

Soil Structure Interaction of Bridges
for Seismic Analysis

by

Ignatius Po Lam[1] and Hubert Law[2]

1   Principal, Earth Mechanics, Inc.
2   Senior Engineer, Earth Mechanics, Inc.

Preface

The Multidisciplinary Center for Earthquake Engineering Research (MCEER) is a national center of excellence in advanced technology applications that is dedicated to the reduction of earthquake losses nationwide. Headquartered at the University at Buffalo, State University of New York, the Center was originally established by the National Science Foundation in 1986, as the National Center for Earthquake Engineering Research (NCEER).

Comprising a consortium of researchers from numerous disciplines and institutions throughout the United States, the Center's mission is to reduce earthquake losses through research and the application of advanced technologies that improve engineering, pre-earthquake planning and post-earthquake recovery strategies. Toward this end, the Center coordinates a nationwide program of multidisciplinary team research, education and outreach activities.

MCEER's research is conducted under the sponsorship of two major federal agencies, the National Science Foundation (NSF) and the Federal Highway Administration (FHWA), and the State of New York. Significant support is also derived from the Federal Emergency Management Agency (FEMA), other state governments, academic institutions, foreign governments and private industry.

The Center's FHWA-sponsored Highway Project develops retrofit and evaluation methodologies for existing bridges and other highway structures (including tunnels, retaining structures, slopes, culverts, and pavements), and improved seismic design criteria and procedures for bridges and other highway structures. Specifically, tasks are being conducted to:
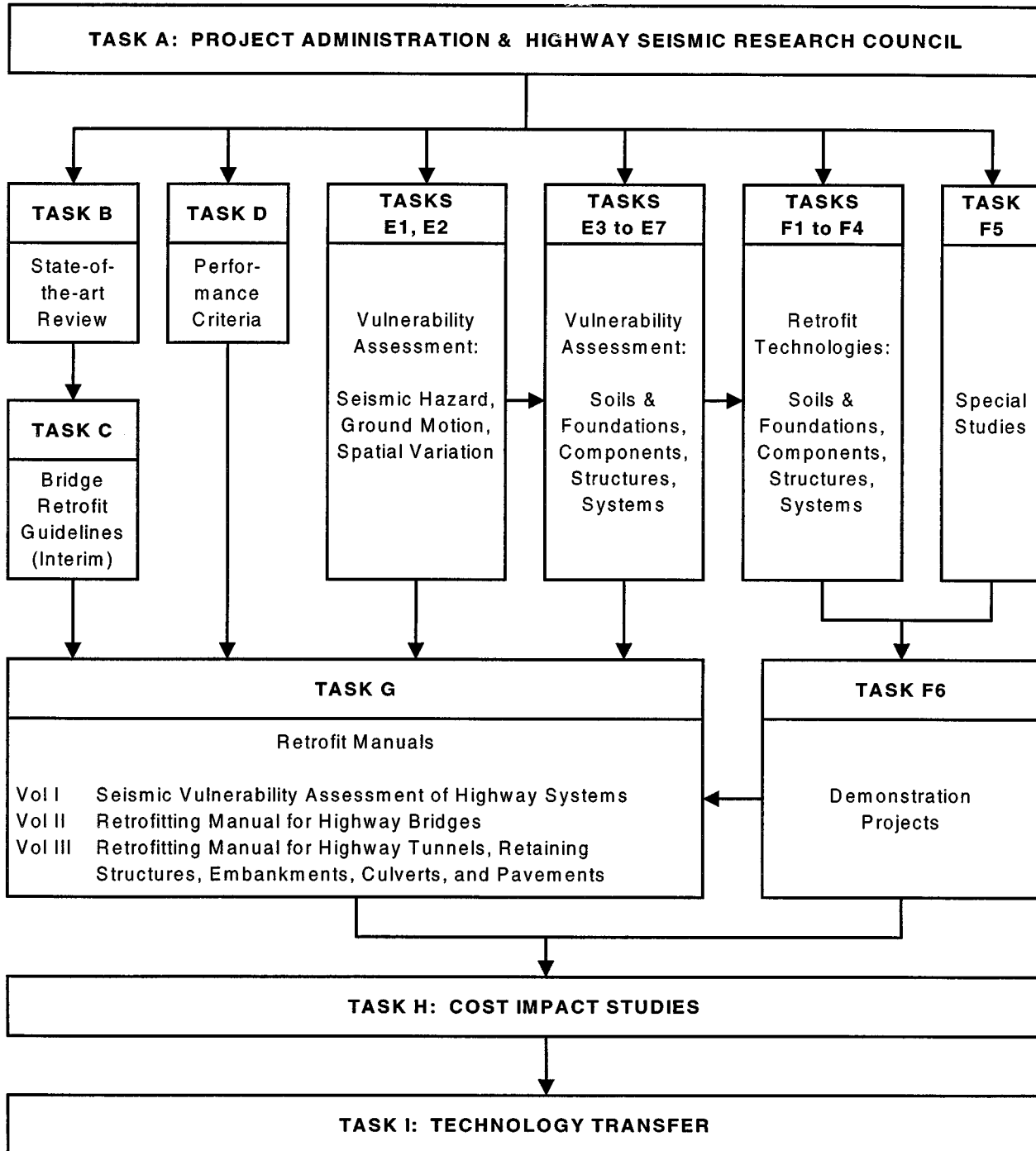* assess the vulnerability of highway systems, structures and components;
* develop concepts for retrofitting vulnerable highway structures and components;
* develop improved design and analysis methodologies for bridges, tunnels, and retaining structures, which include consideration of soil-structure interaction mechanisms and their influence on structural response;
* review and recommend improved seismic design and performance criteria for new highway systems and structures.

Highway Project research focuses on two distinct areas: the development of improved design criteria and philosophies for new or future highway construction, and the development of improved analysis and retrofitting methodologies for existing highway systems and structures. The research discussed in this report is a result of work conducted under the existing highway structures project, and was performed within Task 106-E-4.10, "Synthesis Report: Soil-Structure Interaction and Pile Group Effects" of that project as shown in the flowchart on the following page.

The overall objective of this task was to prepare a report to document the current state-of-practice in soil-structure interaction analysis, and synthesize the latest approaches for analyzing large pile groups for bridge design. Issues such as ground motion aspects for seismic design and soil-structure interaction for typical foundations are discussed. The substructuring technique and applications of kinematic soil-structure interaction in bridge engineering, and an alternate

substructuring method based on inertia interaction are described. Much of the material is based on experience gained during the seismic retrofit and new design programs for major toll bridges in California.

SEISMIC VULNERABILITY OF EXISTING HIGHWAY CONSTRUCTION
FHWA Contract DTFH61-92-C-00106

TASK A: PROJECT ADMINISTRATION & HIGHWAY SEISMIC RESEARCH COUNCIL

TASK B	TASK D	TASKS E1, E2	TASKS E3 to E7	TASKS F1 to F4	TASK F5
State-of-the-art Review	Performance Criteria	Vulnerability Assessment: Seismic Hazard, Ground Motion, Spatial Variation	Vulnerability Assessment: Soils & Foundations, Components, Structures, Systems	Retrofit Technologies: Soils & Foundations, Components, Structures, Systems	Special Studies

TASK C

Bridge Retrofit Guidelines (Interim)

TASK G

Retrofit Manuals

Vol I   Seismic Vulnerability Assessment of Highway Systems
Vol II Retrofitting Manual for Highway Bridges
Vol III Retrofitting Manual for Highway Tunnels, Retaining Structures, Embankments, Culverts, and Pavements

TASK F6

Demonstration Projects

TASK H: COST IMPACT STUDIES

TASK I: TECHNOLOGY TRANSFER

ABSTRACT

This report documents the current state-of-practice in soil-structure interaction analyses for seismic design of bridges. It covers several relevant areas such as ground motion aspects, various issues on soil-structure interaction for typical foundations and methods of substructuring to reduce the number of degrees of freedom for foundation elements.

The ground motion topic includes seismic hazard analyses, seismic performance criteria, spectrum compatible time history, spatial variation of ground motions, effects of local soil condition, and the recent ATC-32 recommendations on standard ARS (Acceleration Response Spectrum) design criteria. The soil-structure interaction area discusses modeling of foundation stiffness and damping for spread footing, gravity caisson, large diameter drilled shaft, and pile group. The concept of substructuring technique is described fully. The technique offers two approaches: one based on kinematic soil-structure interaction and the other based on inertia interaction. Both are intended to reduce the number of degrees of freedom for the foundation to be used in the global bridge analyses.

TABLE OF CONTENTS

LIST OF FIGURES

LIST OF TABLES

SECTION 1
INTRODUCTION

1.1 Overview

The purpose of this report is to document the current state-of-practice in soil-structure interaction analyses for bridge design. Much of the material presented in this report is based on the experience gained during the seismic retrofit and new design programs for major toll bridges in the States of California and Washington.

The function of earthquake engineering is to identify seismic hazards for a given site and to mitigate potential damages. Many advances have been made over the years in the design of seismic-resistant structures and improvements in earthquake design codes. Analytical procedures and modeling methodologies of seismic response studies are regularly refined in order to develop more effective design of structural details. All these improvements are targeted to ensure that new structures will respond satisfactorily to future earthquakes. As earthquake-resistant design has moved from an emphasis on structural strength to both strength and ductility, the need to accurately predict ground motion parameters has increased.

Ground motion estimation is currently based on seismic hazard analyses, which in a broad sense is the analyses of seismicity or the occurrence of earthquakes in space and time. In this report, the framework of seismic hazard analysis is described. Two fundamental types of seismic hazard analysis are currently available: deterministic and probabilistic. Once the seismic hazard is identified, the target performance of the structure is usually guided by a set of seismic performance criteria. For example, two levels of earthquake are defined for new bridges in California: Safety Evaluation Earthquake (SEE) and Functional Evaluation Earthquake (FEE), and the required performance varies for each of these two earthquakes and depends on whether a bridge is classified as Important or Ordinary.

When an earthquake occurs, seismic waves radiate away from a fault and travel rapidly through the earth's crust. As seismic waves travel through both bedrock and soil deposits, the various media act as filters to the seismic waves by attenuating the motion at certain frequencies and amplifying it at others. Soil conditions often vary drastically over relatively short distances, which lead to substantial differences in ground motion characteristics when the seismic waves arrive at the ground surface. Geotechnical engineering practice involves estimating the effect of local soil conditions on ground motion. For a long bridge, the effects of local site conditions become especially important because spatial variations of ground motions would lead to multiple support excitation to the bridge structure. These spatial variations are caused by a combination of local soil conditions and other mechanisms associated with wave propagation through the earth's crust.

The ground motions arriving near the surface would apply loading onto the structure as a form of seismic excitation. Because of the inherent dynamic characteristics of the structure, it would respond differently to a variety of input ground motions. The relative difference between the motions of the soil and the structure will result in the modification of the free-field ground motion in the vicinity of foundation, which is a source of soil-structure interaction. Other sources of soil-structure interaction phenomena that are also discussed in the report include yielding of soil that effectively reduces the soil stiffness, gapping between soil and foundation elements when the structure moves away from the soil which act as a load-fuse mechanism, and boundary effects such as radiation damping.

Much of the soil-structure interaction works are related to mathematical modeling of the soil-foundation system which can then be included in the global bridge analyses. Various modeling techniques currently in use for bridge engineering are presented along with their assumptions and limitations. Depending on the level of effort, mathematical formulation of foundation systems including the supporting soil and the piles, and seismic loading conditions on the superstructure are discussed based on sound principles of mechanics. Some of the techniques are aimed at reducing total number of degrees of freedom in the global bridge model. All these advances in modeling practice are attributed to the seismic safety program initiated by the California Department of Transportation and availability of more powerful personal computers in recent years.

1.2 Organization of the Report

In addition to this introductory section, the remaining sections are organized in the following fashion:

Section 2 summarizes the ground motion aspects for seismic designs. This section includes seismic hazard analyses and performance criteria, methods of generating spectrum compatible time histories, discussion on spatial variation of ground motion, effects of local soil condition, and the recent ATC-32 recommendations on standard ARS (Acceleration Response Spectrum) design criteria.

Section 3 summarizes various issues on soil-structure interaction for typical foundations. This section also includes a discussion on modeling of foundation stiffness for spread footing, gravity caisson, large diameter drilled shaft, and pile group. Foundation damping is another important subject discussed in this section.

Section 4 provides the concept of substructuring technique and application of kinematic soil-structure interaction in bridge engineering. It provides a rational means of establishing site specific ARS design criteria for pile-supported structure where free-field motions vary along the length of the pile. The substructuring method is intended to reduce the number of degrees of freedom for the foundation to be used in the global bridge analyses.

Section 5 discusses the alternate substructuring method based on inertia interaction. This method has been widely used in the nuclear power industry relying on frequency domain approach. The current design practice in bridge engineering allows some damages to take advantage of ductility, which essentially limits the use of linear superposition principle. Recognizing deficiency of frequency domain approach, some modifications have been adopted to use in time domain analysis.

Section 6 provides a summary of the report and conclusions made from the recent seismic retrofit and new design programs for the major toll bridges in California.

Section 7 lists the references cited in the report.

SECTION 2
GROUND MOTION PARAMETERS

2.1   Ground Motion Criteria

A design ground motion describes the level of shaking to structures and facilities that are being designed. The responsibility of the engineer is to design the structure that can withstand the design ground motion without excessive damage. For new bridges in the State of California, the level of damage is guided by a set of seismic performance criteria. In these performance criteria, two levels of earthquakes are defined: Safety Evaluation Earthquake (SEE) and Functional Evaluation Earthquake (FEE).

In the past, the California Department of Transportation (Caltrans), based on deterministic approach, defined Safety Evaluation Earthquake as the Maximum Credible Earthquake which has a small probability of occurring during the useful life of the bridge. Applied Technology Council (ATC-32) recently recommended an alternative definition of Safety Evaluation Earthquake as an earthquake with a 1000- to 2000-year return period through a site-specific study based on a probabilistic approach. The Functional Evaluation Earthquake is intended to represent an earthquake with a reasonable probability of not being exceeded (approximately 60%) during the life span of the bridge.

Required performance varies for each of the two earthquakes defined above and depends on whether a bridge is classified as Important or Ordinary. As limited ductility is recommended for Important Bridges, repairable damage must be maintained after the Safety Evaluation Earthquake. On the other hand, Ordinary Bridges can take maximum advantage of plastic hinging to utilize full ductile behavior. This type of structural action implies significant damage to the bridge structure. Table 2.1 summarizes the recommended seismic performance criteria for bridges classified as Important or Ordinary.

Table 2.1 Seismic Performance Criteria

Ground Motion at Site	Ordinary Bridge	Important Bridge
Functional Evaluation Earthquake	Immediate Service Level [Repairable Damage]	Immediate Service Level [Minimal Damage]
Safety Evaluation Earthquake	Limited Service Level [Significant Damage]	Immediate Service Level [Repairable Damage]

2.2   Seismic Hazard Analysis

Seismic hazard analyses estimate ground shaking hazard at a particular site in a quantitative manner. Two distinct procedures generally used are: deterministic approach and probabilistic approach. The deterministic seismic hazard analysis (DSHA) assumes a

particular earthquake scenario while the probabilistic seismic hazard analysis (PSHA) considers uncertainties in earthquake size, location and occurrence explicitly.

The deterministic seismic hazard analysis involves development of a seismic scenario consisting of the postulated occurrence of an earthquake of a specified size occurring at a particular location. The analysis requires the specification of three basic elements; an earthquake source, a controlling earthquake fault of specified magnitude and a means of determining the hazard (usually peak ground acceleration at the site). The basic steps in this procedure is schematically shown in Figure 2.1, and each step can be described as follows (Reiter, 1990):

1   All seismic sources capable of generating significant ground motion at the site are identified. Each of the earthquake sources is characterized by defining source geometry such as point, line or area source.
2   A source-to-site distance parameter for each seismic source is chosen, usually the closest distance between source and the site of interest. An epicentral distance or hypocentral distance can be used.
3   Using an attenuation relation (e.g., Abrahamson and Silva, 1997), a level of shaking produced by each of the seismic sources identified in step 1 and the corresponding source-to-site distance chosen in step 2 is determined. The controlling earthquake is chosen to produce the strongest level of shaking.
4   The seismic hazard is formally defined at the site by the controlling earthquake using one or more ground motion parameters such as peak acceleration, peak velocity and response spectrum.

Although the procedure outlined above for DSHA provides a straightforward framework for evaluation of worst-case scenario, it does not deal with likelihood of occurrence of the controlling earthquake, the likelihood of seismic source occurring where it is assumed to occur, or uncertainties in computing ground motion characteristics.

In recent years, the use of PSHA receives wider acceptance among the engineers and seismologists because the probabilistic concept allows uncertainties in the size, location, and rate of recurrence of earthquake. The PSHA provides a framework in which these uncertainties can be identified, quantified, and combined in a rational manner to provide a more complete picture of the seismic hazard. The hazard description is not restricted to scenario-like statements; they incorporate the effects of all the earthquakes believed to be capable of affecting the site in question, the probability of different magnitude earthquakes occurring is included in the analysis.

Cornell (1968) defined the methodology used in most PSHA. A four-step procedure as shown in Figure 2.2 provides basic mechanics of probabilistic seismic hazard analysis. The steps can be described as (Reiter, 1990)

1   As in the case of DSHA, seismic sources capable of producing significant ground motion at the site are identified and characterized. Again, sources may range from small planer faults to large seismotectonic provinces. The probability
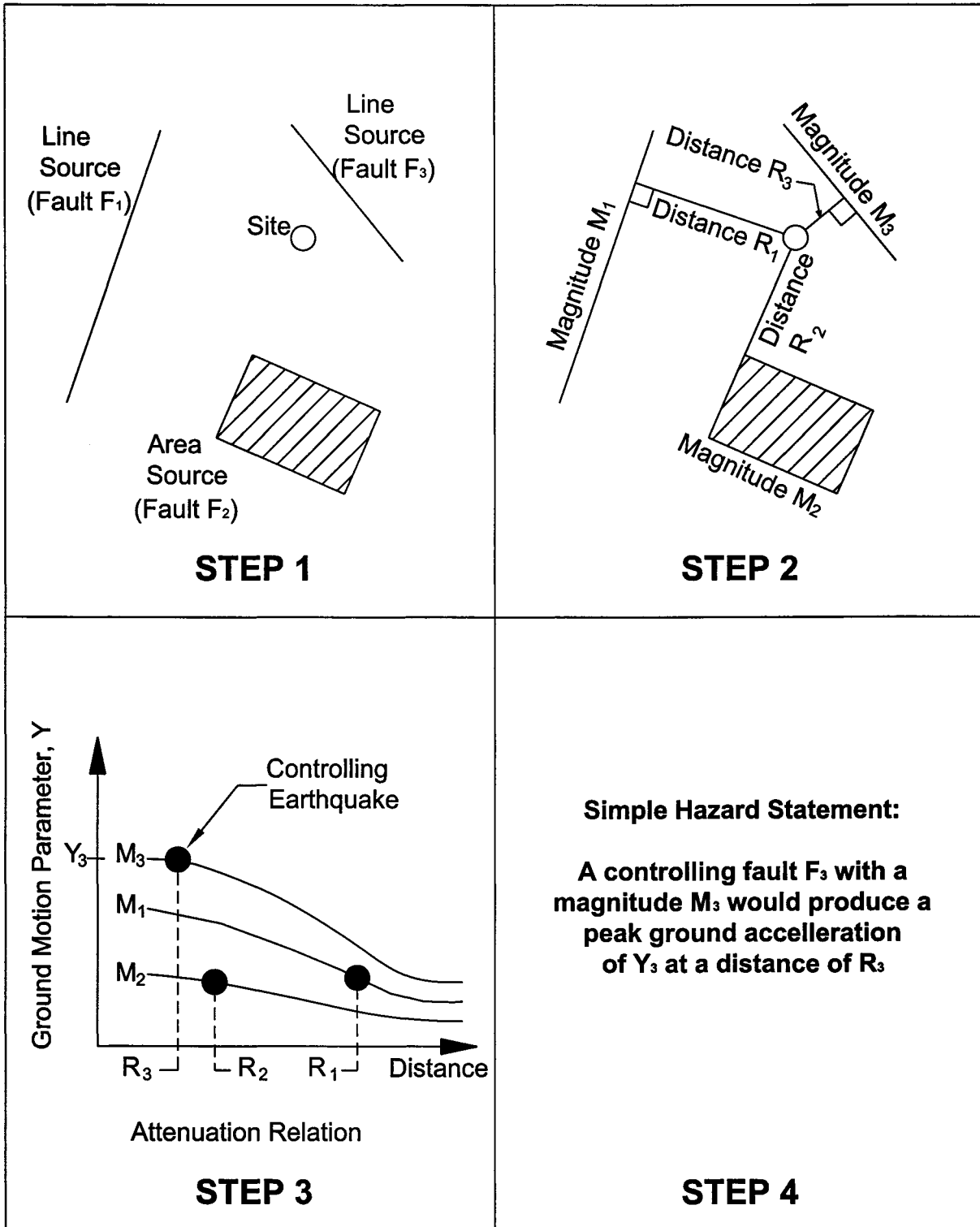
Figure 2-1   Four steps of a deterministic seismic hazard analysis.

STEP 1

Line Source (Fault F$_1$)

Line Source (Fault F$_3$)

Site

Area Source (Fault F$_2$)

STEP 2

Log of No. of Earthquakes with Equal or Greater M

F$_1$

F$_2$

F$_3$

Magnitude, M

STEP 3

Ground Motion Parameter, Y

Uncertainity in Attenuation

M$_3$

M$_2$

M$_1$

Distance

STEP 4

Probability of exceedance

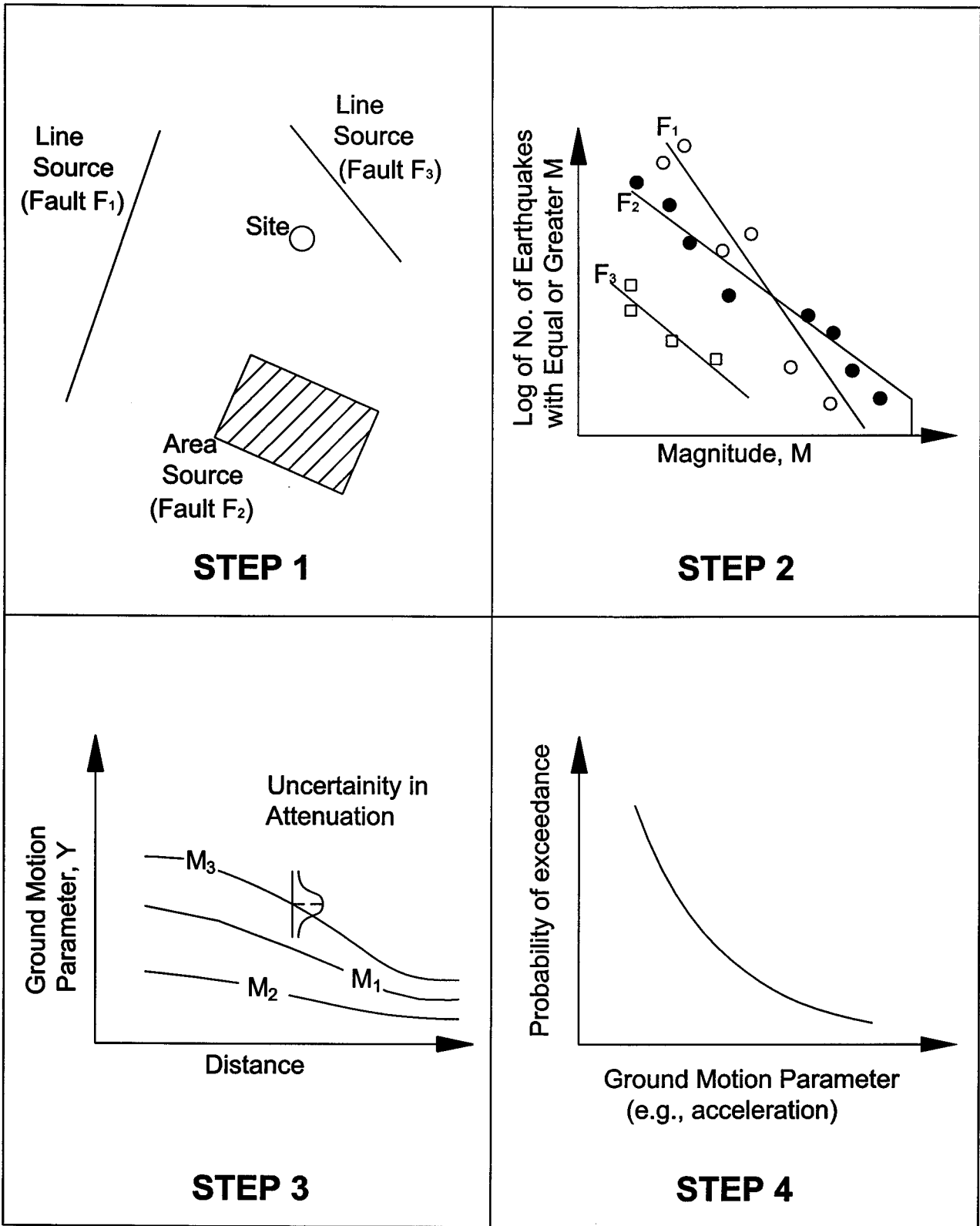Ground Motion Parameter (e.g., acceleration)

Figure 2-2   Four steps of a probabilistic seismic hazard analysis.

distribution of potential rupture locations within the source is also characterized. It is usual to assume uniform probability distribution to each source zone implying that earthquakes are equally likely to occur at any point within the source zone.

2   Instead of picking one controlling fault, a recurrence relationship of each earthquake source is characterized. The recurrence relationship indicates the average rate at which an earthquake of some size will be exceeded and hence quantifies the seismicity of each source zone. The recurrence curve in a simple case is:

$$\log N = A - BM \qquad (2.1)$$

where N is the cumulative number of earthquakes larger than magnitude M that are expected to occur during a specified period of time, A is the log of the number of earthquake of magnitude zero or greater to occur during the same time and B is the slope of the curve.

3   The ground motion produced at the site by earthquakes of any possible size occurring at any possible point in each source zone is determined using a family of earthquake attenuation or ground motion curves. Each curve relates a ground motion parameter, such as peak acceleration, to distance for an earthquake of a given size. The uncertainties inherent in the attenuation relation are also considered in the analysis.

4   The effects of all the earthquakes of different sizes, occurring at different locations in different earthquake sources at different probabilities of occurrence are integrated into one curve. The curve shows the probability of exceeding different levels of ground motion, such as peak acceleration, at the site during a specified period of time.

The probabilistic seismic hazard analysis usually assumes that earthquakes have no "memory"; that is, each earthquake occurs independent of any other earthquake. If an earthquake of magnitude 6.5 occurred on a given fault today it would have no influence on where the next earthquake of any size would occur. Obviously this assumption is not consistent with a data set which includes foreshocks and aftershocks.

The consideration of systematic uncertainty often results in seismic hazard estimates accompanied by large bands of uncertainty which is only a reflection of the state of knowledge on seismology. Therefore, the proper performance of a PSHA requires careful attention to the problems of source characterization and ground motion parameters prediction.

2.3   Ground Motion Time History

The ground motion parameters, such as peak accelerations, peak velocities, or response spectra as developed from seismic hazard analysis, are often not sufficient to describe the effects of ground shaking. For certain structural analyses that take into account the

nonlinear behavior of the structure, time history analysis is necessary. In these cases, time histories of ground motion that match target ground motion parameters are artificially developed. If the target ground motion parameter is solely based on peak velocity, peak acceleration or dominant frequency, direct scaling of the actual recorded ground motion by multiplying with an amplitude-scaling factor or changing the time step to alter the frequency content may be adequate. However, the current state of practice in civil engineering application relies on matching of a target response spectrum to ensure a broad range of frequency is included in the ground motion time history generated for design. In this case, a reference ground motion time history (usually actual earthquake record) is chosen as a seed motion and is gradually modified through an iterative process so that the response spectrum the modified time history is compatible with the target spectrum.

Various methods have been developed to perform the spectrum matching. A commonly used method adjusts the Fourier amplitude spectrum based on the ratio of the target response spectrum to the time history response spectrum while keeping the Fourier phase of the reference history fixed. An alternative approach for spectral matching adjusts the time history in the time domain by adding wavelets to the reference time history. A formal optimization procedure for this type of time domain spectral matching was first proposed by Kaul (1978) and was extended to simultaneous matching at multiple damping values by Lilhanand and Tseng (1987, 1988). While this procedure is more complicated than the frequency domain, it has good convergence properties.

Figures 2.3 through 2.5 show an example of spectral matching for the fault normal component of motion obtained from the 1940 Imperial Valley earthquake recorded at El Centro. Figure 2.3 is the initial time history of the original ground motion and Figure 2.4 is the modified time history after spectral matching. The comparison of response spectra from the original and modified motions is shown in Figure 2.5.

Other than matching of response spectrum for each of the ground motion components developed for structural designs, checking of cross-correlation of the two horizontal orthogonal directions is also important for ensuring no deficiency in shaking level at any rotated axis. The concept of cross-correlation is derived from digital signal processing to examine dissimilarity of two signals. When the ground motions of two orthogonal directions are dissimilar, the chance of adding up or canceling each other is small after rotating the axes, and therefore this set of ground motions is likely to excite the structure at any oblique angle with reasonable energy. For example, if time history analysis of a structure is conducted with two orthogonal components where the X component motion is identical to the Y component motion, shaking level along the direction +45° from the X axis would be $\sqrt{2}$ times higher than that along the principal axis. On the other hand, the direction -45° from the X axis would not be excited at all. Clearly, this set of input ground motions is not robust for design as the time history analysis would fail to examine the structural elements whose behavior is of critical along or about the direction -45° from the X axis.
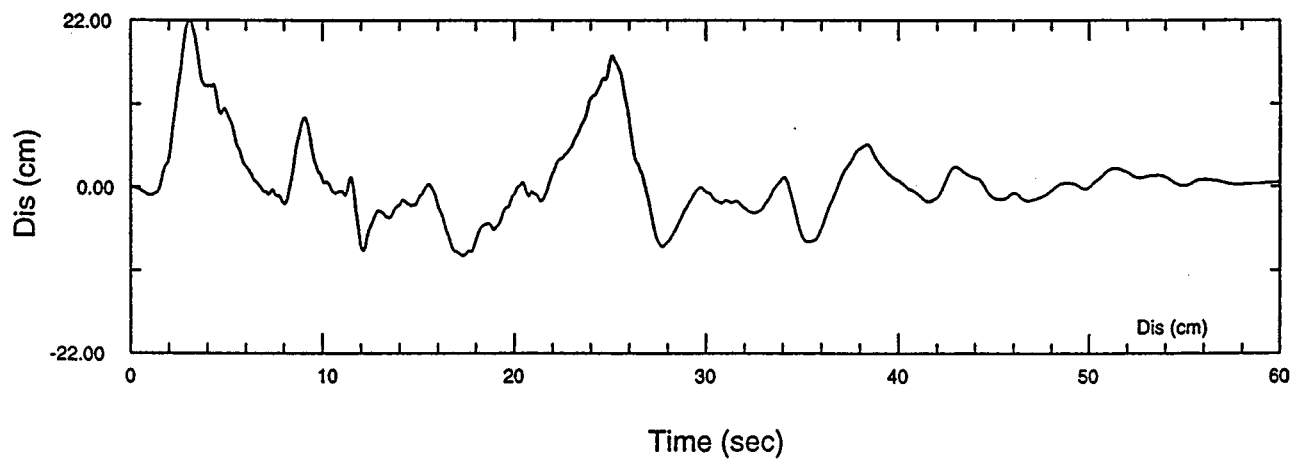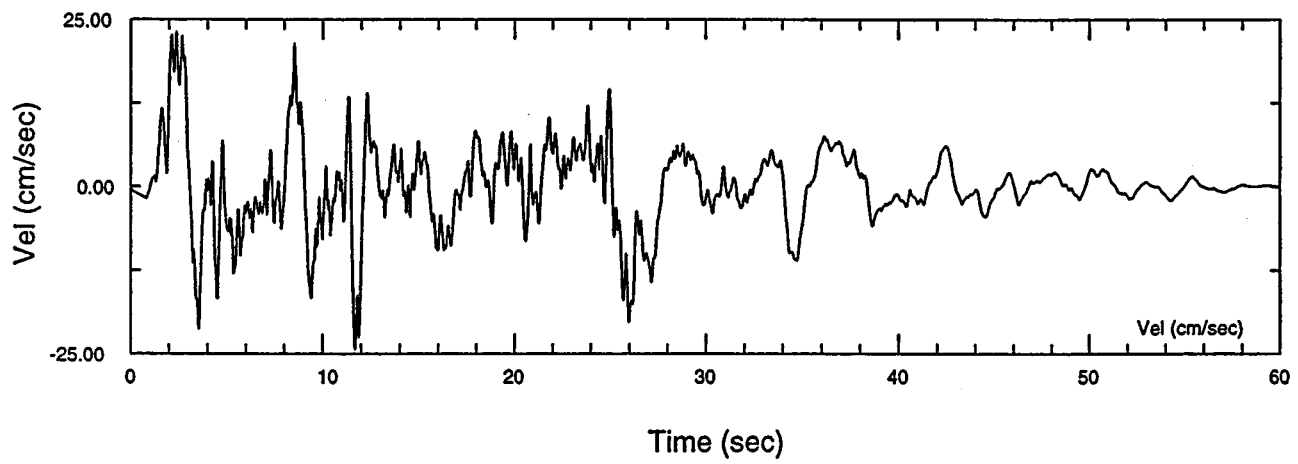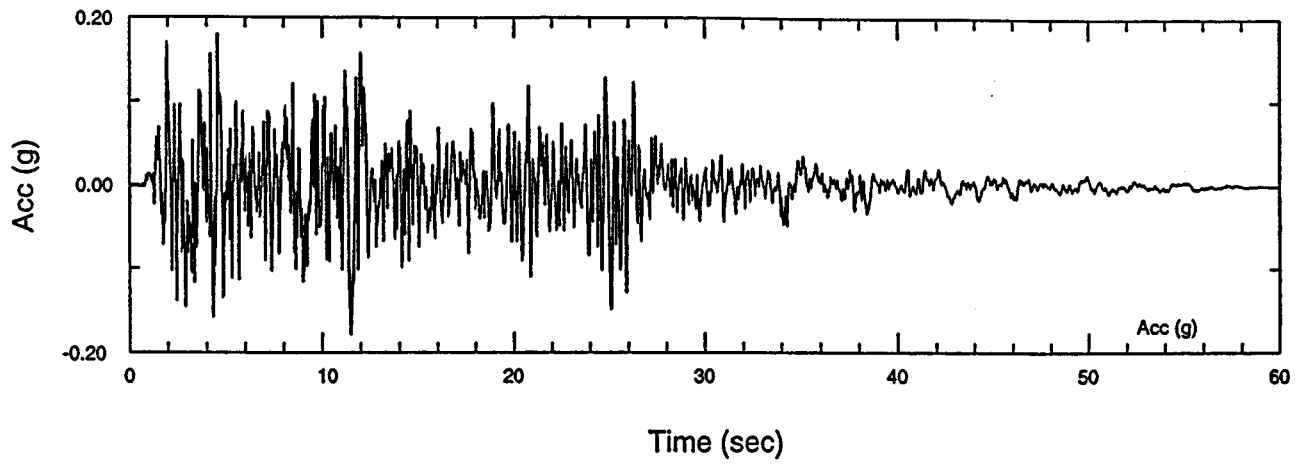
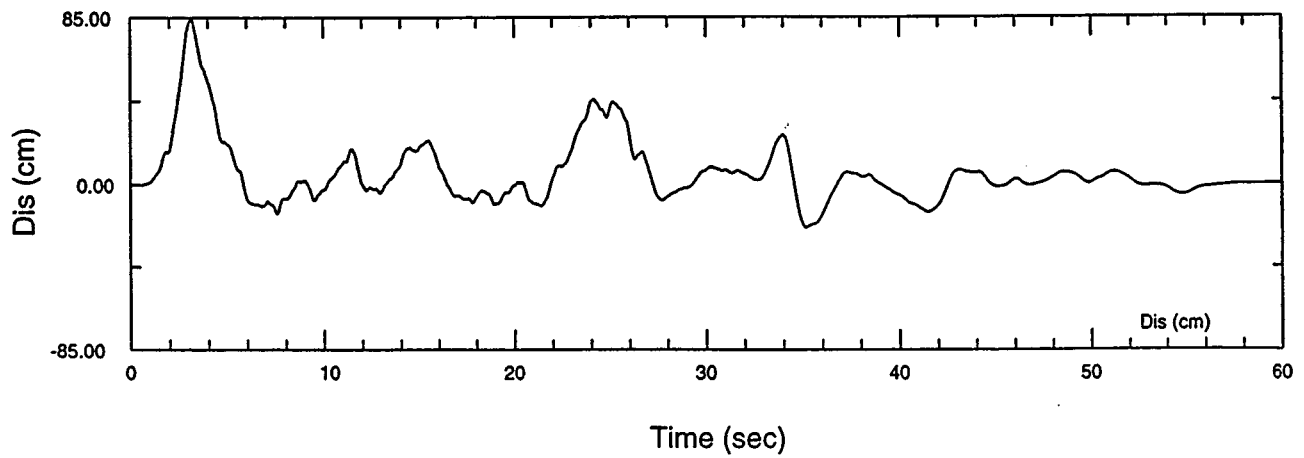**Figure 2-3** Initial time history for fault normal component of El Centro record from 1940 Imperial Valley earthquake.
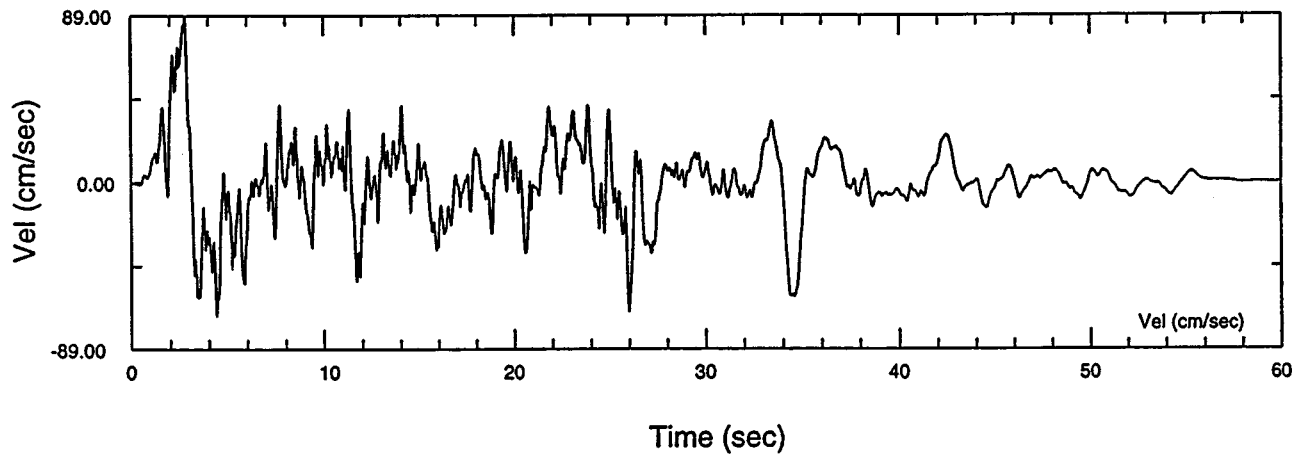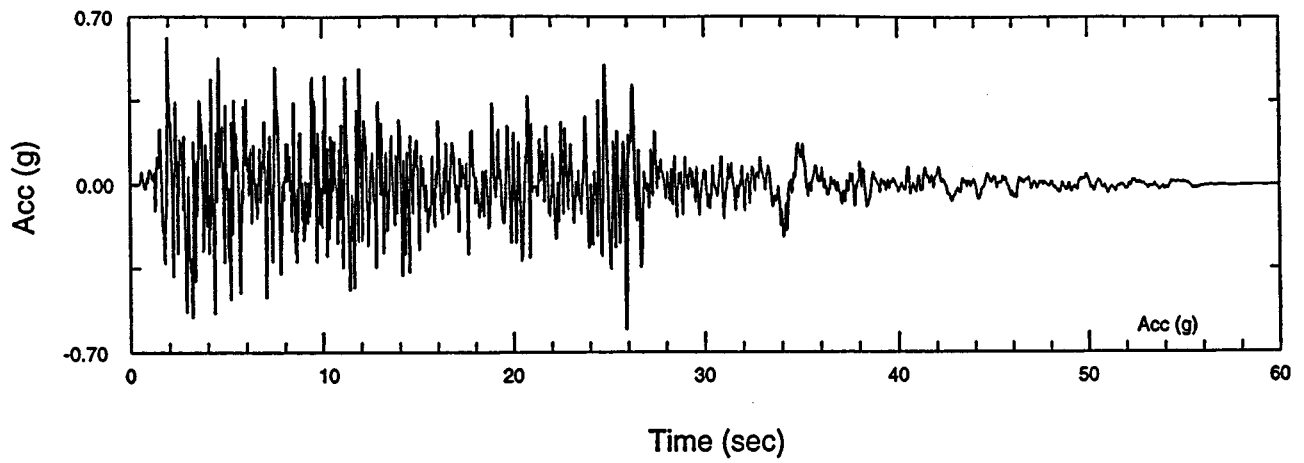
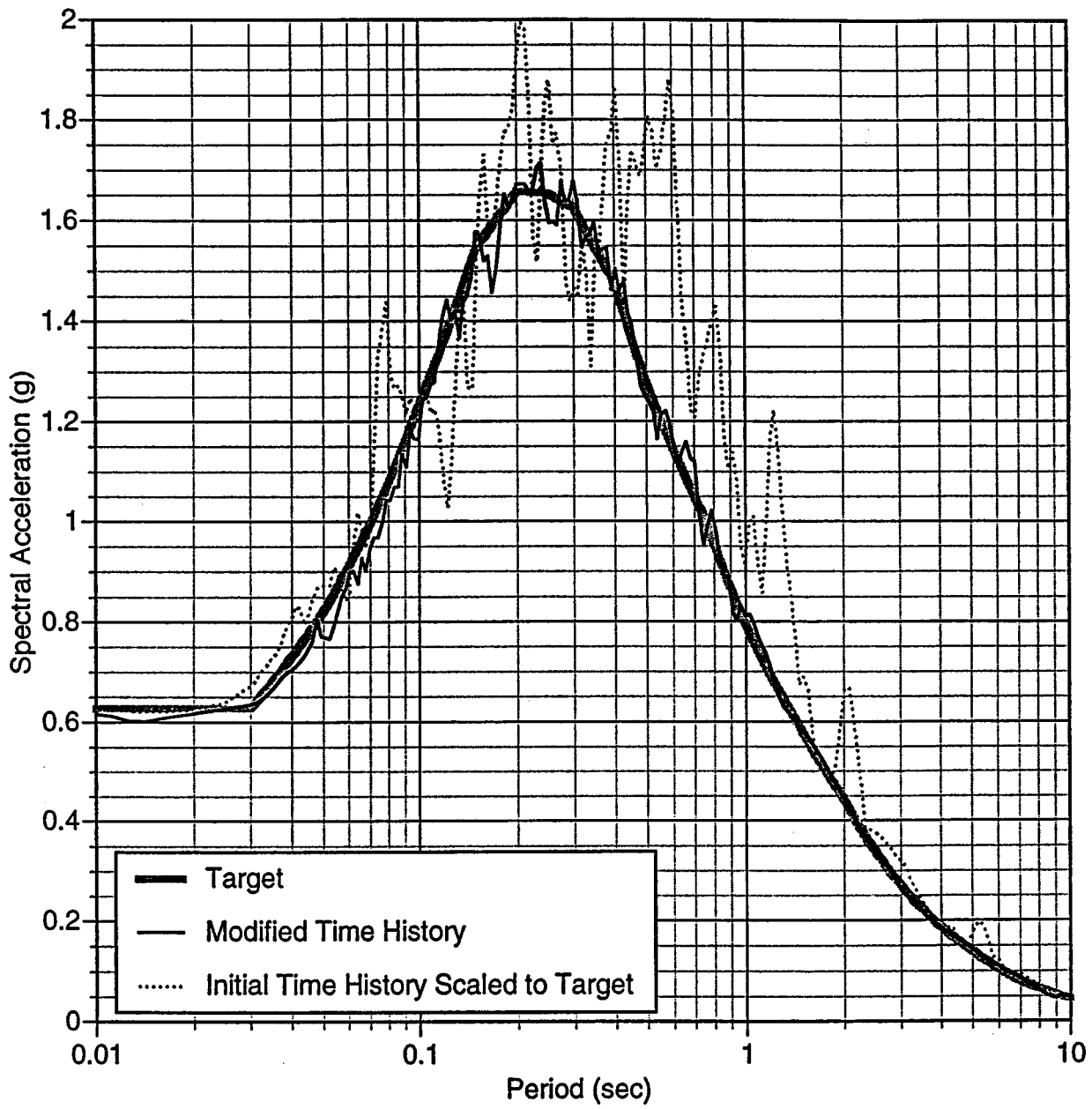**Figure 2-4** Modified motion after spectrum matching.

12

Figure 2-5   Comparison of 5% damped response spectra for the modified
fault normal component and initial time history scaled to the target PGA.

A better representation of shaking level at any direction may be examined by computing spectral accelerations for the periods of interest along the rotated axis. This can be done by first rotating the motion in 360° angles at say every 10° and then computing spectral acceleration for selected periods. Figure 2.6 shows polar plots of spectral acceleration at each rotated azimuth from two-component spectrum compatible motions developed for bridge design. A circular pattern from this polar plot indicates equal shaking intensity for all directions; deficiency of shaking intensity in any direction can be seen on the plot as substantial deviation from a circular pattern.

2.4   Spatial Variation of Rock Motions

Ground motions can vary spatially on a local scale due to scattering and complex wave propagation, and this local variation can be important for long structures such as bridges and pipelines that extend over considerable distance. The spatial variability or incoherence is caused by a number of factors, such as:

1   Wave Passage Effect: nonvertical waves reach different positions on the ground surface at different times causing a time shift between the motions at those locations

2   Extended Source Effect: mixing of wave types and source directions due to differences in the relative geometry of the source and the site

3   Ray Path Effect: scattering of seismic wave by heterogeneity of earth along the travel path causing different waves to arrive at different locations at different times

4   Attenuation Effect: variable distance from the different locations to the seismic source

5   Local Site Effect: variable soil conditions produce different motions at the ground surface

The spatial variation of ground motions at different locations can be characterized by cross covariance in time domain representation or coherency in frequency domain representation.

Considering two points j and k with their acceleration time histories $a_j(t)$ and $a_k(t)$, respectively, the cross covariance is defined as

$$C_{jk}(\tau) = \sum_{i=1}^{N} a_j(t_i)a_k(t_i + \tau)$$ (2.2)

where τ is a time increment and N is the number of time samples. Coherency of the same two motions can be described in the frequency domain as

$$\gamma_{jk}(\omega) = \frac{S_{jk}(\omega)}{\sqrt{S_{jj}(\omega)S_{kk}(\omega)}}$$ (2.3)

14
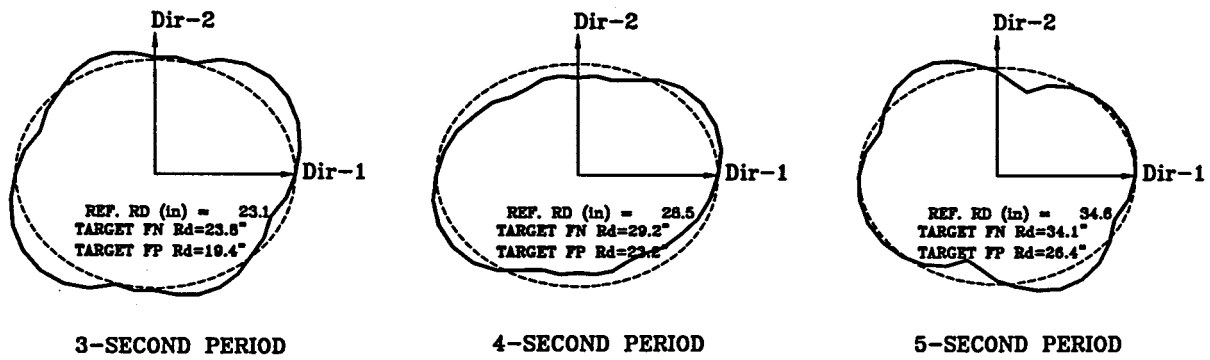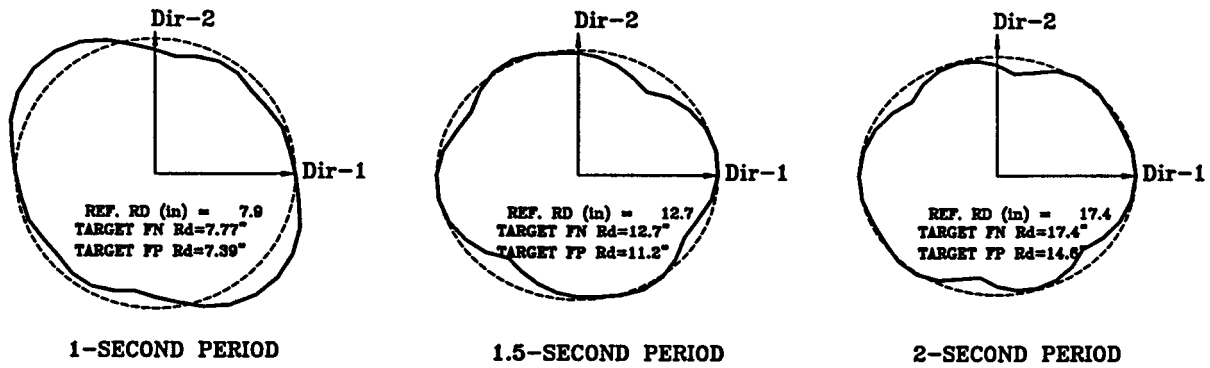
SHAKING INTENSITY AT VARIOUS AZIMUTHS

at Dir-1 = FAULT NORMAL
at Dir-2 = FAULT PARALLEL

CROSS–CORRELATION STATISTICS FOR Dir-1 and Dir-2

ACCELERATION	VELOCITY	DISPLACEMENT
CROSS CORREL. COEFF. = .01	CROSS CORREL. COEFF. = −.03	CROSS CORREL. COEFF. = −.06
PRINC. DIR. AT (DEG) = 2.0	PRINC. DIR. AT (DEG) = −3.7	PRINC. DIR. AT (DEG) = −2.7
MAX. COEFFICIENT = .105	MAX. COEFFICIENT = .255	MAX. COEFFICIENT = .541
AT DIRECTION (DEG)= 140.0	AT DIRECTION (DEG)= 130.0	AT DIRECTION (DEG)= 130.0
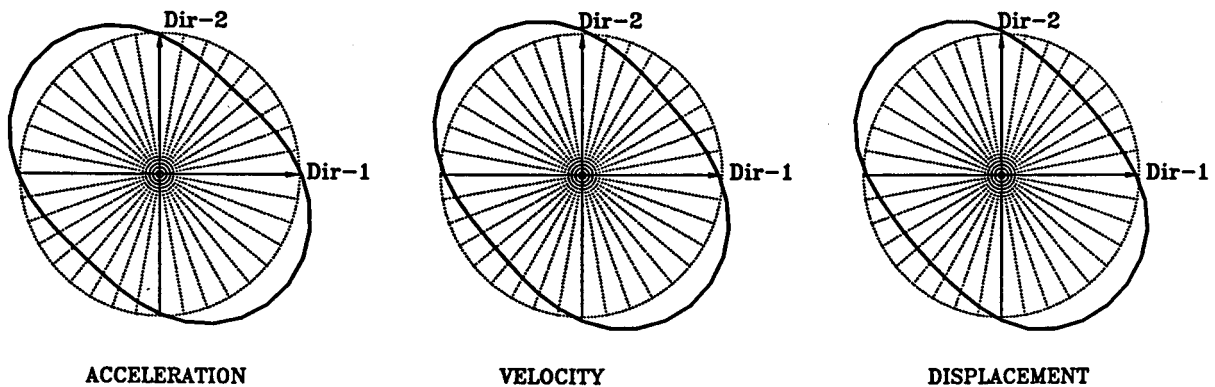
CROSS CORRELATION COEFFICIENT OF RECORDS UNDER ROTATION

Figure 2-6   Checking of shaking intensity for rotated axes.

where $S_{jk}(\omega)$ is the complex-valued cross power spectral density function to the two accelerations, $S_{jj}(\omega)$ and $S_{kk}(\omega)$ are real-valued power spectral density functions. The coherency function describes the degree of positive or negative correlation between the amplitudes and phase angles of two time histories at each of their component frequencies. A value of 1 indicates full coherence while a value of zero indicates complete incoherence.

SMART-1 recording array at Lotung, Taiwan has provided numerous ground motion records which show that coherency decreases with increasing distance between measuring points and with increasing frequency. This is illustrated in Figure 2.7. Other measurements from elsewhere in U.S and Japan show a similar trend suggesting that the coherence functions may be applicable to other part of the world as well. Detailed discussion on generation of spatial incoherent motion is described by Abrahamson et al., 1991. The spatial variation of ground motions has been implemented in the recent seismic retrofit program as well as in the new design for California toll bridges. In these projects, the empirical coherency function as obtained from the dense arrays provides a basis for developing incoherent motions at different bridge supports.

2.5   Effects of Local Site Conditions

Theoretical evidence as well as actual measurements show that local site conditions profoundly affect the ground motion characteristics in terms of amplitude, frequency content, and duration. As these factors play an important role in earthquake resistant design, the effects of local site conditions must be properly accounted for.

The influence of local site conditions can be demonstrated analytically using a simple site response analyses. Two soil deposits with an identical depth are considered with soil deposit at one site being stiffer than the other. Assuming linearly elastic behavior for soil, the amplifications as a function of frequency are shown in Figure 2.8. The softer site (site A) amplifies bedrock motion at a low frequency range while the stiffer site (site B) amplifies high frequency rock motion. Since earthquakes produce bedrock motion over a range of frequencies, some components of the bedrock motion will be amplified more than others.

The effects of local soil conditions are also evident in interpretation of strong motion data from many instrumented sites. For example, recordings of ground motion at several locations in San Francisco during the 1957 earthquake show remarkable variations in ground motion characteristics in terms of peak horizontal acceleration and response spectra along the a 4-mile stretch through the city, as shown in Figure 2.9. While the rock outcrop motions are very similar, the amplitude and frequency content of the surface motions are quite different at the sites underlain by thick soil deposit. Similar effects have been observed in other earthquakes.

It is of particular interest to compare the response of two seismic records from Yerba Buena Island and Treasure Island in the San Francisco Bay. Yerba Buena Island is a rock
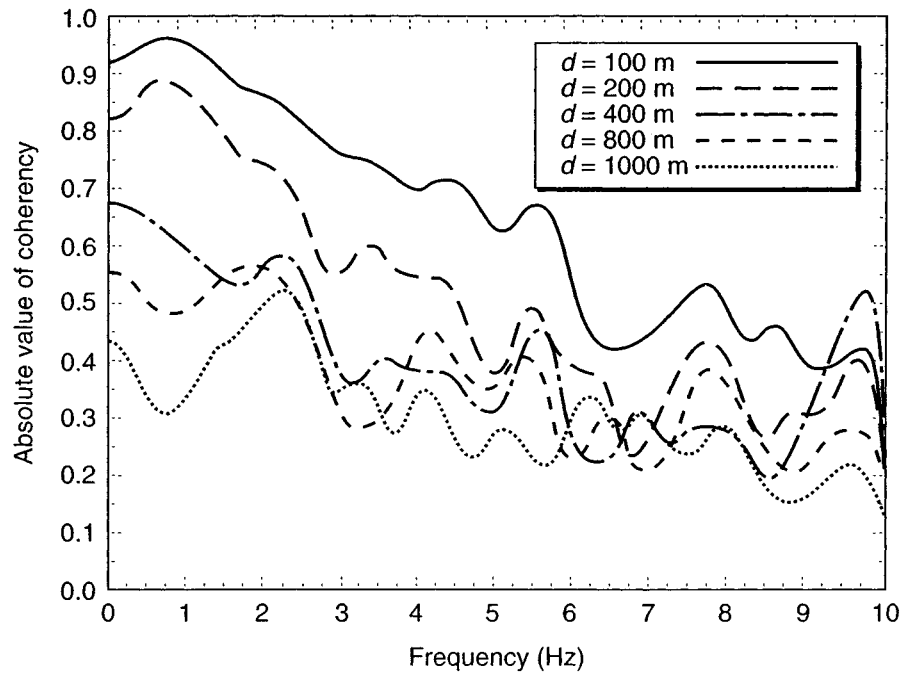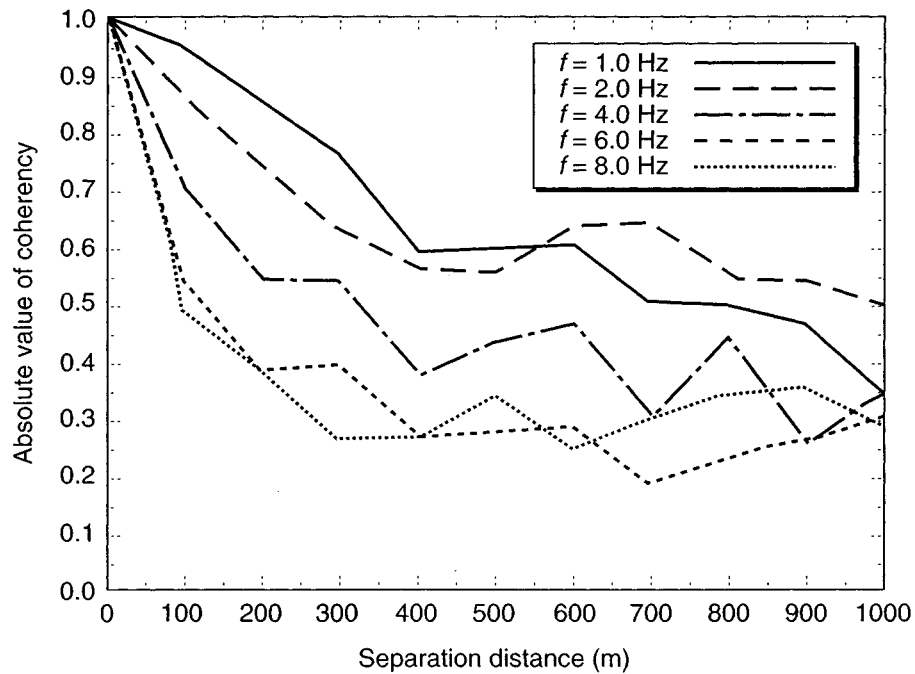
Figure 2-7 Measured decay of coherency with increasing frequency and separation distance for M = 6.9 event at hypocentral depth of 30.6 Km and epicentral distance of 116.6 Km from SMART-1 dense array at Lotung, Taiwan. (Source: Kramer, 1996).

Figure 2-8 Comparison of amplification functions for two soil deposits. (Source: Kramer, 1996).

18

Figure 2-9   Variation of spectral velocity, spectral acceleration, and peak horizontal acceleration along a 4-mile section through San Francisco in the 1957 San Francisco earthquake. (After Seed and Idriss, 1976).

outcrop and Treasure Island is a man-made hydraulic fill placed partially on the Yerba Buena shoals. Although Yerba Buena Island and Treasure Island are located at the same distanc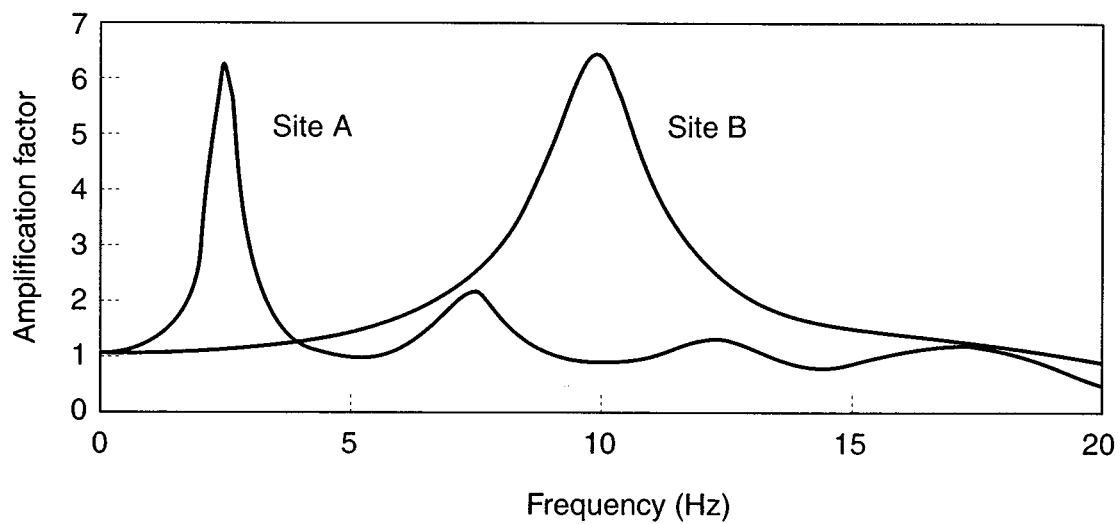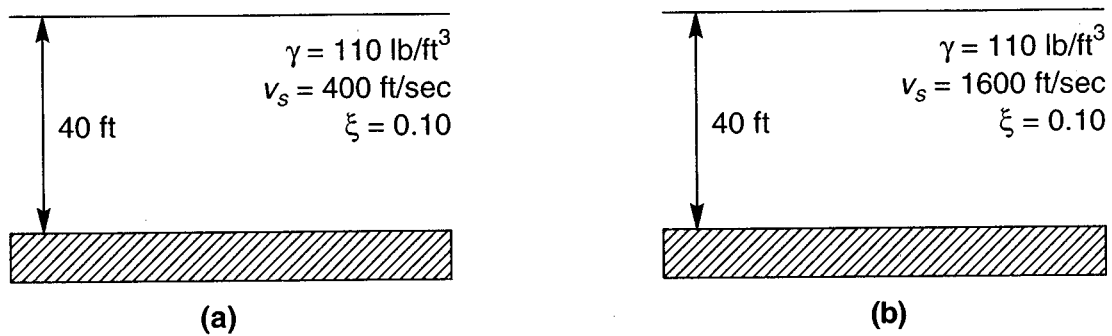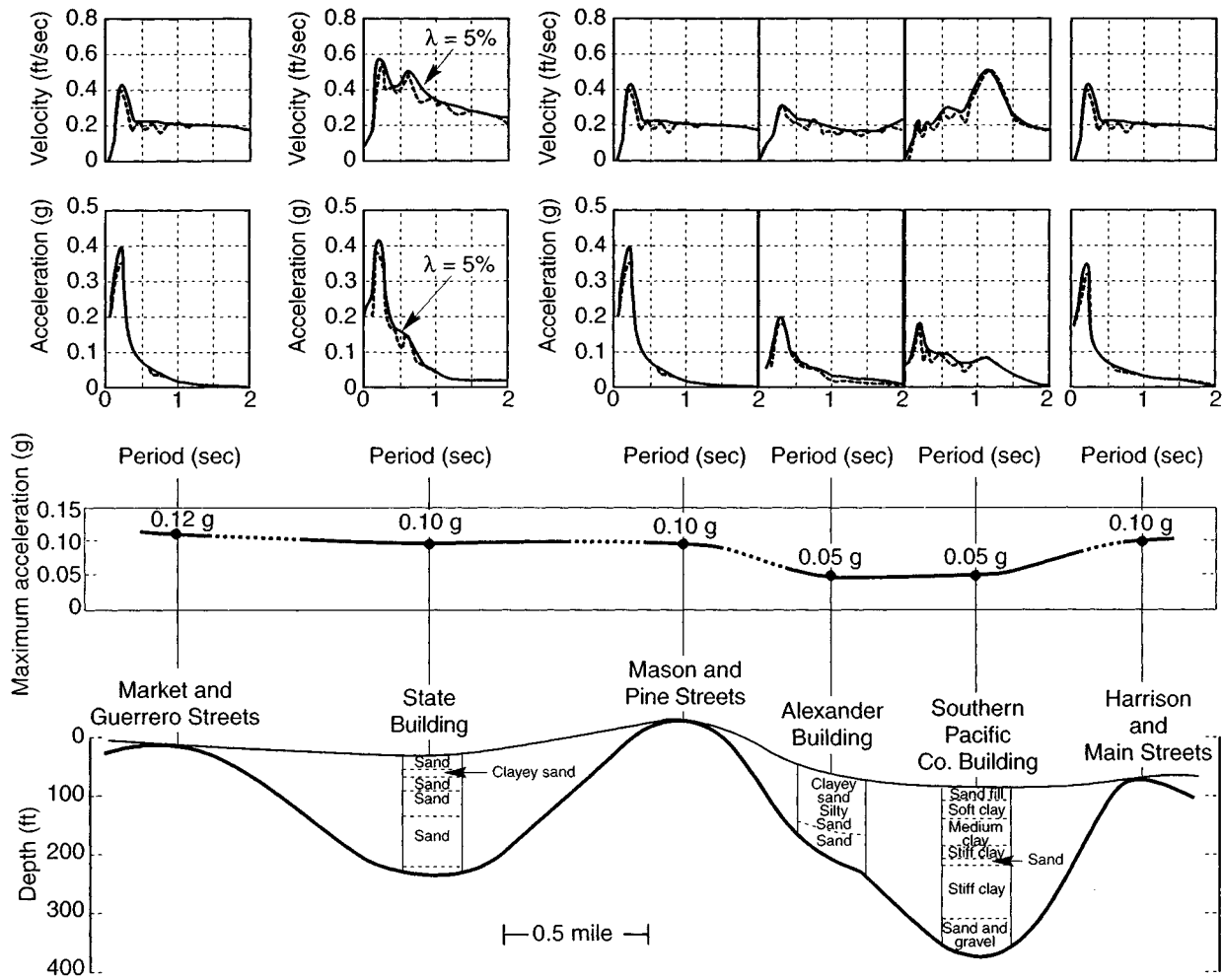e from the seismic source, the ground motion recorded at these two sites during the 1989 Loma Prieta Earthquake are very different. Figure 2.10 shows the comparison of acceleration time histories and response spectra in the east-west component. Clearly, the presence of the soft soils at the Treasure Island site caused significant amplification of the underlying bedrock motion.

Seed et al. (1976) computed average response spectra from ground motion records at sites underlain by four categories of site conditions: rock sites, stiff soil sites of less than 200 feet, deep cohesionless soil sites greater than 250 feet, and sites underlain by soft to medium-stiff clay deposits. Normalizing the computed spectra by dividing spectral accelerations by the peak ground acceleration illustrates the effects of local soil conditions of the shape of spectra, as shown in Figure 2.11. At periods above 0.5 sec, spectral amplifications are much higher for soil sites than rock sites; this phenomena is significant for long-period structures, such as tall bridges, that are founded on soft soils.

2.6   ATC-32 Design Spectra

Response spectra from actual earthquakes are highly irregular and their shape reflects the details of their specific frequency contents and phasing. Design spectra are generally smooth as they were developed by a means of averaging, enveloping, and/or smoothing. The use of smooth design spectra implicitly recognizes the uncertainty in many ground motions parameters.

Newmark and Hall (1973) recommended that design response spectra be developed from a series of straight lines on a tripartite plot corresponding to the acceleration-, velocity-, and displacement-controlled portions of the spectrum. However, the recent ATC-32 proposed a family of site-dependent design spectra based on four standard sites. These standard sites are primarily characterized by the typical shear wave velocity of the upper 100 feet of the soil profile, as shown in Table 2.2.

Table 2.2 Site Characteristics for Standard Design Spectra

Site Designation	Site Description	Shear Velocity in Upper 100 feet of soil
B	Medium Rock	2500 to 5000 ft/sec
C	Soft Rock/Dense Soil	1200 to 2500 ft/sec
D	Stiff Soil	600 to 1200 ft/sec
E	Soft Soil	<600 ft/sec

The spectral shapes for acceleration values between 0.1 and 0.7 g in 0.1 g increments for three magnitude groups (6.5, 7.25, 8.0) are shown in Figures 2.12 through 2.23. However the standard design spectra are not appropriate for near fault sites because of directivity
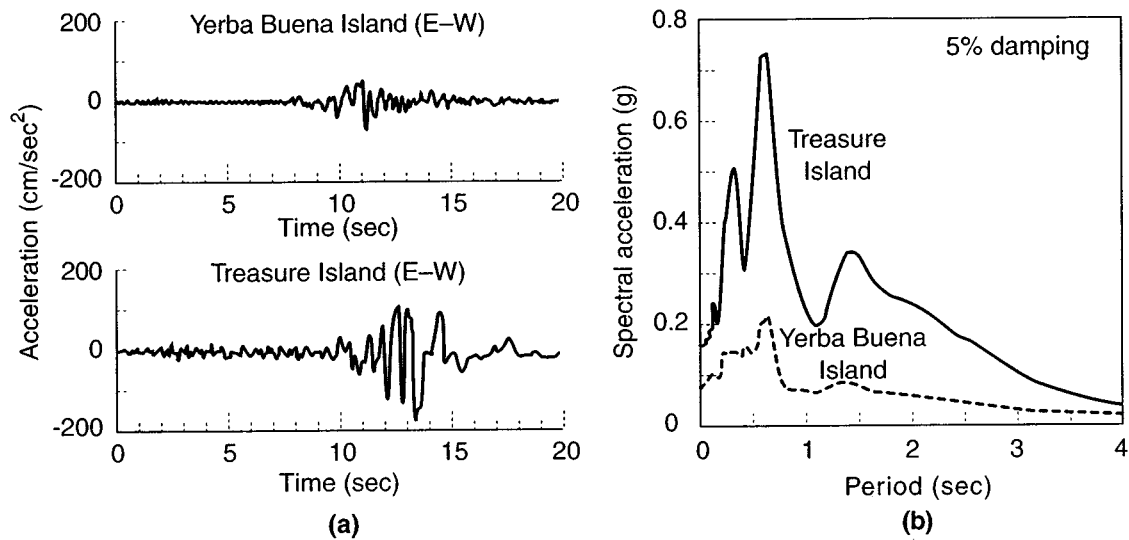
Figure 2-10 Ground surface motions at Yerba Buena Island and Treasure island in the 1989 Loma Prieta earthquake: (a) time histories; (b) response spectra. (After Seed et al., 1990).
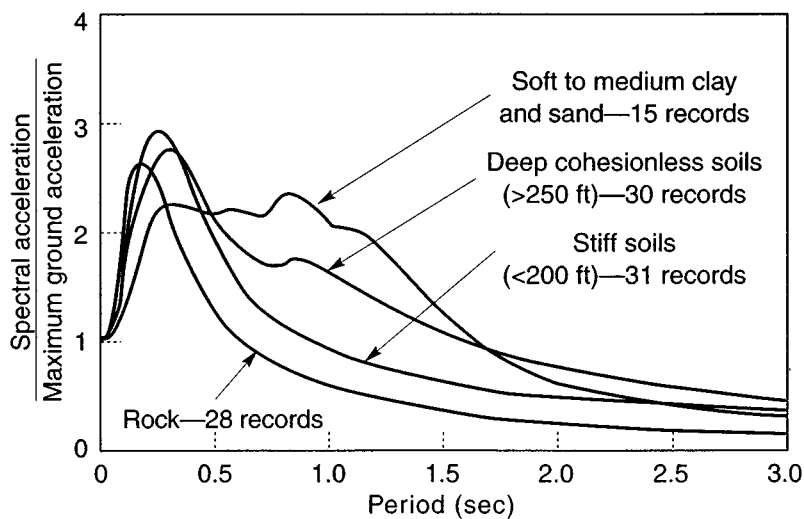
Figure 2-11 Average normalized response spectra (5% damping) for different local site conditions. (After Seed and Idriss, 1976).

21
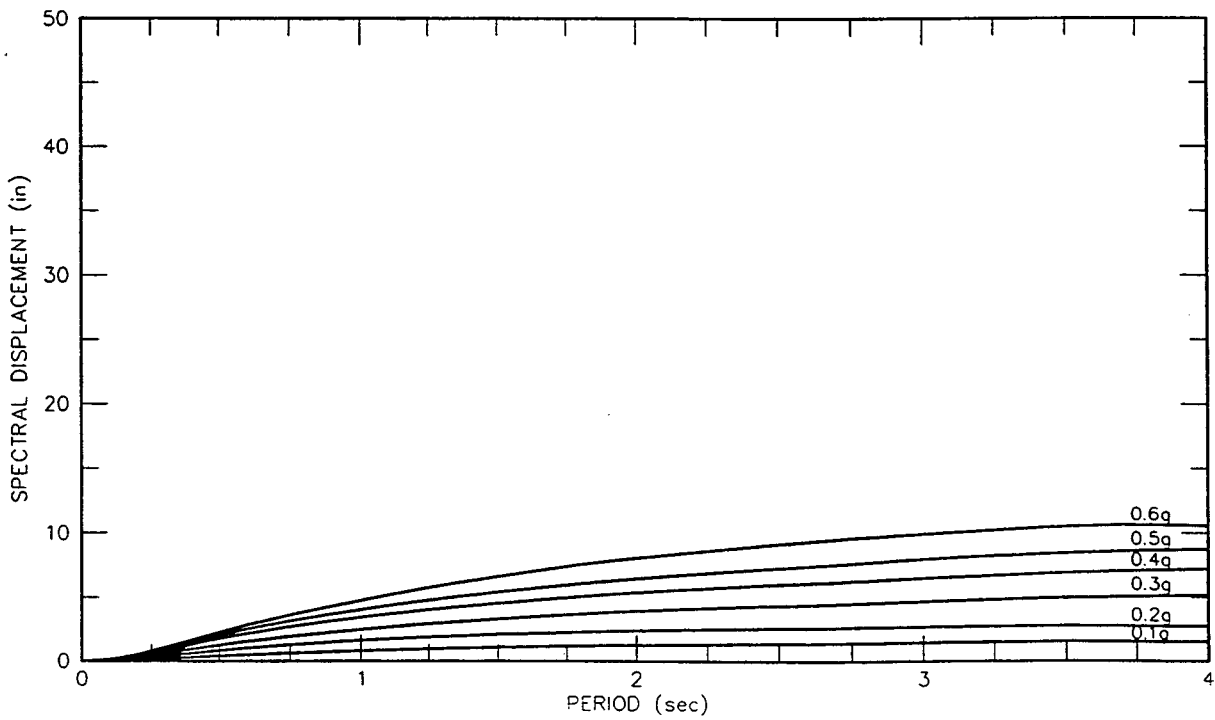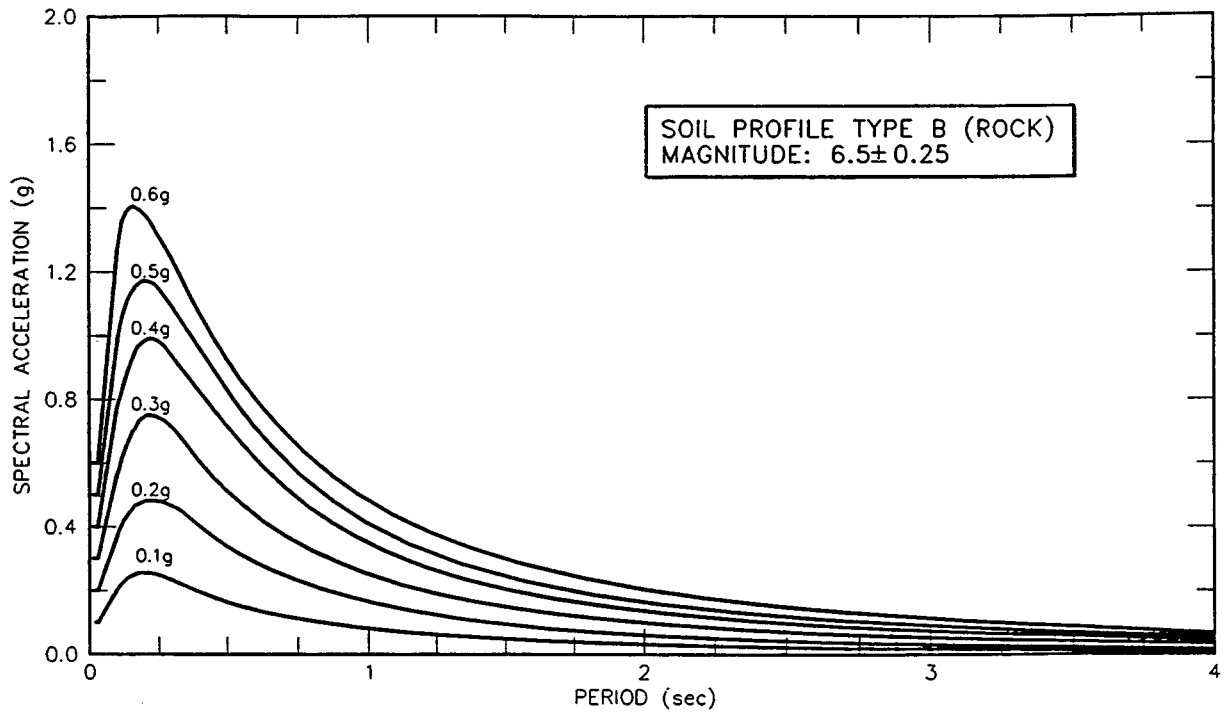
Figure 2-12 ATC proposed ARS curves for rock (M = 6.50 ± 0.25). (After ATC 32, 1996).
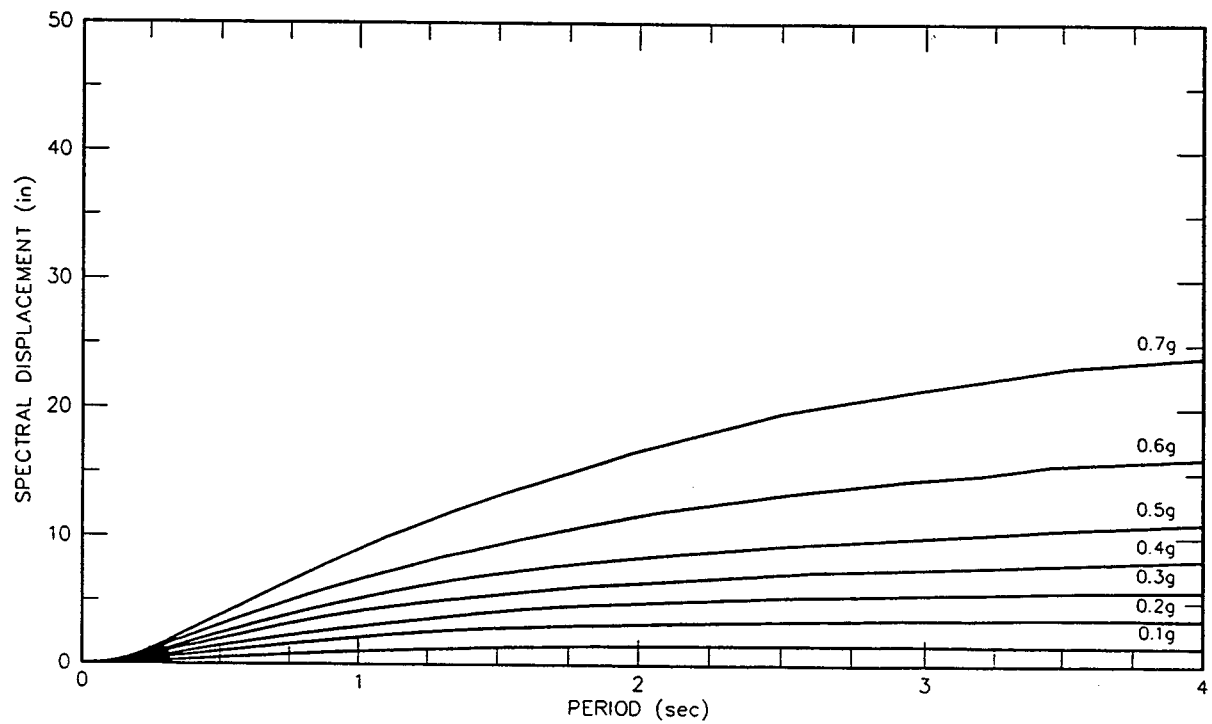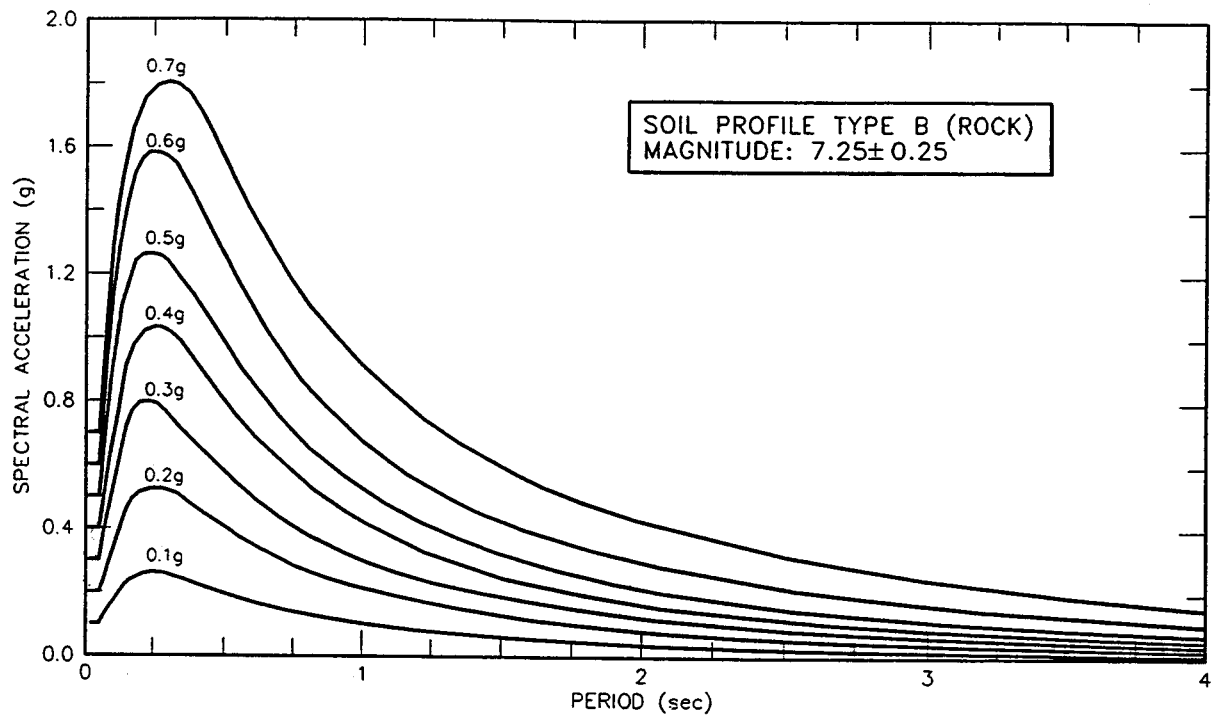
Figure 2-13 ATC proposed ARS curves for rock (M = 7.25 ± 0.25). (After ATC 32, 1996).
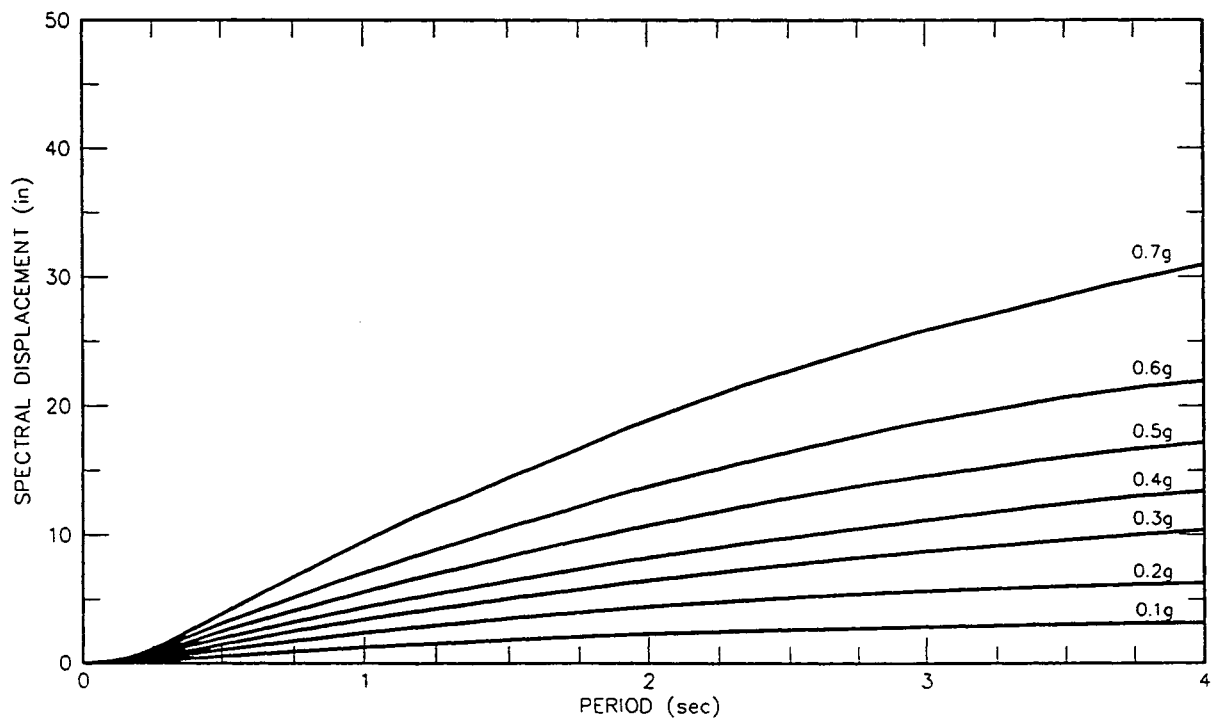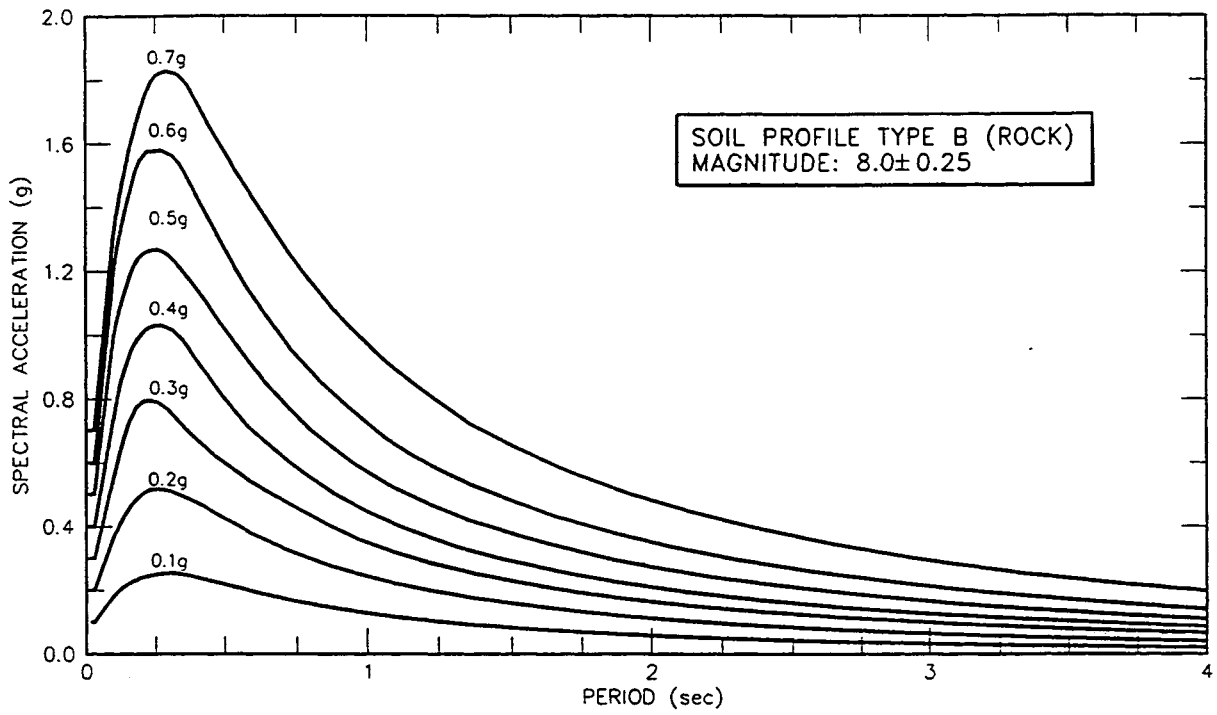
Figure 2-14 ATC proposed ARS curves for rock (M = 8.0 ± 0.25). (After ATC 32, 1996).

24
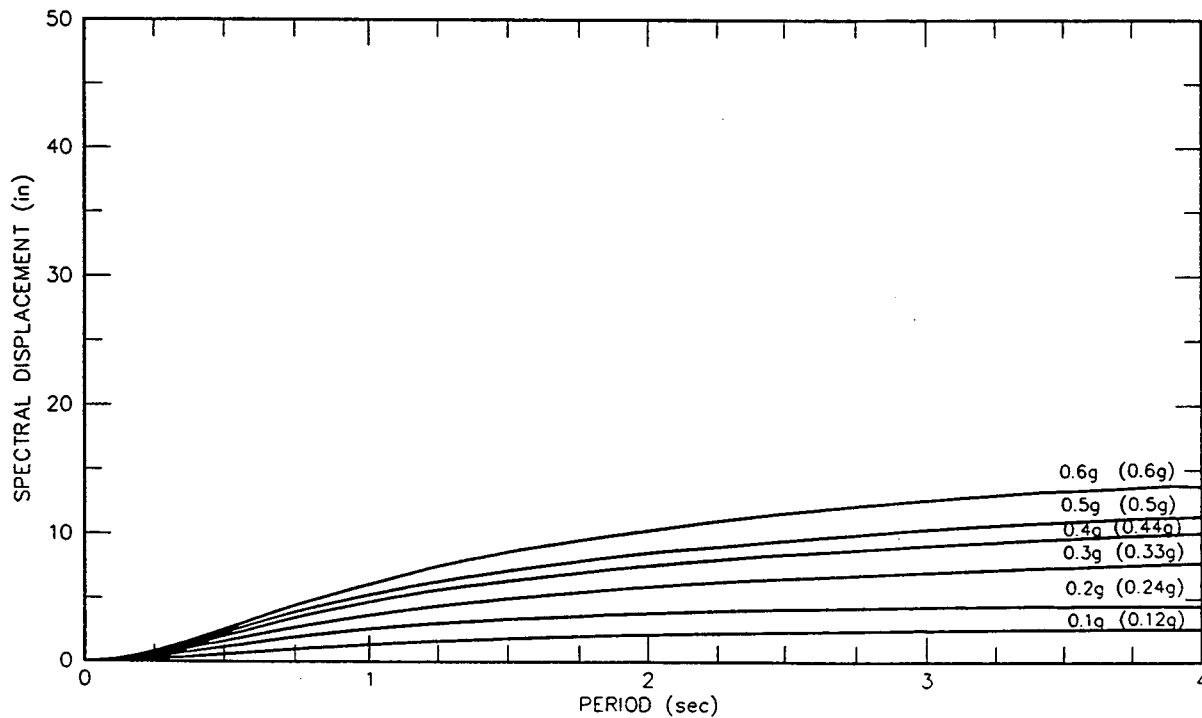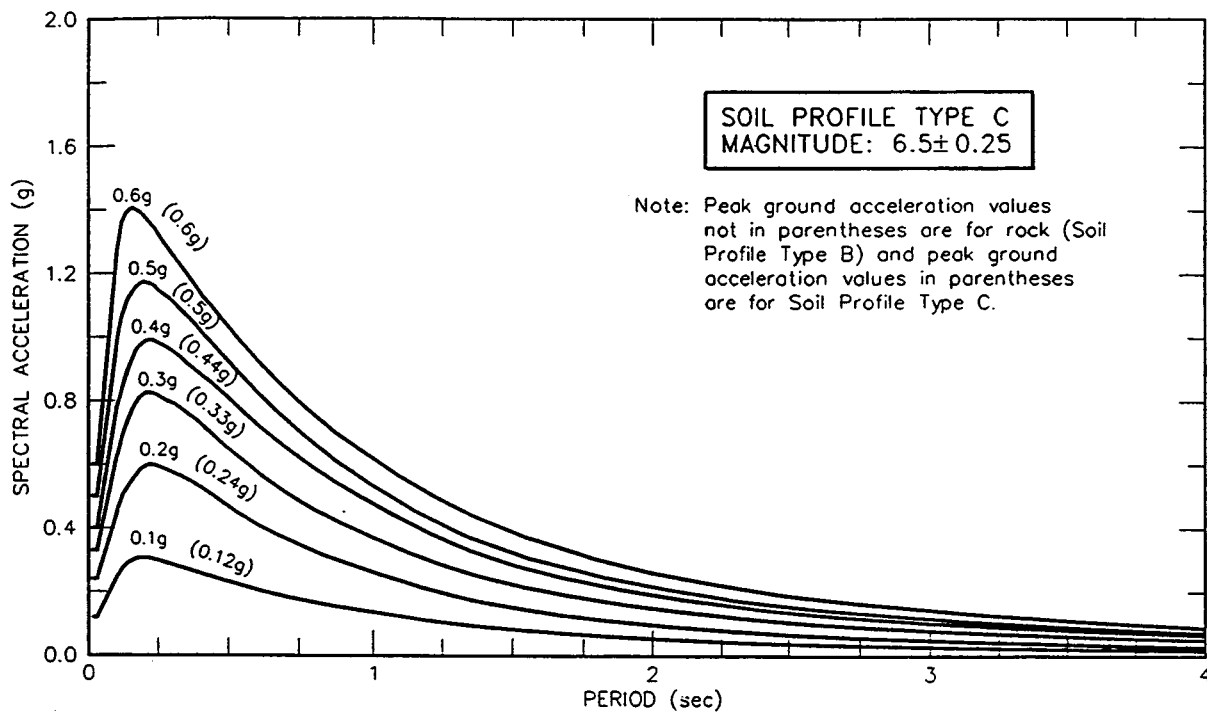
Figure 2-15   ATC proposed ARS curves for soil type C (M = 6.50 ± 0.25).
(After ATC 32, 1996).

Top graph:

SPECTRAL ACCELERATION (g)

2.0

1.6

1.2

0.8

0.4

0.0

0.7g (0.7g)

0.6g (0.6g)

0.5g (0.5g)

0.4g (0.4g)

0.3g (0.33g)

0.2g (0.24g)

0.1g (0.12g)

SOIL PROFILE TYPE C
MAGNITUDE: 7.25±0.25

Note: Peak ground acceleration values
not in parentheses are for rock (Soil
Profile Type B) and peak ground
acceleration values in parentheses
are for Soil Profile Type C.

0   1   2   3   4

PERIOD (sec)

Bottom graph:

SPECTRAL DISPLACEMENT (in)

50

40

30

20

10

0

0.7g (0.7g)

0.6g (0.6g)

0.5g (0.5g)

0.4g (0.4g)

0.3g (0.33g)

0.2g (0.24g)

0.1g (0.12g)

0   1   2   3   4

PERIOD (sec)

Figure 2-16 ATC proposed ARS curves for soil type C (M = 7.25 ± 0.25). (After ATC 32, 1996).

26
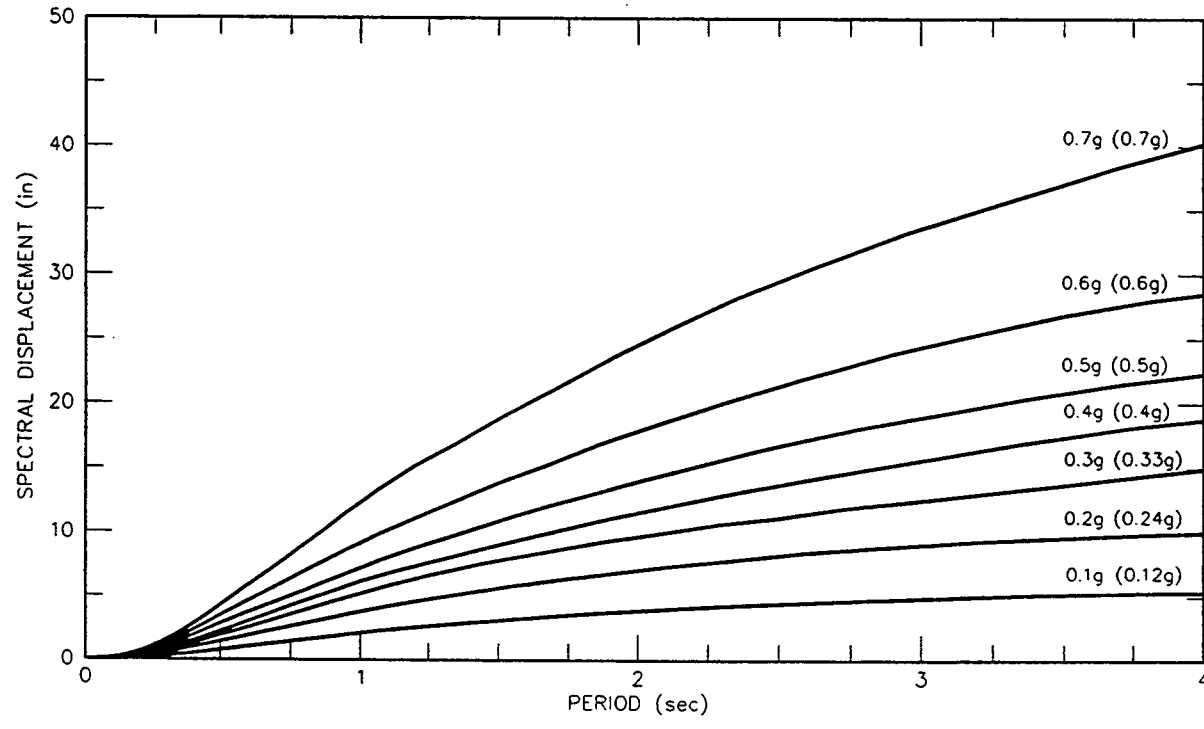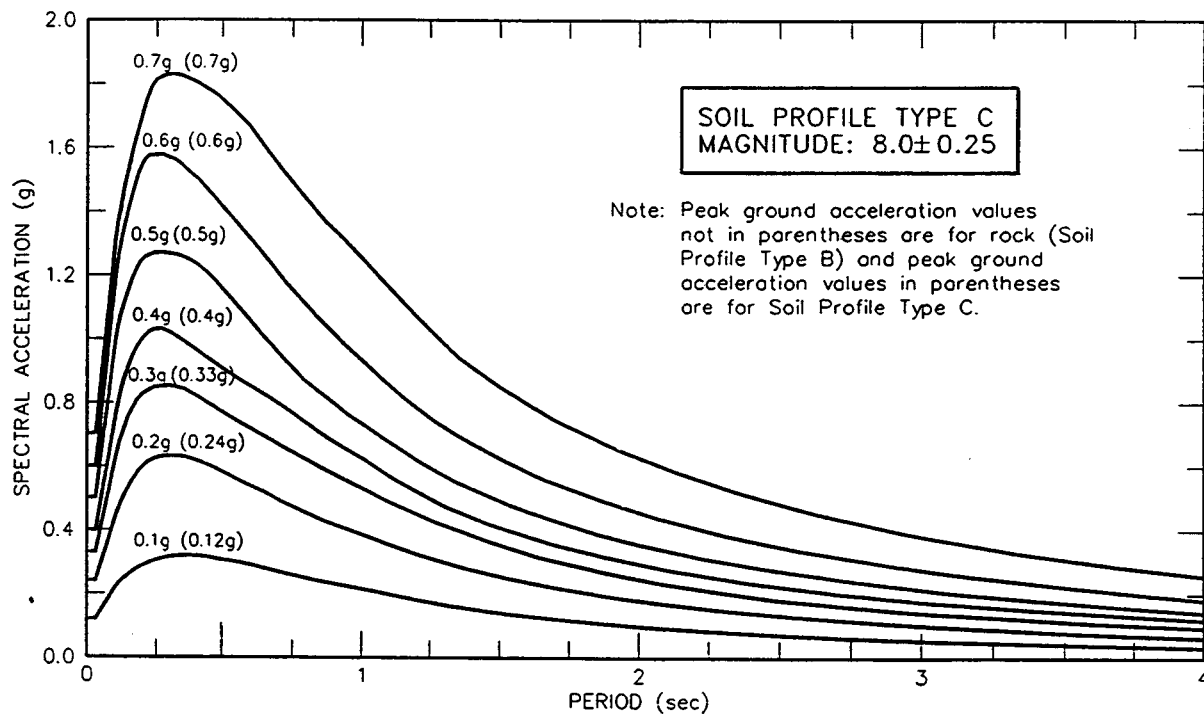
Figure 2-17 ATC proposed ARS curves for soil type C (M = 8.0 ± 0.25). (After ATC 32, 1996).
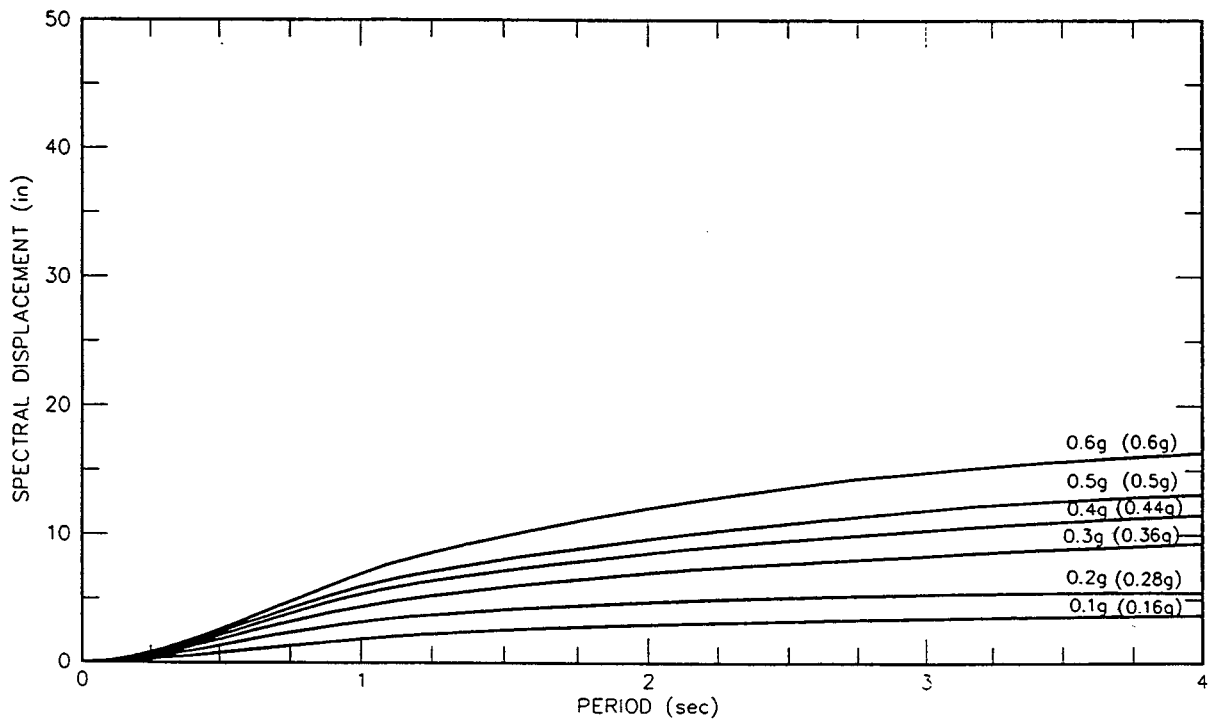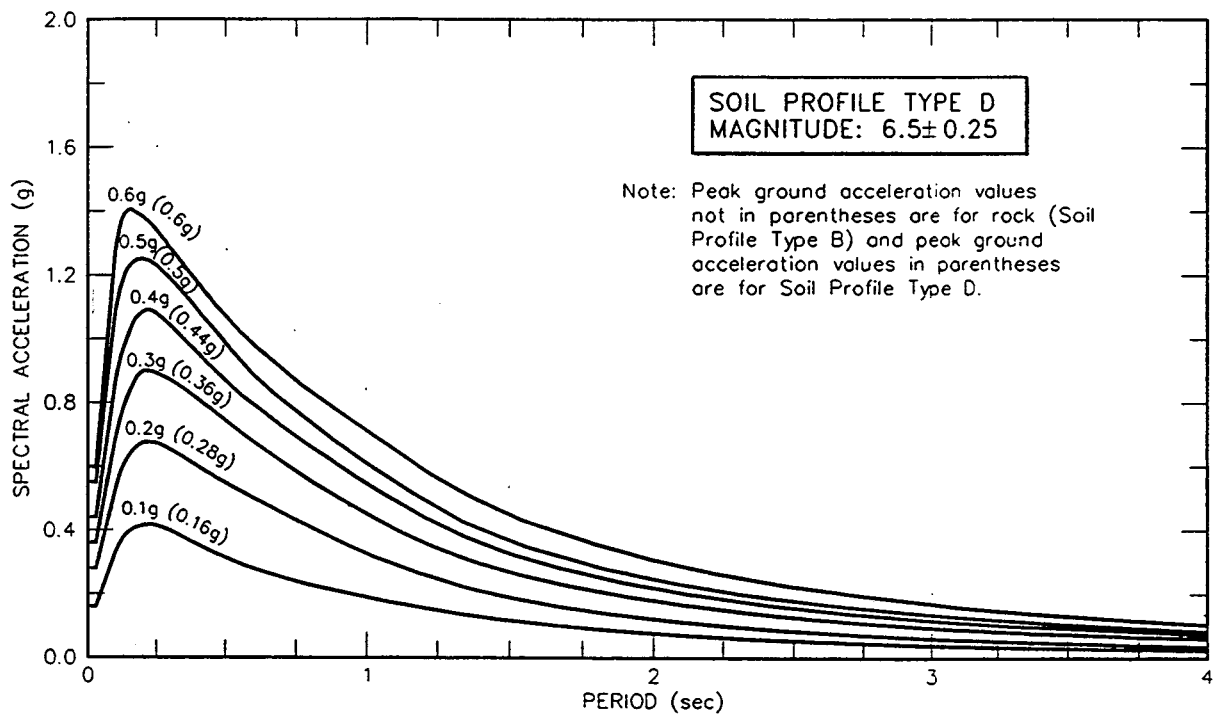
Figure 2-18 ATC proposed ARS curves for soil type D (M = 6.50 ± 0.25). (After ATC 32, 1996).
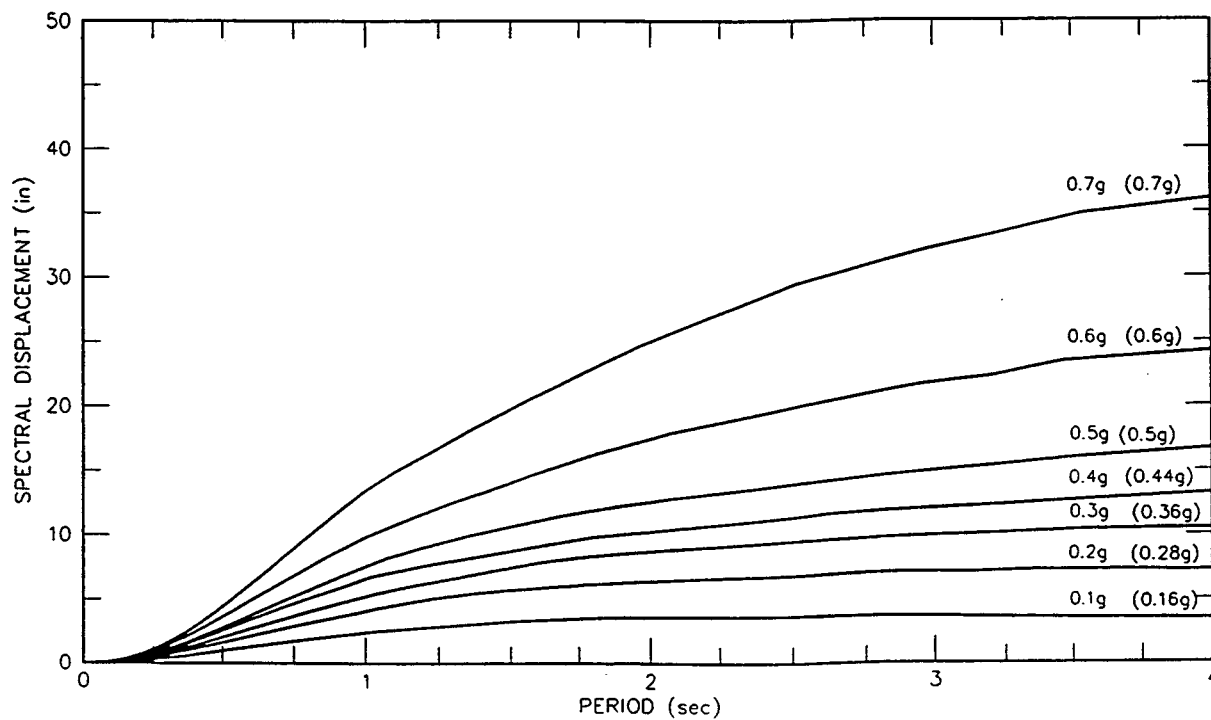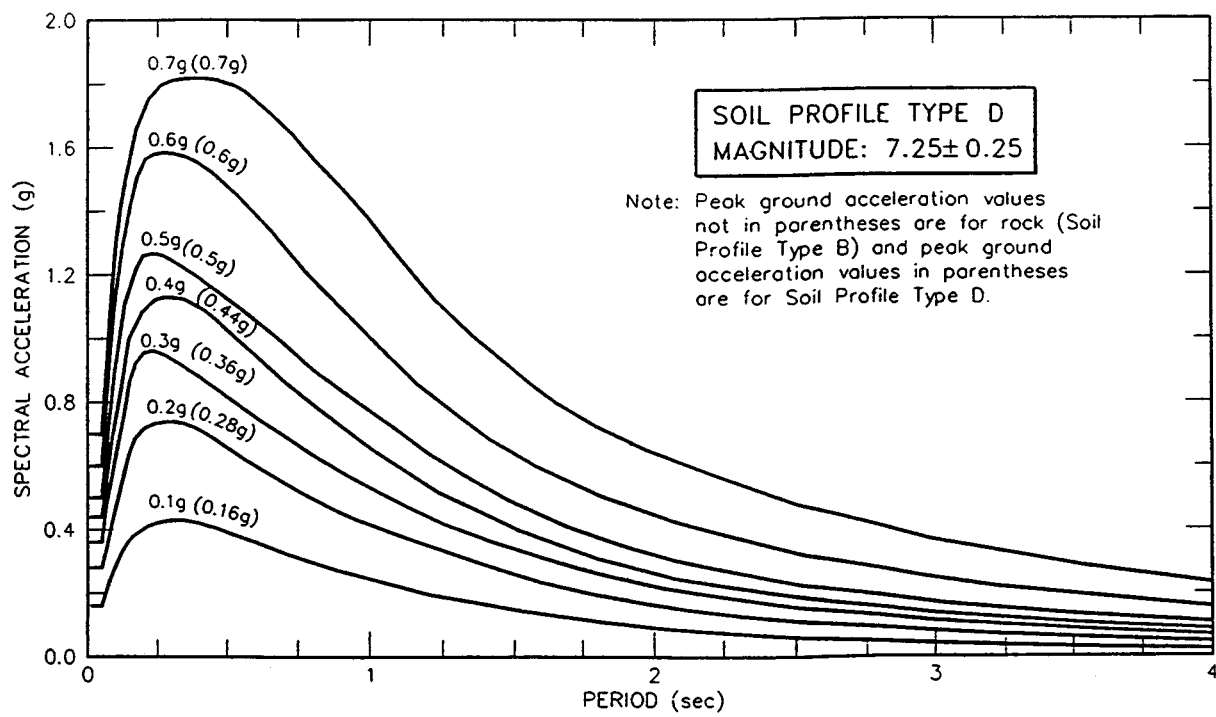
Figure 2-19 ATC proposed ARS curves for soil type D (M = 7.25 ± 0.25). (After ATC 32, 1996).
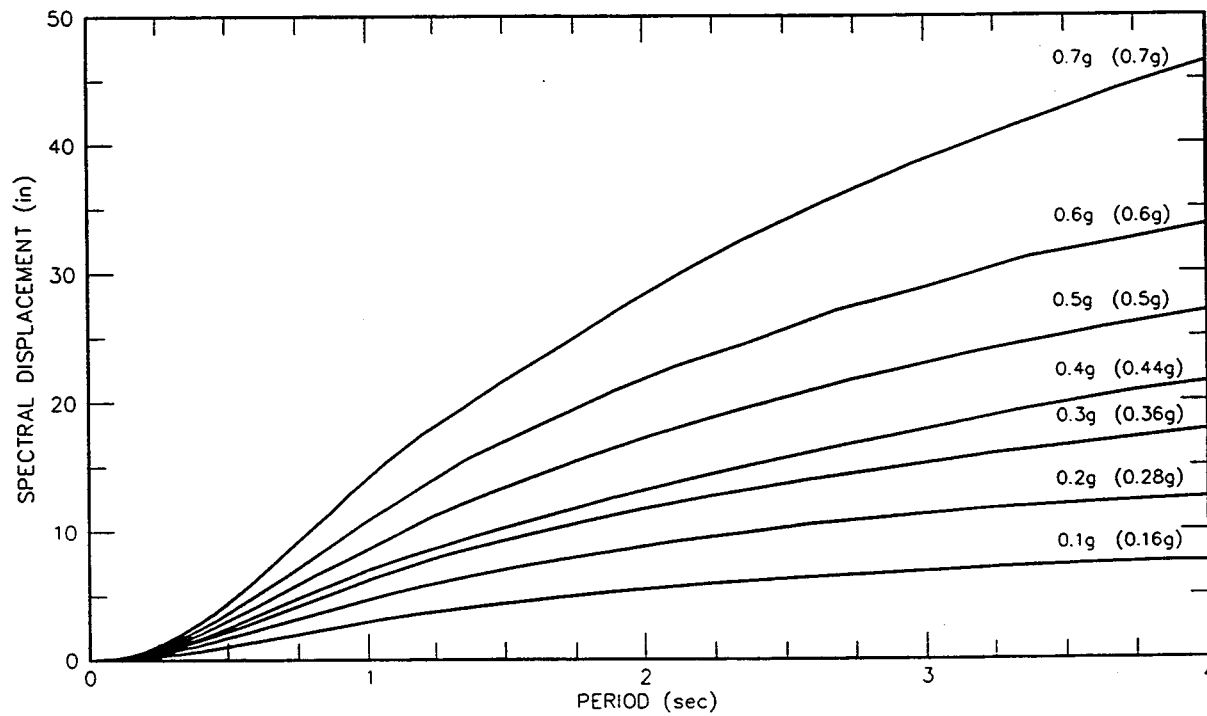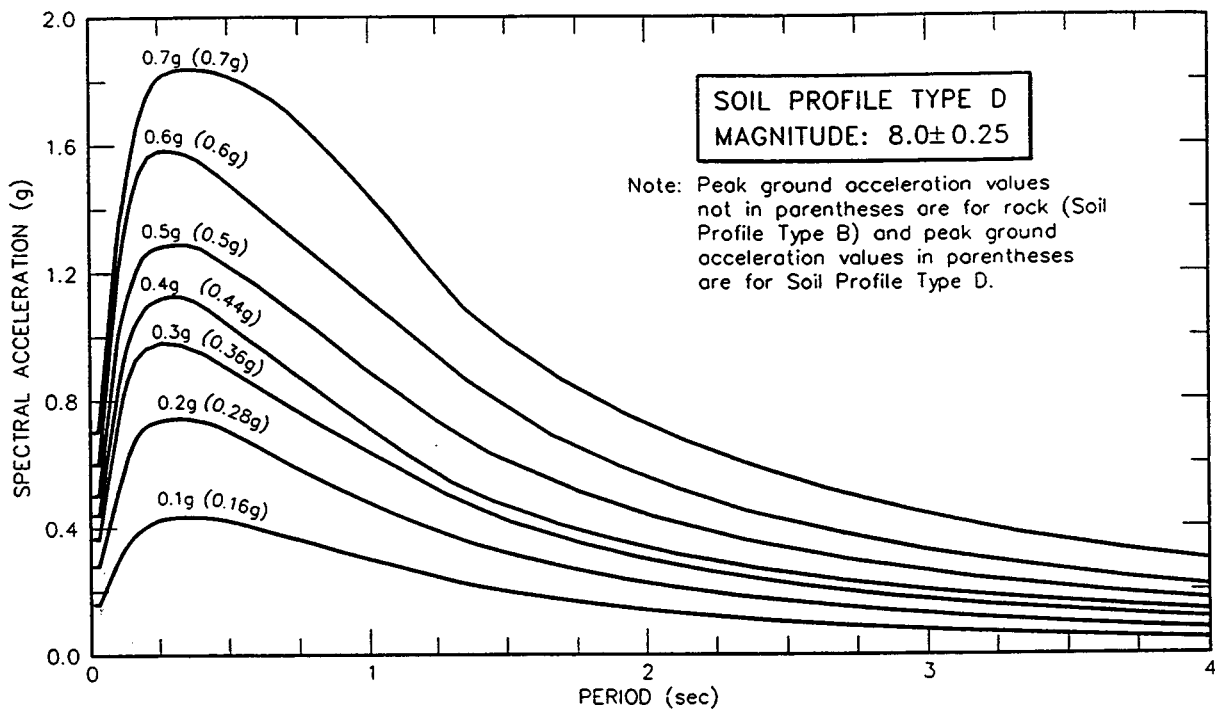
Figure 2-20   ATC proposed ARS curves for soil type D (M = 8.0 ± 0.25). (After ATC 32, 1996).
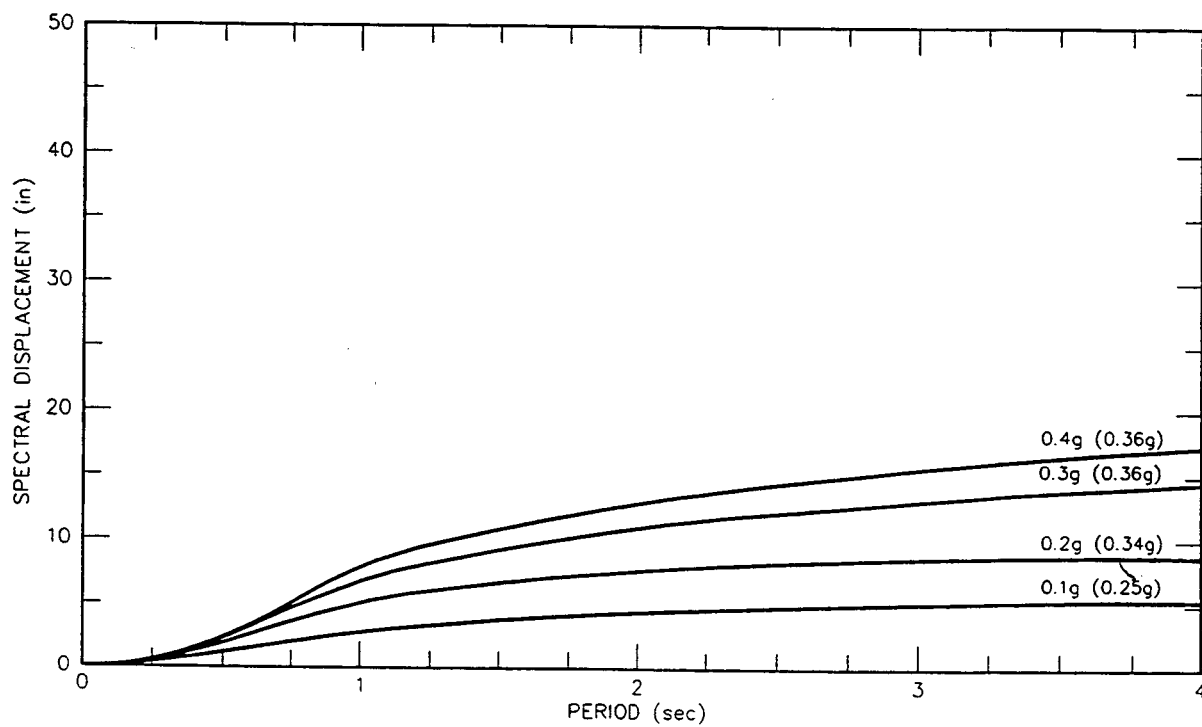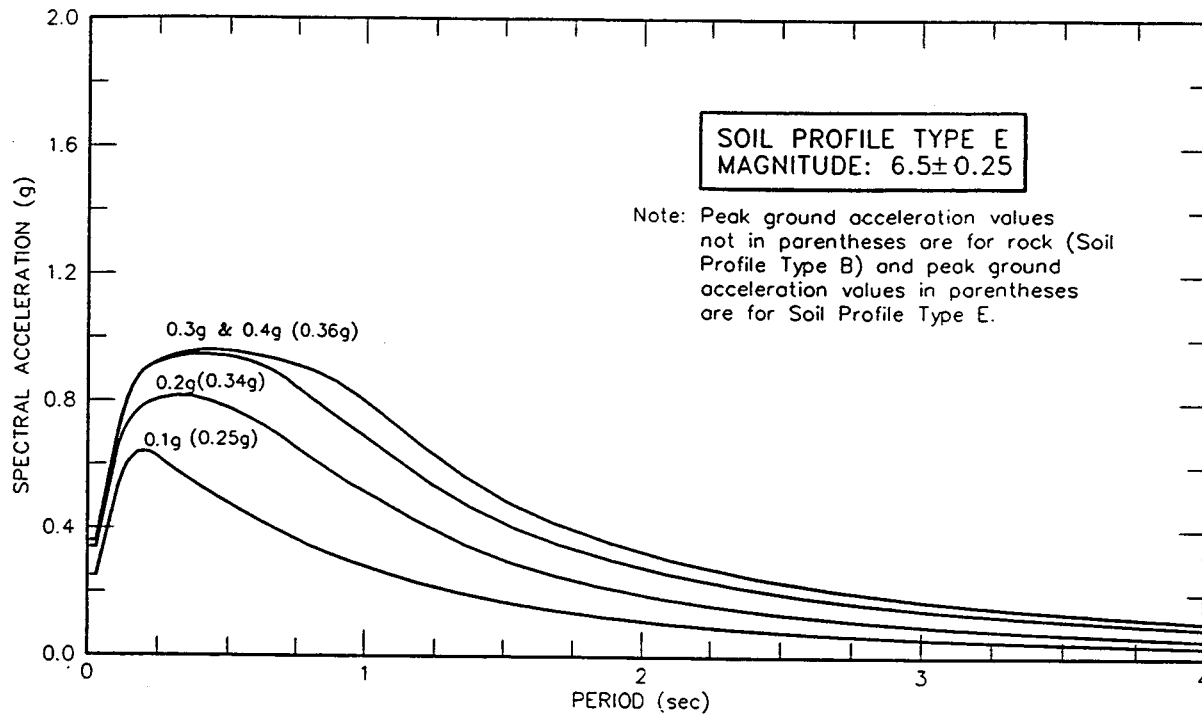
Figure 2-21 ATC proposed ARS curves for soil type E (M = 6.50 ± 0.25). (After ATC 32, 1996).

31

The upper chart shows spectral acceleration. The y-axis is labeled SPECTRAL ACCELERATION (g) ranging from 0.0 to 2.0, and the x-axis is labeled PERIOD (sec) ranging from 0 to 4.

Box label:
SOIL PROFILE TYPE E
MAGNITUDE: 7.25 ± 0.25

Note: Peak ground acceleration values
not in parentheses are for rock (Soil
Profile Type B) and peak ground
acceleration values in parentheses
are for Soil Profile Type E.

Curve labels: 0.4g(0.36g), 0.3g(0.36g), 0.2g(0.34g), 0.1g (0.25g)

The lower chart shows spectral displacement. The y-axis is labeled SPECTRAL DISPLACEMENT (in) ranging from 0 to 50, and the x-axis is labeled PERIOD (sec) ranging from 0 to 4.

Curve labels: 0.4g(0.36g), 0.3g(0.36g), 0.2g(0.34g), 0.1g(0.25g)

Figure 2-22   ATC proposed ARS curves for soil type E (M = 7.25 ± 0.25).
(After ATC 32, 1996).
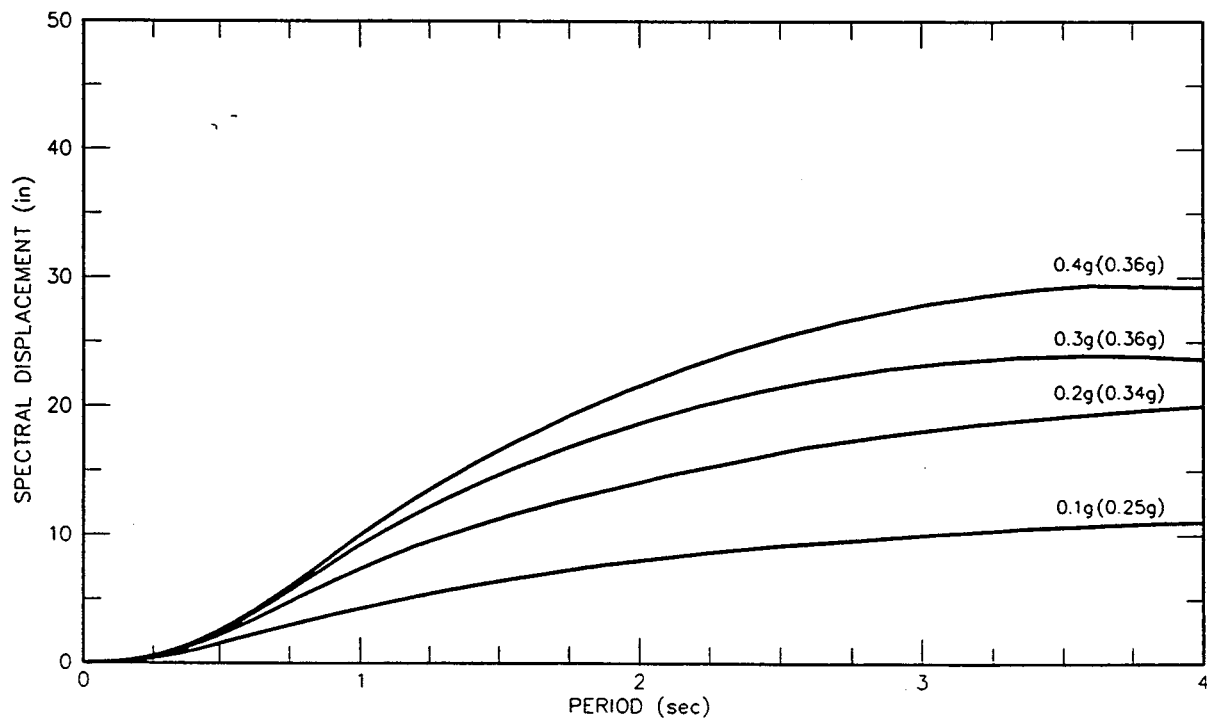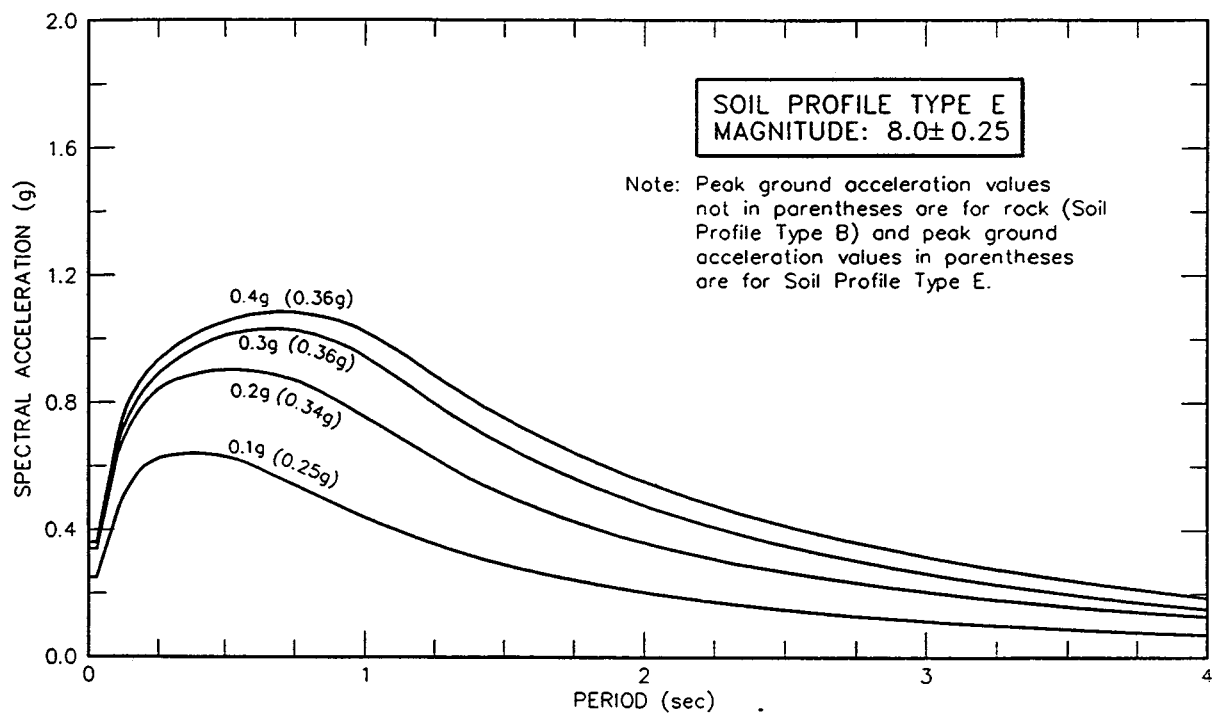
Figure 2-23 ATC proposed ARS curves for soil type E (M = 8.0 ± 0.25).
(After ATC 32, 1996).

effects which has been observed in past earthquakes. The effects of near fault motion on structural response need to be determined from inelastic dynamic analysis using spectrum-compatible motions that contain the appropriate velocity pulses.

The nature of vertical earthquake loading is complex; it depends on fault rupture mechanism, proximity of earthquake source, local soil conditions and other factors. Many researchers have studied propagation of vertical ground through downhole strong motion array data. To date, well-calibrated site response techniques for vertical component motion are not available. ATC-32 recommends the vertical earthquake design spectra may be taken as 2/3 of horizontal design spectra for typical sites not adjusted for proximity to active faults. This recommendation is largely based on comparisons of vertical and horizontal peak ground accelerations from far field earthquakes.

SECTION 3
ASPECTS OF SOIL STRUCTURE SYSTEM

3.1   Current Modeling Practice

Almost all man-made structures are built on soil or rock medium. Assessing response of a structure under static and dynamic loading conditions requires some knowledge of soil-structure interaction (SSI) aspects. The topic of seismic loading on structures has been a major driving source for advancement in understanding of many SSI problems faced regularly in civil engineering. Evidence from major earthquake damages around the world clearly demonstrates the importance of vibratory response of structure and its interaction with the supporting media. In a general sense, the soil-structure interaction problem depends on the loading mechanism, foundation type as well as the nature of the superstructure.

After the 1989 Loma Prieta Earthquake, a statewide major retrofit program was initiated by the California Department of Transportation to ensure satisfactory performance of the existing bridges and new bridges for future earthquakes. The program also called for improvement of the existing design codes, advancement in seismic analysis and design procedure and development of more effective structural detailing and construction methods. The analytical procedure dealing with the soil-structure interaction problems has been refined and improved since then.

Long bridges pose a special challenge to the designers because these structures are supported on multiple piers with varying foundation types, subsurface conditions and loading conditions. For this type of structures, multiple-support excitation is a valid form of loading during seismic events. Multiple support time history analysis is the best suited for the study of effects of spatial variation in the ground motion. To perform multiple support time history analyses, time histories of the ground motion arriving at each individual foundation are evaluated. Depending on the level of efforts, modeling of the bridge can be a complete system or a simplified substructured system, as shown in Figure 3.1. In the complete system, every essential elements of the foundation such as all the piles and all the soil support springs are explicitly included in the bridge model. On the other hand, the substructured model simplifies the foundation as a reduced degree-of-freedom system by using the substructuring techniques based on the principle of structural mechanics. As illustrated in Figure 3.1, substructuring can be conducted for individual piles or for the entire pile group. Substructuring methods are discussed in Sections 4 and 5.

3.2   Multiple Support Motion

All the toll bridges in the State of California cross a bay or strait with bridge lengths ranging from 1 to 3 kilometers. As outlined in the previous chapter, spatial variation of the ground motion due to incoherency and local site condition leads to multiple support
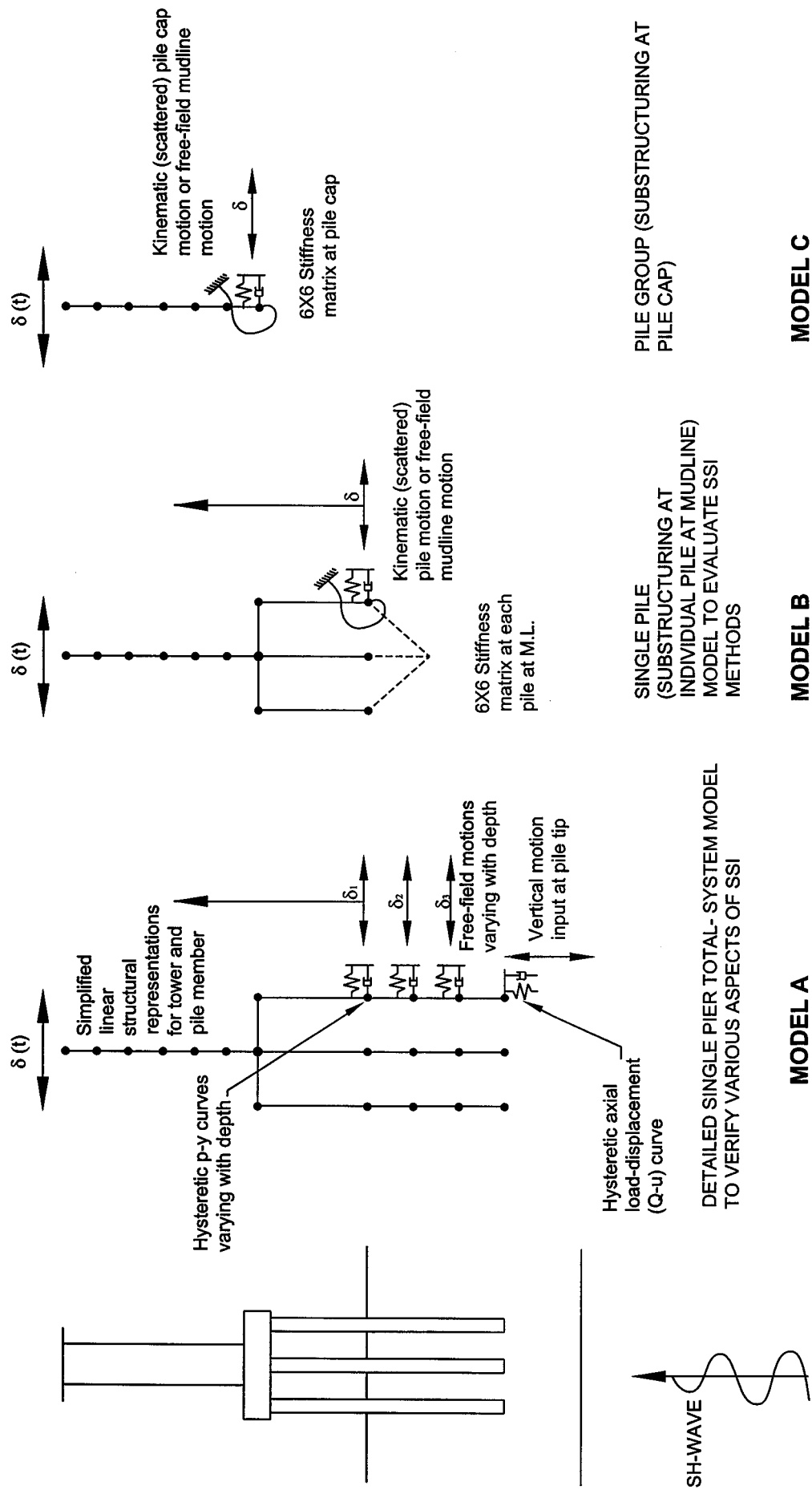
Figure 3-1   Various SSI models to evaluate a bridge structure.

excitation for the long bridge. As a result, the conventional response spectrum approach of designing the global bridge as a primary design tool becomes inadequate unless some measures are implemented to consider the variation in the multiple support motions.

Recognizing the deficiencies in the response spectrum procedure, multiple-support time history analyses have been implemented in the designs (both seismic retrofits and new designs) of all California toll bridges. This procedure also allows the designers to address inelastic behavior of the structure and to incorporate such ground motion issues as multiple support excitation and near-field directivity effects. Table 3.1 lists the California toll bridges that have been designed with multiple support time history analyses.

Table 3.1 Seismic Design of Toll Bridges in California and Washington

Bridge	Bridge Type	No. of Multiple Support Motions	Directivity Effects
Seismic Retrofit of Existing Structure			
Golden Gate Bridge	Suspension	Three	Not Considered
Carquinez Bridge	Steel Truss	Three	Considered
Benicia-Martinez Bridge	Box Girder	Three	Considered
San Mateo Bridge	Box Girder	Three	Considered
Richmond-San Rafael Bridge	Steel Truss	Three	Considered
San Diego-Coronado Bridge	Box Girder	Three	Considered
Vincent-Thomas Bridge	Suspension	Three	Considered
Design of New Structure			
New Carquinez Bridge	Suspension	Three	Considered
New Benicia-Martinez Bridge	Box Girder	Three	Considered
New East Span San Francisco – Oakland Bay Bridge	Suspension/ Box Girder	Six	Considered
New Tacoma-Narrows Bridge	Suspension	Three	Not Considered

As mentioned earlier, the effects of multiple-support excitation and directivity cannot be fully addressed by the response spectrum procedure. All the bridges listed in Table 3.1 were initially designed with some ARS criteria and were later checked against multiple-support time history analyses. The use of appropriate ARS criteria during the initial phase of design was necessary to reduce the analysis time because execution of multiple-support time analysis is often very time consuming. The success of seismic response analysis for a bridge depends largely upon how well the initial design ARS criteria represent the actual loading conditions including potential for variations in multiple support excitation and incorporating all essential features of soil-structure interaction

elements. In the foregoing section, discussions on development of ARS criteria are provided.

Irrespective of whether a complete total system or a substructured system is modeled, multiple support motions are needed at different support piers. This involves conducting site response analyses to evaluate wave propagation at the pier location using the local soil conditions and performing soil-pile interaction study to derive effective forcing function at the foundation level. The outcome of the study, in fact, includes spatial variation of ground motion, effects of local site condition, and foundation consideration. The forcing function estimated at each pier is then used in the global bridge model to determine seismic response of the bridge.

3.3   Spread Footing

Spread footings are commonly used as foundations for piers and abutment walls. The current state of practice in soil-structure interaction analyses for spread footing involves solving for the response of a rigid footing on a semi-infinite elastic half space. From elasto-dynamic formulation, the stiffness characteristics of foundation consist of two parts; static component and dynamic component. However for most typical highway bridge application, the dynamic effects can be ignored because the periods of interest for earthquake problems are relatively long generally more than 0.7 seconds.

The general form of stiffness matrix for a rigid footing is of the following form:

$$[K] = \begin{bmatrix} k_{11} & 0 & 0 & 0 & -k_{15} & 0 \\ 0 & k_{22} & 0 & k_{24} & 0 & 0 \\ 0 & 0 & k_{33} & 0 & 0 & 0 \\ 0 & k_{42} & 0 & k_{44} & 0 & 0 \\ -k_{51} & 0 & 0 & 0 & k_{55} & 0 \\ 0 & 0 & 0 & 0 & 0 & k_{66} \end{bmatrix} \qquad (3.1)$$

Degrees of freedom 1 through 3 are translation and degrees of freedom 4 through 5 are rotation. The degree of freedom 3 is the translation in the vertical direction. The vertical translational degree of freedom (k_{33}) and torsional degree of freedom (k_{66}) are uncoupled with the other degrees of freedom in the stiffness matrix. However, the two components of horizontal translation are coupled with the two degrees of freedom in rocking rotation in the stiffness matrix. When embeddment of the footing is shallow, the off-diagonal (cross-coupling) terms are generally neglected. Therefore, the following form of uncoupled stiffness matrix is quite adequate for most spread footing problems

38

$$[K] = \begin{bmatrix} k_{11} & 0 & 0 & 0 & 0 & 0 \\ 0 & k_{22} & 0 & 0 & 0 & 0 \\ 0 & 0 & k_{33} & 0 & 0 & 0 \\ 0 & 0 & 0 & k_{44} & 0 & 0 \\ 0 & 0 & 0 & 0 & k_{55} & 0 \\ 0 & 0 & 0 & 0 & 0 & k_{66} \end{bmatrix} \qquad (3.2)$$

The solution for a circular footing bonded to the surface of an elastic half space provides the basic stiffness coefficients for the various components of displacement as summarized below:

$$k_{33} = \frac{4GR}{1-v} \qquad (3.3)$$

$$k_{11} = k_{22} = \frac{8GR}{2-v} \qquad (3.4)$$

$$k_{66} = \frac{16GR^3}{3} \qquad (3.5)$$

$$k_{44} = k_{55} = \frac{8GR^3}{3(1-v)} \qquad (3.6)$$

where R is the radius of the footing, G and v are the shear modulus and Poisson's ratio for the elastic half space, respectively. For rectangular footings, the radius of an equivalent circular footing can be approximated which can then be used in the above equations to compute individual stiffness coefficients. The procedure to calculate the radius of an equivalent circular footing is summarized in Figure 3.2. The appropriate value of shear modulus requires some degree of engineering judgement to account for strain compatibility. In addition to the spread footing stiffness, a damping parameter is required for seismic response analysis of the bridge especially when the foundation is represented by linear elastic representation. Some discussion on foundation damping is given later.

The stiffness matrix as derived from the elastic half space theory is a linear representation of the problem. For tall bridges, the most important mode of foundation behavior is rocking stiffness term where base separation can have major effects on the resultant global bridge behavior. To appreciate the importance of this behavior, it is recommended that pseudo-static pushover analysis be conducted to examine moment-rotation characteristics of spread footing considering the effects of geometric nonlinearity (uplift of the footing) and soil yielding. Analytical results from these pushover analyses not only yield rotational stiffness parameters, but also provide the geotechnical mode of ultimate moment capacity which can be treated as load fuse in the overall bridge system. For the spread footing problem, geometric nonlinearity (uplift) is a most severe form of nonlinearity, and the foundation cannot develop overturning moments that are higher than
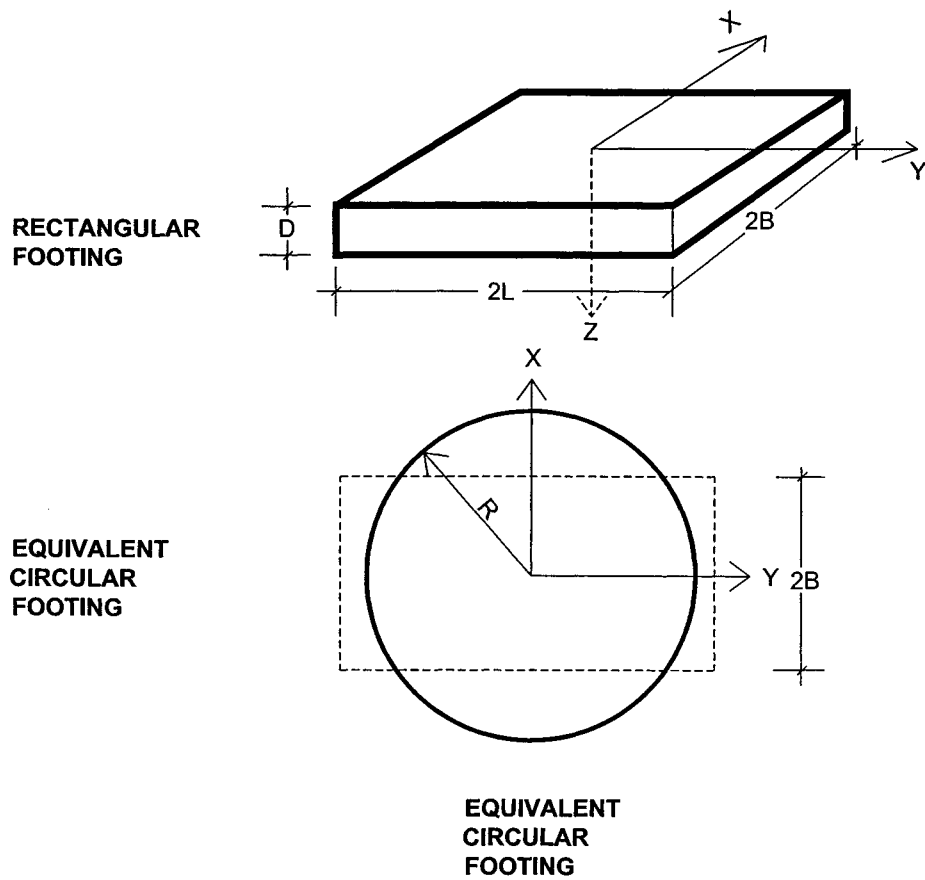
EQUIVALENT RADIUS:

TRANSLATIONAL: $R = \sqrt{\dfrac{4BL}{\pi}}$

ROTATIONAL: $R = \left[\dfrac{(2B)\,(2L)^3}{3\pi}\right]^{\frac{1}{4}}$ ....(x−AXIS ROCKING)

$R = \left[\dfrac{(2B)^3\,(2L)}{3\pi}\right]^{\frac{1}{4}}$ ....(y−AXIS ROCKING)

$R = \left[\dfrac{4BL\,(4B^2 + 4L^2)}{6\pi}\right]^{\frac{1}{4}}$ ....(z−AXIS TORSION)

Figure 3-2   Procedure for calculating equivalent radius of a rectangular footing.

the ultimate moment capacity. Since the pushover analyses would provide rotational stiffness for seismic analysis of the bridge structure, it is important not to use artificially low soil strength and stiffness parameters because engineers find difficult to judge what is meant by being conservative for foundation stiffness when used in seismic analyses. In this case, using best estimated soil parameters (as opposed to lower bound strength and stiffness) would be most desirable for pushover analyses.

Figure 3.3 presents an example of pushover (rocking) analyses conducted for a spread footing on dense sand at San Diego-Coronado Bay Bridge (EMI, 1997a). Vertical dead load was imposed on the spread footing before increasing moment was applied. From the limit equilibrium, the upper bound value of the ultimate moment capacity may be evaluated from the product of dead load on the footing and the half width of the footing.

3.4   Gravity Caisson

Caissons are large structural foundations commonly used at deep-water sites. They are usually in the form of a large cellular rectangular box or cylindrical shell structure with a seal base. When a bridge is supported on gravity caissons, in addition to solving for the dynamic response of the bridge during earthquakes, the stability of caisson itself needs to be addressed in the design. Unlike most spread footings, gravity caissons are massive and sometimes constitute a major portion of the weight of the entire bridge. The fundamental mode of vibration for most gravity caissons can be characterized as very short period motion and it would be very different from the long period response of the bridge. Because of two distinct modes of vibration between the caisson and the bridge, uncoupled seismic analyses would provide reasonable estimates of the caisson behavior.

For modeling of a total system comprising of bridge structure and foundations, the caisson foundation may be represented by a lumped mass model using the same stiffness matrix formulation as the spread footing as a first cut approximation. Since the center of gravity for the caisson is relatively high, the controlling mode of vibration is usually rocking. End bearing of the caisson base and the passive soil resistance on the vertical wall of the caisson provide resisting mechanisms against seismic loading. The following form of coupled linear stiffness matrix as derived from elasto-dynamic theory may be used

$$[K] = \begin{bmatrix} k_{11} & 0 & 0 & 0 & -k_{15} & 0 \\ 0 & k_{22} & 0 & k_{24} & 0 & 0 \\ 0 & 0 & k_{33} & 0 & 0 & 0 \\ 0 & k_{42} & 0 & k_{44} & 0 & 0 \\ -k_{51} & 0 & 0 & 0 & k_{55} & 0 \\ 0 & 0 & 0 & 0 & 0 & k_{66} \end{bmatrix} \tag{3.7}$$
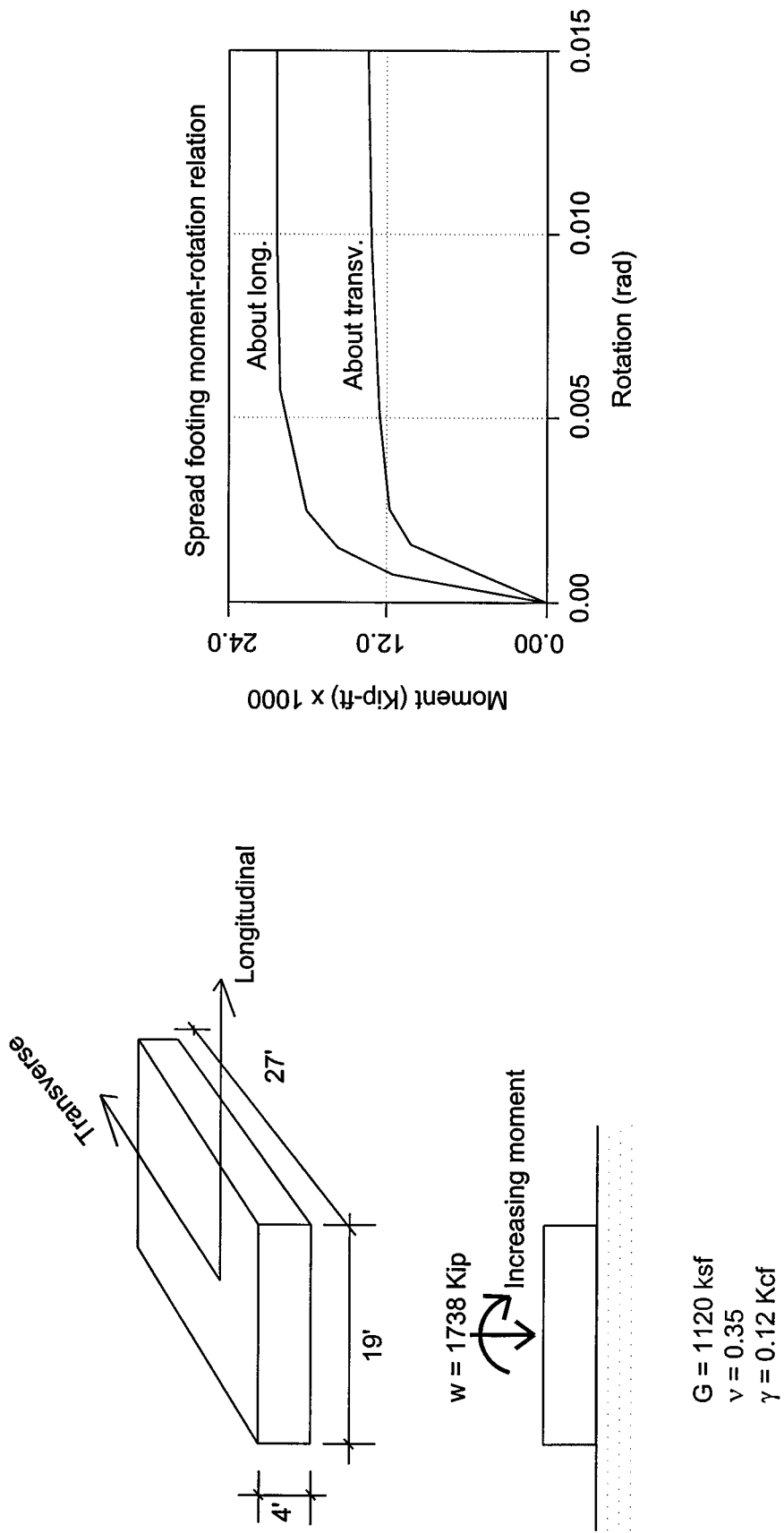
Figure 3-3 Typical rocking analysis of a spread footing.

The coupling terms in the stiffness matrix are due to the embeddment of the caisson in soils. The foundation stiffness matrix can be used in the seismic response analysis of the bridge, which would also need a foundation damping parameter to be discussed later. However, most of the earthquake response analyses make use of Raleigh damping in terms of a certain percentage of the critical damping for the entire system.

As in the case of spread footing, excessive overturning moment due to large excitation could lead to gapping at the base of the caisson. Therefore, the classical elasto-dynamic approach, which assumes full contact with the underlying soil, tends to overestimate the stiffness. Although the stiffness matrix presented above provides reasonable characteristics of foundation behavior at a small displacement range, it can lead to erroneous results for large deformations, especially when a force-based design approach is taken. The errors are attributed the lack of a load-fuse mechanism when the limiting force or moment is reached.

Static pushover analyses with allowance for base separation and soil yielding is highly recommended to appreciate the effects of geometric and material nonlinearity as well as to establish proper load-fuse mechanisms. The results of the pushover analyses would form a basis for refining the lumped mass model to capture essential elements of soil-structure interaction phenomena including the load-fuse.

Figure 3.4 shows one-half model for three dimensional pushover analysis conducted on a large gravity caisson at the Carquinez Bridge in Northern California. These analyses were conducted as part of the seismic retrofit program for the existing bridge structure. The plan dimensions of the caisson are 102 feet in the transverse direction and 53 feet in the longitudinal direction (EMI, 1997b). The foundation is largely embedded in 45 feet of dense to very dense sand and is underlain by shale. Two load cases were considered in the finite element pushover studies; the first load case was to simulate effective vertical load, and the second load case was to apply increasing horizontal load at the center of gravity after the first load case. The computation was conducted using a computer program DYNAFLOW. Soil material properties soils are modeled by an appropriate constitutive relation such as von Mises type stress-strain behavior and contact elements are used at all the nodes at the soil/structure interface to allow tensile separation between the soil and the structure.

Figure 3.5 presents moment-rotation characteristics deduced from the finite element solutions. The moment values have been calculated based on the horizontal force applied at the center of gravity of the caisson multiplied by the height of the loading point above the base. The applied force at the center of gravity is also plotted against the lateral deflection at the base of the caisson to deduce lateral load-deflection characteristics, as shown in Figure 3.6. These resultant curves can be used for dynamic response of the caisson itself and for overall performance of the global bridge model.

Figure 3.7 presents a lumped mass model of the gravity caisson to study the rocking behavior without the influence of the bridge superstructure. It is represented by a two degree of freedom with a rotational and a translational degree of freedom. The nonlinear
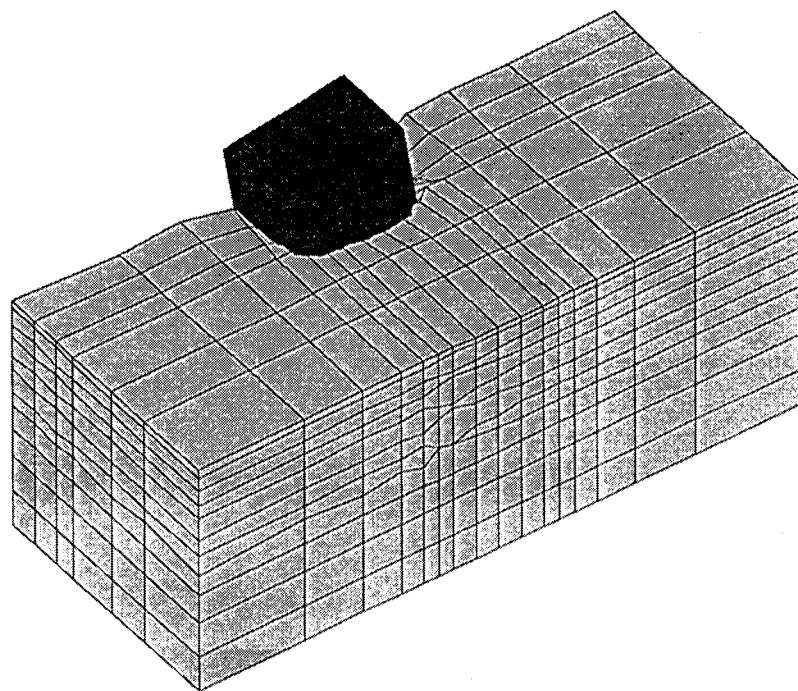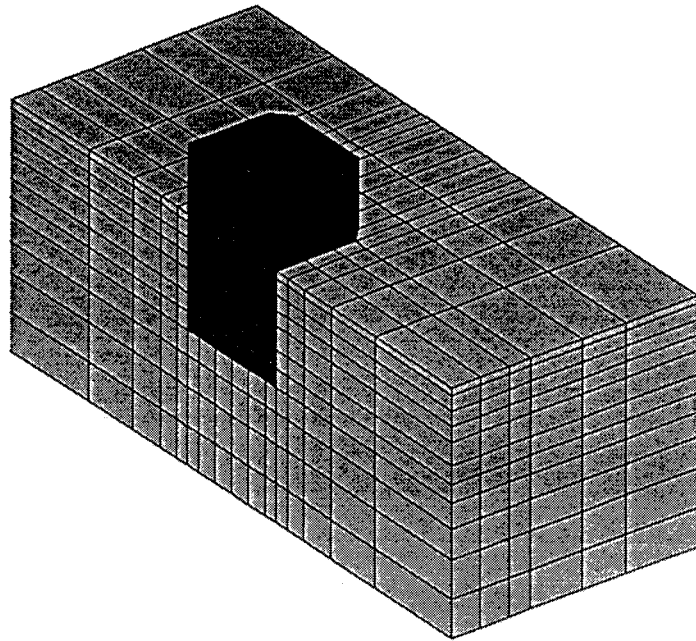
Figure 3-4 One half model for 3-dimensional pushover analysis of a gravity caisson.
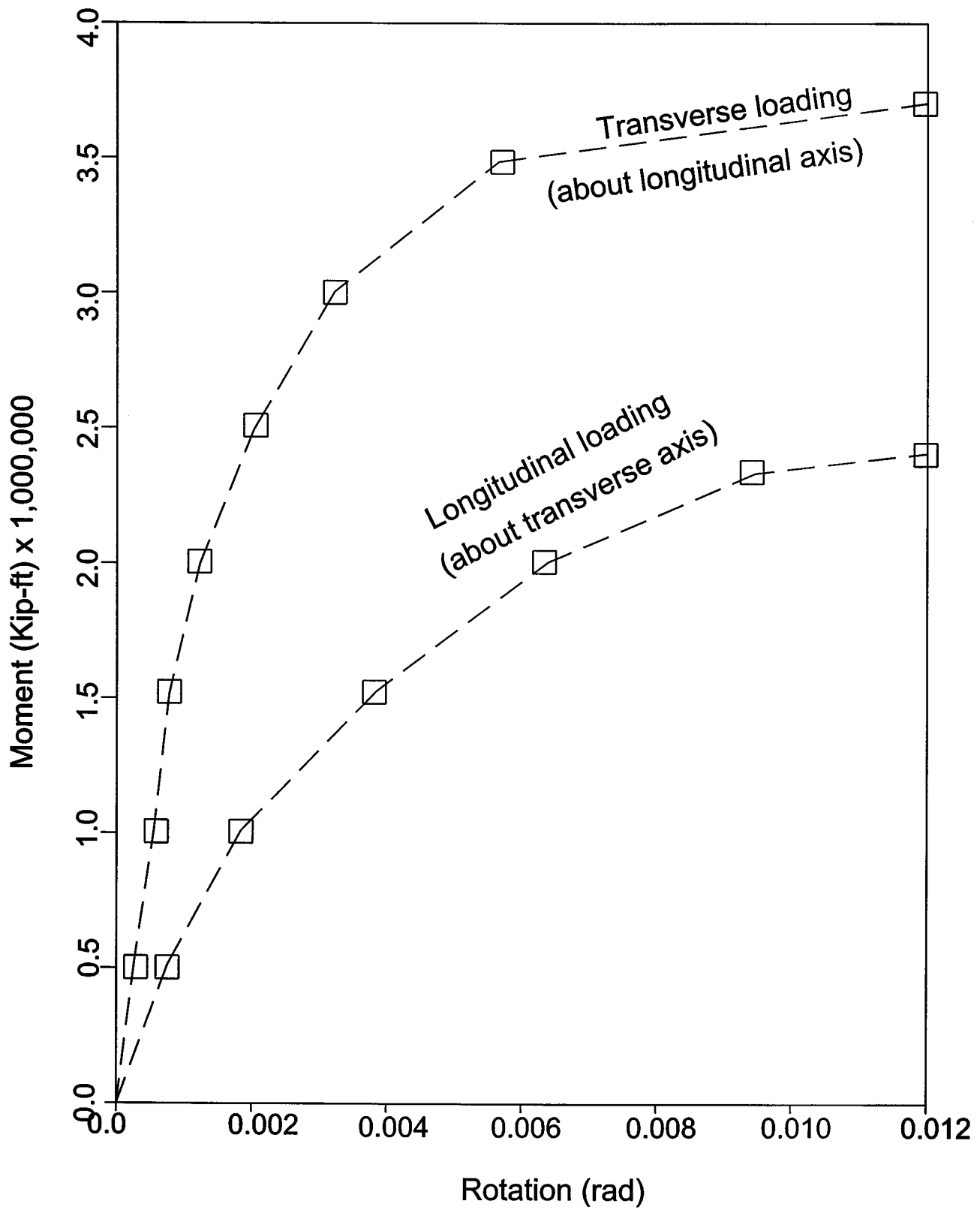
Figure 3-5 Foundation moment-rotation characteristics of a gravity caisson from pushover analysis.
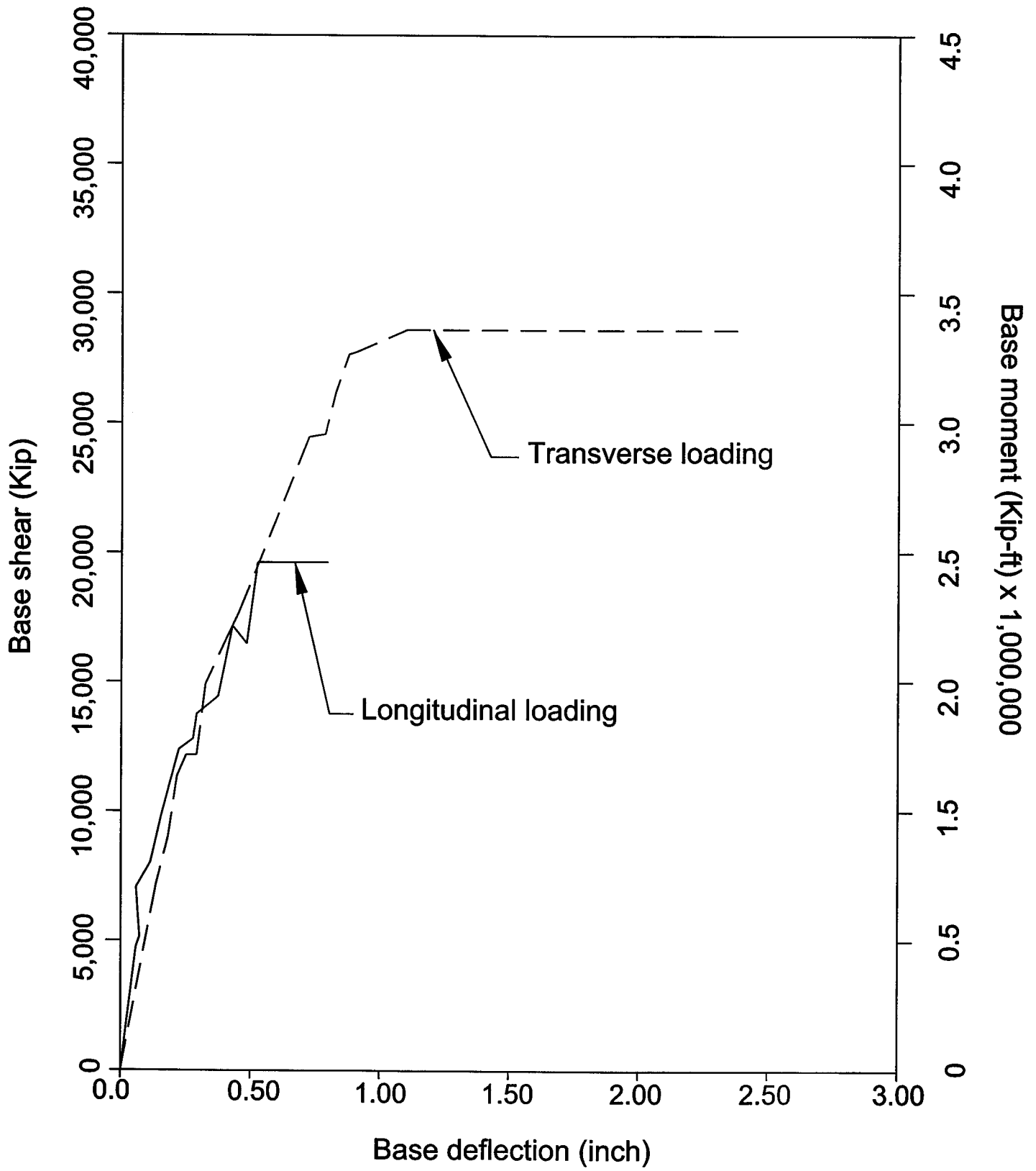
Figure 3-6 Lateral force-deflection relationship of a gravity caisson for pushover analysis.
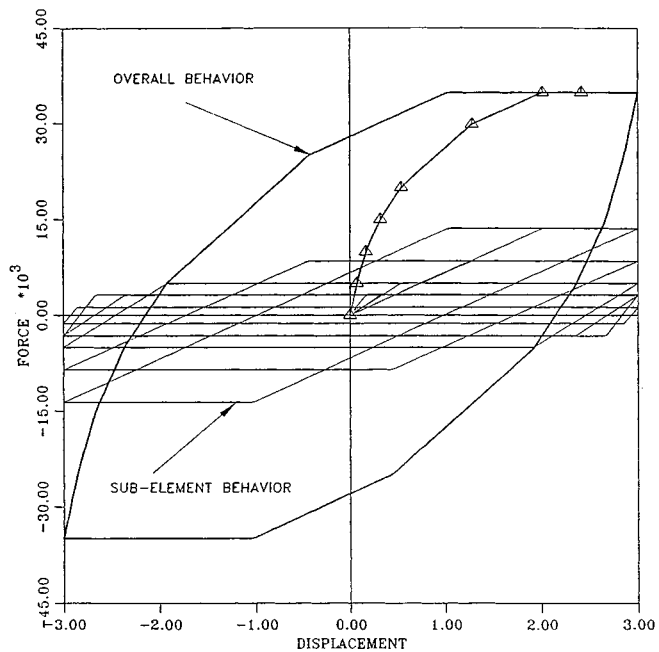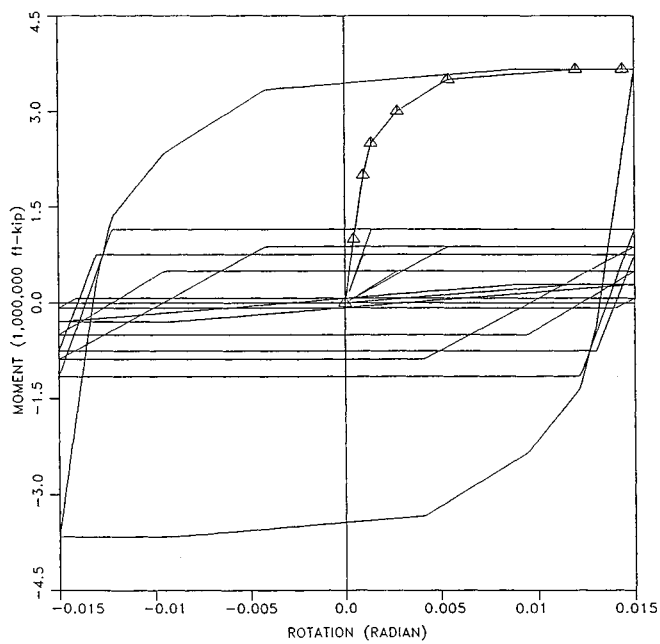
GROUND ACCELERATION
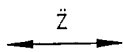
TRANSLATIONAL EQUILIBRIUM:

$$M\ddot{Y} + MH\ddot{\Theta} + C_x\dot{Y} + K_x Y = -M\ddot{Z}$$

MOMENT EQUILIBRIUM:

$$I\ddot{\Theta} + MH\ddot{Y} + MH^2\ddot{\Theta} + C_\theta\dot{\Theta} + K_\theta\Theta = -MH\ddot{Z}$$
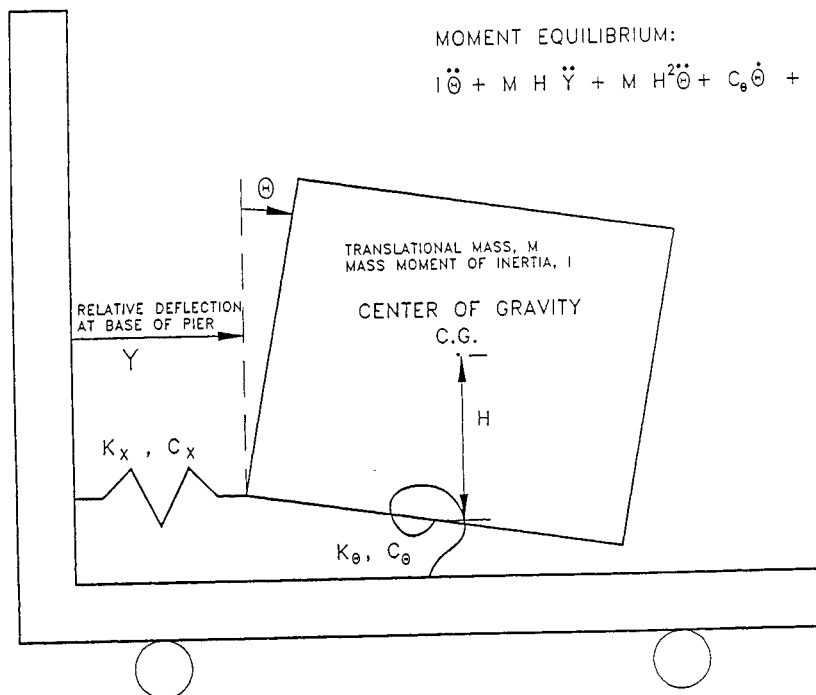
Figure 3-7   2 Degree of freedom lumped mass model for caisson response.

foundation moment-rotation and lateral force-deflection characteristics as obtained from pushover analyses are simulated by the nonlinear hysteretic rotational and translational springs. The time histories of the design earthquake are shown in Figure 3.8 and the solutions of the lumped mass model are shown in Figure 3.9 in the longitudinal shaking direction.

3.5   Large Diameter Drilled Shaft

Lateral loads on piles are resisted by the surrounding soil whose behavior is characterized by lateral soil resistance per unit length of pile, p, as a function of lateral displacement, y. The p-y relation is generally developed on the basis of a semi-empirical curve, which reflects nonlinear resistance of the local soil surrounding the pile at specified depth.

A number of p-y models have been proposed by different authors for different soil conditions. The two most commonly used p-y models are those proposed by Matlock (1970) for soft clay and by Reese et al. (1974) for sand. These models are essentially semi-empirical and have been developed on a basis of a limited number of full-scale lateral load tests on piles of smaller diameters ranging from 12 to 16 inches. To extrapolate the p-y criteria to conditions that are different from the one from which the p-y models were developed requires some judgement and consideration.

Matlock's and Reese's nonlinear p-y approaches can be regarded as an extension of the widely used linear subgrade modulus approach by Terzaghi (1955). Terzaghi's linear subgrade modulus represents the soil stiffness corresponding to a normal working load level. If the Matlock's clay and Reese's sand p-y criteria are used in load deflection analyses for typical piles to develop a nonlinear load-deflection curve, they typically give solutions comparable to results from Terzaghi's linear subgrade modulus approach at 0.5 to 2 inches of pile head deflection.

Based on some field test results, there are indications that stiffness and ultimate lateral load carrying capacity of a large diameter drilled shaft are larger than the values estimated using the conventional p-y criteria as reported by Stevens and Audibert (1979). Pender (1993) suggests that subgrade modulus used in p-y formulation would increase linearly with pile diameter. Using nonlinear three dimensional finite element analyses, Lam and Law (1994) demonstrated that the increases in stiffness and lateral capacity of large diameter shafts are attributed to additional soil resistance mobilized due to pile rotation.

In order to model drilled shaft behavior in a global bridge system for seismic response studies, the soil-pile stiffness can be represented in several ways. The most common methods are

- Beam supported on nonlinear p-y springs
- Coupled foundation stiffness matrix
- Equivalent cantilever model

48
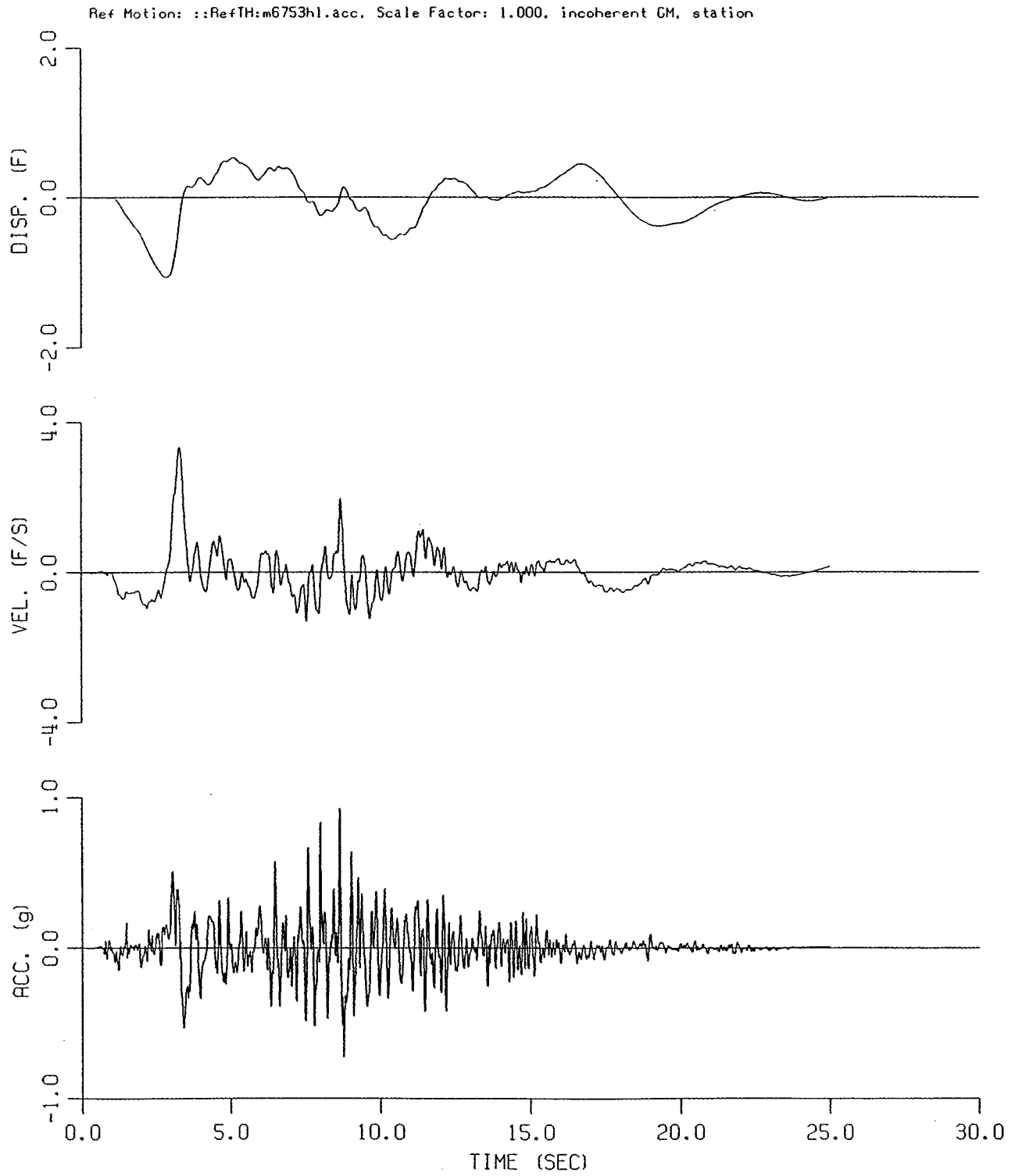
Figure 3-8   Input time histories used in rocking analysis for gravity caisson.
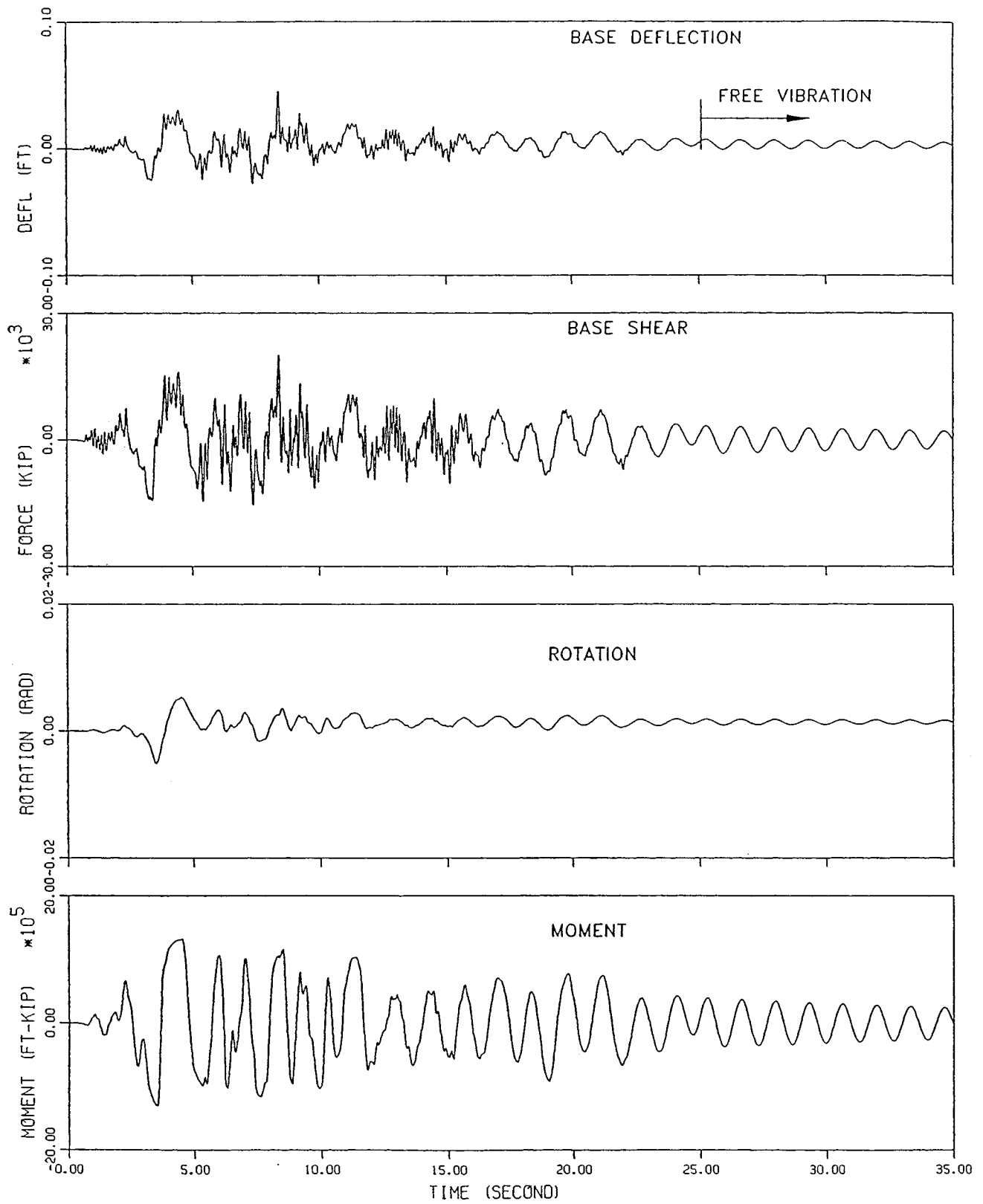
Figure 3-9 Solutions for lumped mass response analysis.

50

- Uncoupled base spring model

<u>Beam supported on nonlinear p-y springs</u>: As the number of large diameter drilled shafts for a typical bridge is very limited, the entire drilled shaft can be included in the bridge model by using a structural beam supported on nonlinear soil springs without much difficulty. This model, shown in Figure 3.10, offers a complete feature of soil-structure interaction and such nonlinear behaviors as plastic hinging of the shaft and soil yielding can be properly accounted in the analysis. When hysteretic behavior of the p-y curve is fully implemented, energy dissipation associated with material damping is automatically included in the model. The radiation damping component can be separately modeled by attaching additional viscous dashpots.

<u>Coupled foundation stiffness matrix</u>: Figure 3.11 illustrates a 6x6 coupled stiffness matrix representing the stiffness of a single shaft at the ground line. This stiffness matrix can be estimated to match the soil-pile behavior for all six degrees of freedom (e.g., Lam & Martin, 1986). The common form of the stiffness matrix in the local pile coordinate system is given by the following expression:

$$[K] = \begin{bmatrix} k_x & 0 & 0 & 0 & 0 & 0 \\ 0 & k_y & 0 & 0 & 0 & k_{y\theta z} \\ 0 & 0 & k_z & 0 & -k_{z\theta y} & 0 \\ 0 & 0 & 0 & k_{\theta x} & 0 & 0 \\ 0 & 0 & -k_{y\theta z} & 0 & k_{\theta y} & 0 \\ 0 & k_{z\theta y} & 0 & 0 & 0 & k_{\theta z} \end{bmatrix} \tag{3.8}$$

in which k_x, k_y, k_z, $k_{\theta x}$, $k_{\theta y}$ and $k_{\theta z}$ are stiffness coefficients corresponding to translational and rotational degrees of freedom associated with the local x (along the pile axis), y and z axes, respectively. The x-coordinate is taken as the axis along the pile. The off-diagonal terms represent coupling between two degrees of freedom for two orthogonal axes perpendicular to the pile axis. For development of a 6x6 coupled stiffness matrix, linearization of p-y curves is needed or Terzaghi's linear subgrade modulus can be used.

<u>Equivalent cantilever model</u>: In the equivalent cantilever method, the drilled shaft foundation is replaced by a cantilever beam that has equivalent stiffness properties to that of the drilled shaft with the surrounding soil. The model is schematically depicted in Figure 3.12. It is possible to calculate equivalent length of the cantilever beam by equating the terms of the pile head stiffness matrix. The corresponding stiffness matrix of a cantilever beam of length L_c and flexural stiffness EI_c is given by

Figure 3-10 A complete total system for a drilled shaft.

Figure 3-11 Coupled stiffness matrix model for a drilled shaft.

Superstructure

Ground Line

Drilled shaft

Superstructure

E I

K_{6x6}

6x6 stiffness matrix
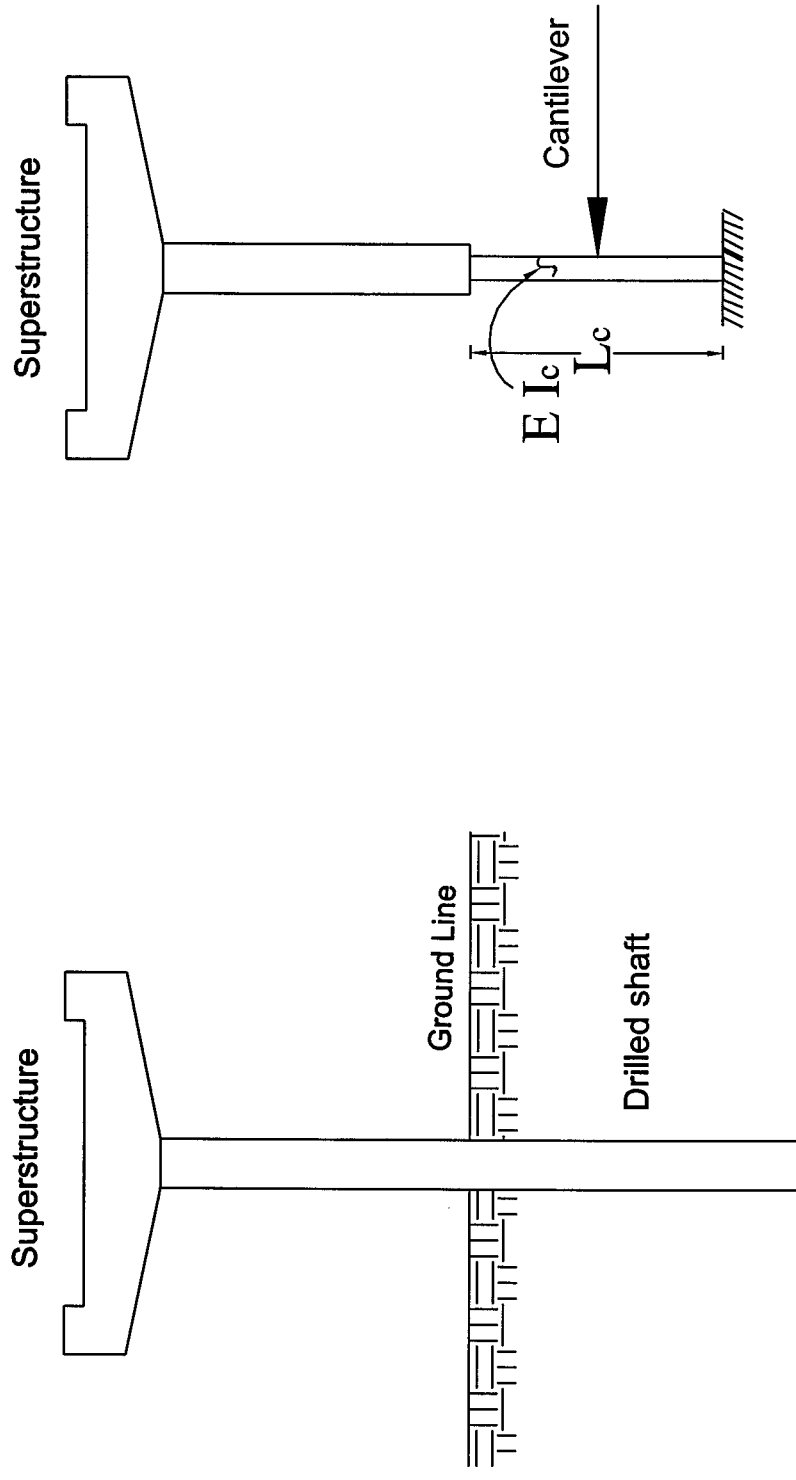
Figure 3-12 Equivalent cantilever model for a drilled shaft.

54

$$K_{cantilever} = EI_c \begin{bmatrix} \dfrac{12}{L_c^3} & \dfrac{6}{L_c^2} \\ \\ \dfrac{6}{L_c^2} & \dfrac{4}{L_c} \end{bmatrix} \tag{3.9}$$

The stiffness matrix of the soil pile system is approximated by the equivalent cantilever model using the appropriate value of EI_c and equivalent cantilever length $L_c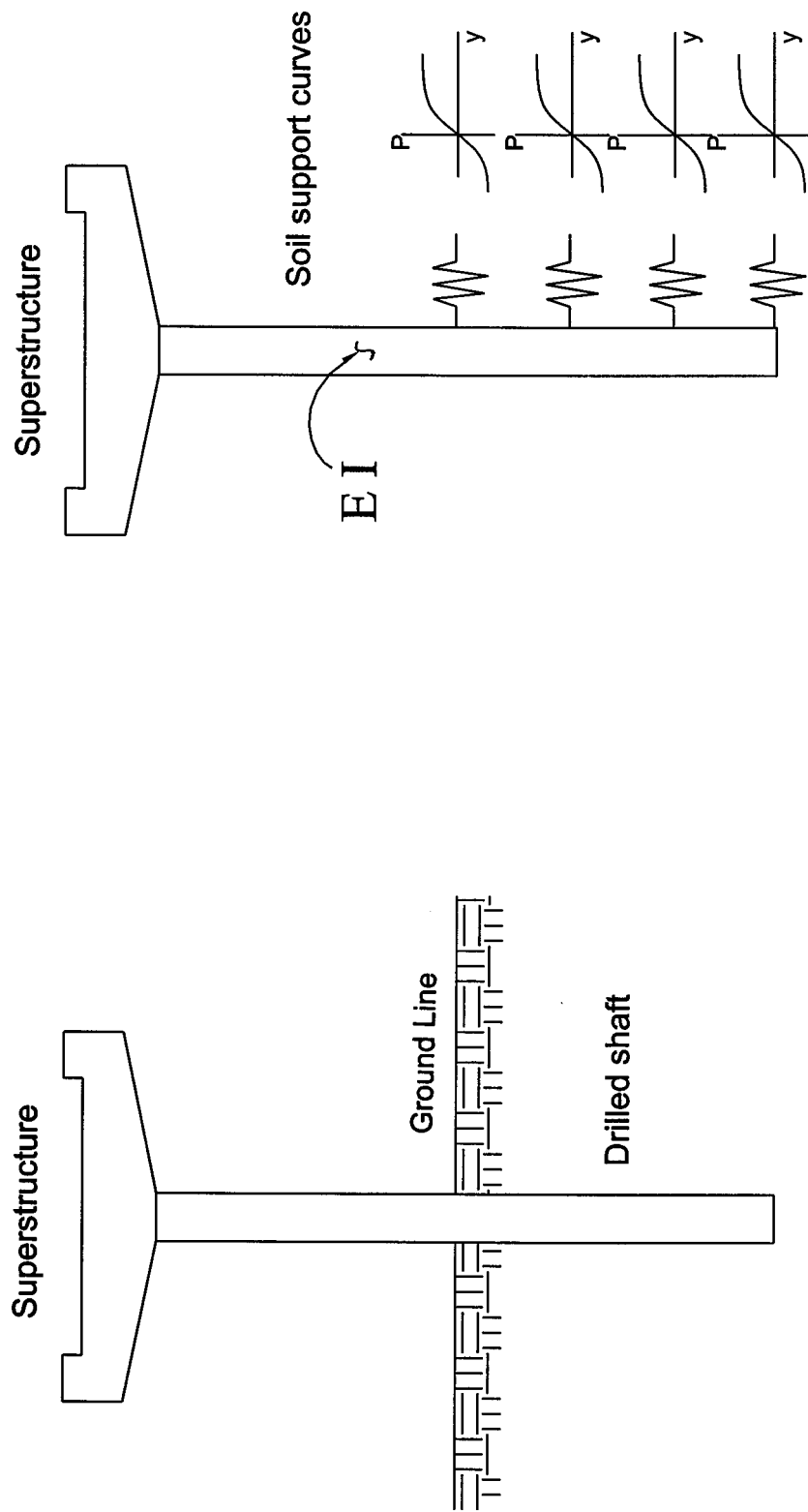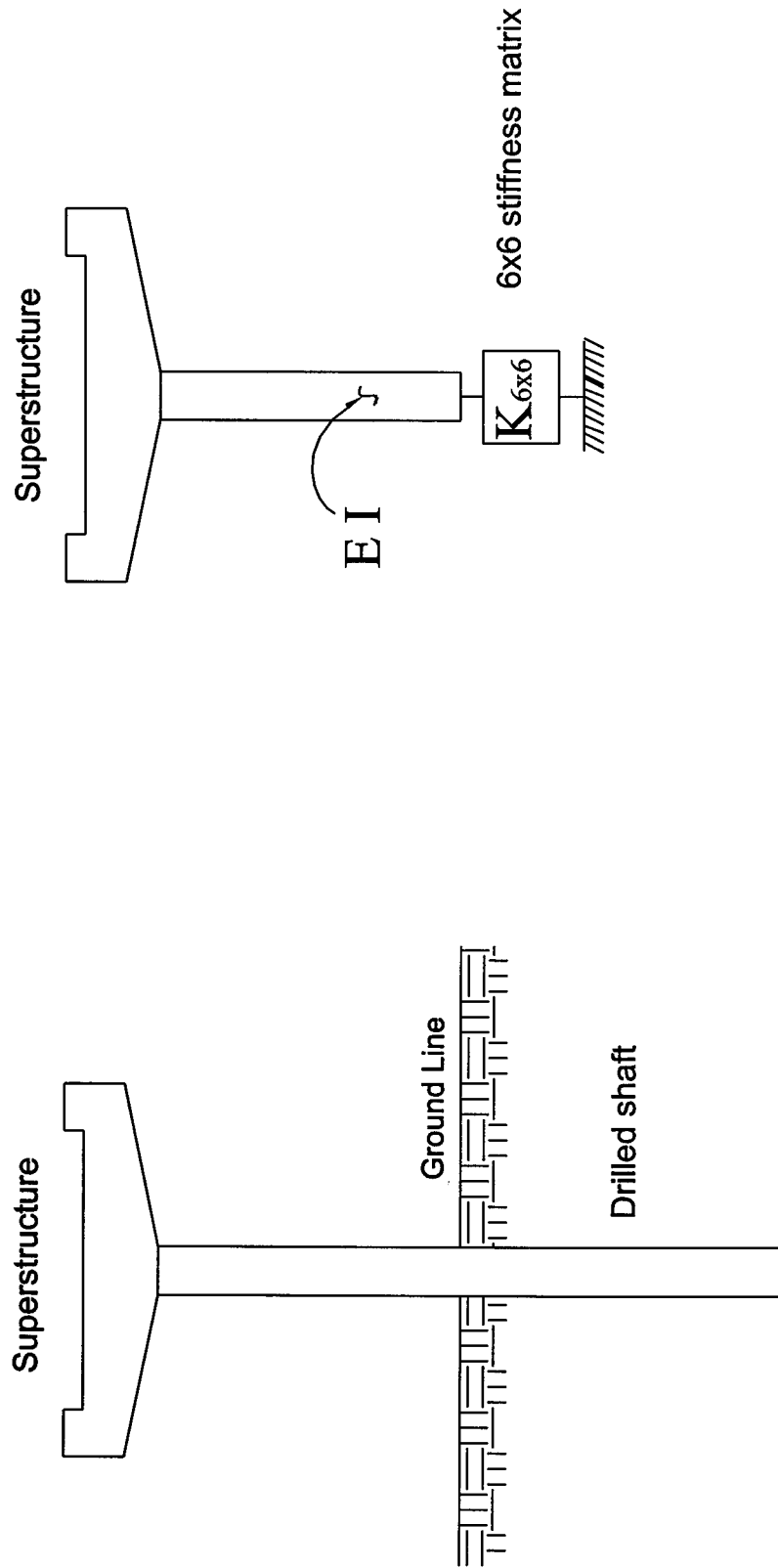$. It is obvious that only two cantilever model parameters are not sufficient to satisfy all three stiffness coefficients (two diagonal stiffness and one cross-coupling stiffness coefficients) in the above mentioned equation. A decision needs to be made to choose two significant terms in the stiffness matrix for matching of the equivalent cantilever model.

<u>Uncoupled base spring model</u>: In this particular method, the drilled shaft is replaced by two springs which can be nonlinear, one representing the translational and the other representing the rotational stiffness, as shown in Figure 3.13. The cross-coupling between lateral and rotational movement is not maintained.

3.6   Pile Group

Pile designs based on p-y curves or the Terzaghi's subgrade modulus approach have been widely adopted by the industry. Studies have shown that Matlock and Reese p-y criteria give reasonable pile design solutions, and their procedures have been recommended for design in the American Petroleum Institute (API) code. However, the p-y criteria were originally conceived for design against storm wave loading conditions based on observation of monotonic static and cyclic pile load test data. The monotonic static loading data formed the static p-y criteria and are still applicable for developing the backbone p-y curves for seismic design application. Therefore, Matlock and Reese's static p-y curves can serve as the benchmark for design to represent the initial monotonic loading path for typical small diameter driven isolated piles.

If a complete total system of a bridge is modeled for seismic response study, individual piles and p-y curves can be included in the analytical model. For a large pile group, group effects become important. Although the group effects have been a popular research topic within the geotechnical community, currently there is no common consensus on the design approach to incorporate group effects. Full scale and model tests by a number of authors show that in general, the lateral capacity of a pile in a pile group is less than that of a single isolated pile due to so-called group efficiency. The reduction is more pronounced as the pile spacing is reduced. Other important factors that affect the efficiency and lateral stiffness of the pile are the type and strength of soil, number of pile, and type and level of loading.

In the past, the analysis of group effects were based mostly on elastic halfspace theory due to the absence of costly full-scale pile experiments. In recent years, a number of major studies yielded some high quality experimental data from full-scale or centrifuge

Figure 3-13 Uncoupled bas spring model for a drilled shaft.

56

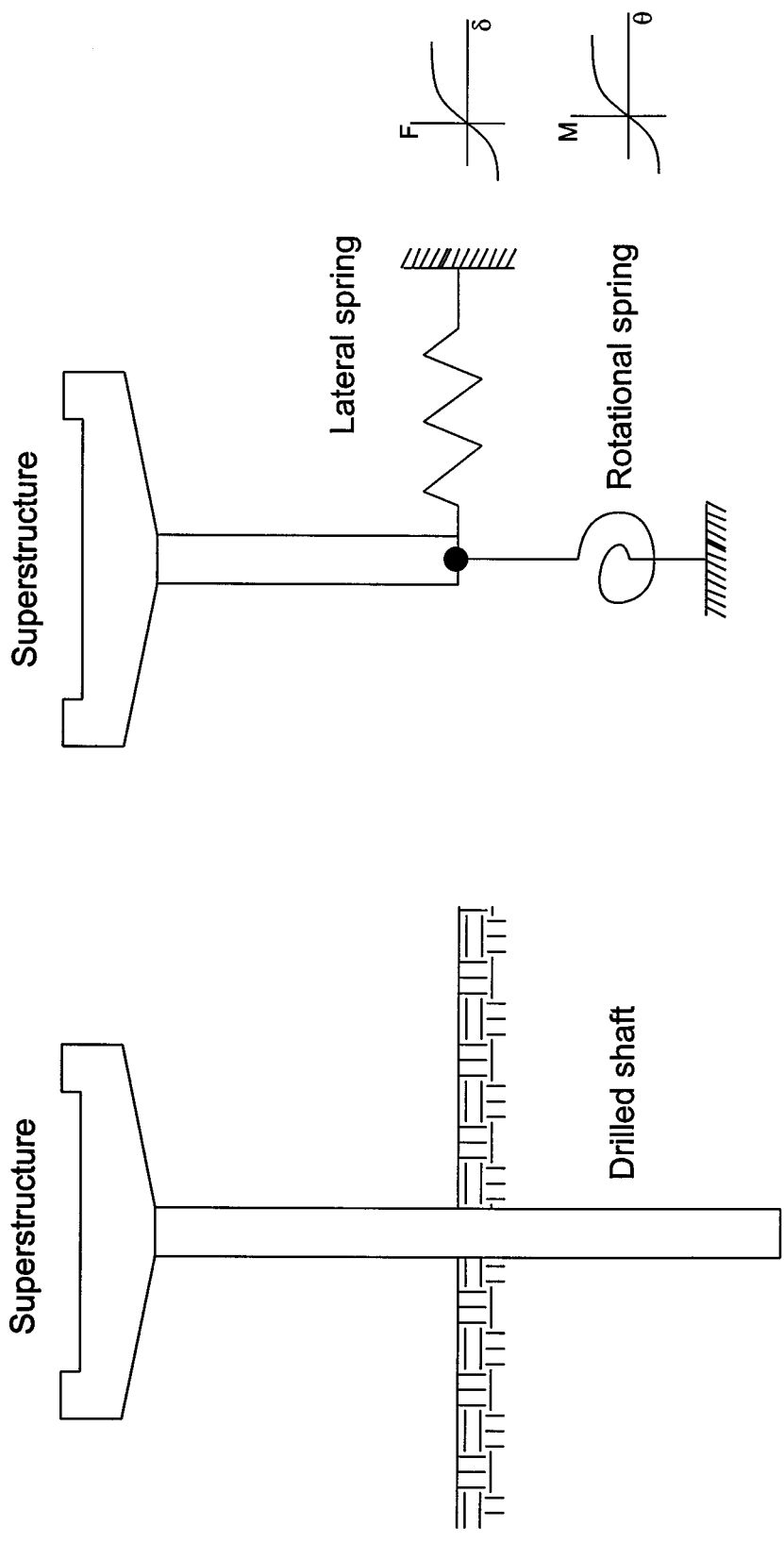model tests (e.g., Ashford, et al., 1999, Brown, et al., 1987, McVay, et al., 1995). In addition to group effect, gapping and potential cyclic degradation have been considered in the recent studies. It has been shown that a concept based on p-multiplier applied on the standard static loading p-y curves works reasonably well to account for pile group and cyclic degradation effects (e.g., Bogard and Matlock, 1983; Brown, et al., 1987; Brown, et al., 1988) . Most of the full-scale pile load tests have been conducted on relatively small pile groups involving 9 or 16 piles. Foundations for major bridges often utilize extremely large piers supported by several hundred piles where the horizontal dimension of the footing can be easily a couple of hundred feet. A full-scale experiment for such a huge pile group would be impossible and there is no recourse but to rely on numerical prediction for these problems. A concept based on periodic boundary condition has been recently used to solve the lateral pile response for an infinite repeating pile pattern (Lam et al., 1998). The study was implemented with three-dimensional finite element method to examine the group effects on p-y curves for a huge pile group consisting of 390 piles. The results indicate that both p-multiplier and y-multiplier can be used to scale the p-y curves of the single isolated pile in order to account for the group effect. The values of the p-multiplier and y-multiplier are dependent on the spacing of the piles.

In terms of foundation stiffness, it can be observed that uncertainties in p-y curves may not be a insignificant problem compared to other sources of uncertainty, including the pile head fixity, the choice of bending stiffness of the pile and the loading conditions.

When the substructuring technique is used to simplify the foundation in the global bridge model, the pile group can be represented by a linear 6x6 stiffness matrix, and the approach has been described by Lam and Martin (1986). Since the p-y curves are nonlinear, the first step towards developing the foundation stiffness matrix involves linearization of the p-y curves by performing lateral pushover analysis of the single pile to a representative displacement level expected during the earthquake. Once the p-y curves are linearized on the basis of lateral pushover analysis, the problem become beam on elastic springs, and the method of substructuring was applied to obtain the condensed stiffness matrix. The pile-head stiffness matrix of a single pile, computed using static condensation, has the following form

$$[K_{single}] = \begin{bmatrix} k_x & 0 & 0 & 0 & 0 & 0 \\ 0 & k_y & 0 & 0 & 0 & k_{y\theta z} \\ 0 & 0 & k_z & 0 & -k_{z\theta y} & 0 \\ 0 & 0 & 0 & k_{\theta x} & 0 & 0 \\ 0 & 0 & -k_{y\theta z} & 0 & k_{\theta y} & 0 \\ 0 & k_{z\theta y} & 0 & 0 & 0 & k_{\theta z} \end{bmatrix} \qquad (3.10)$$

The coordinate system for an individual pile is shown in Figure 3.14 in relationship to the global pile group coordinate system, and k_x, k_y, k_z, $k_{\theta x}$, $k_{\theta y}$ and $k_{\theta z}$ are stiffness coefficients of translational and rotational degrees of freedom in the local pile axis. The global stiffness of the pile group is computed by the summation of individual pile-head
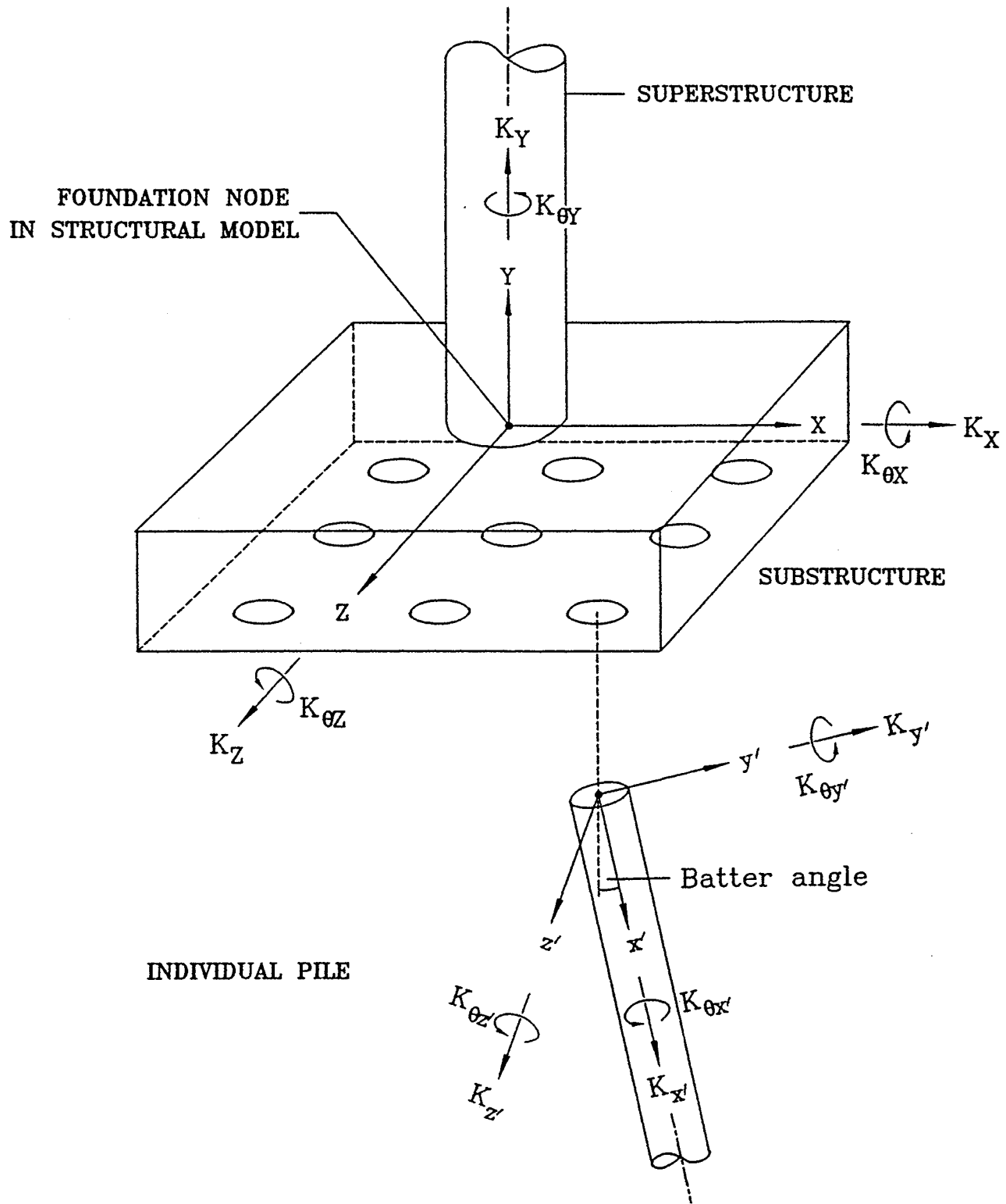
Figure 3-14 Coordinate systems for individual pile vs. global pile group.

58

stiffness, invoking static equilibrium. The procedure, which can be applied to any number of piles and geometric pile group configuration, assumes that the pile cap is infinitely rigid.

For a vertical pile group, the form of pile group stiffness matrix will be identical to the individual single pile. The pile group stiffness for the translational displacement terms (two horizontal terms and one vertical term) and the cross-coupling terms can be obtained by merely multiplying the corresponding stiffness components of the individual pile by the number of piles. However, the rotational stiffness terms (two rocking terms and one torsion term) require consideration of an additional component. In addition to individual pile-head bending moments at each pile head, a unit rotation at the pile cap will introduce translational displacements and corresponding forces at each pile head. These pile-head forces will work together among the piles and will result in an additional moment reaction on the overall pile group. The following equation can be used to develop the rotational stiffness terms of a vertical pile group (Lam, et al., 1991):

$$K_\theta = \sum_{piles} k_\theta + \sum_{piles} k_\delta R^2 \tag{3.11}$$

where K_θ and k_θ are rotational stiffness of the pile group and an individual pile, respectively, k_δ is the appropriate translational axial stiffness coefficient of an individual pile, and R is the distance between the individual pile and the center of the pile group.

For a general case, the stiffness matrix is a full matrix representing coupling among various displacement terms. A pile group at Richmond – San Rafael Bridge is an example of full stiffness matrix due to a large number of battered HP piles arranged in circular patterns (EMI, 1999). The configuration of the pile group is shown in Figures 3.15 and 3.16 showing a total of 308 piles. The directions of strong axis for these HP piles are oriented tangential to the circumference of circular pattern. The stiffness matrix of this pile group is presented in Table 3.2.

Table 3.2 Pile Group Stiffness Matrix of at Richmond – San Rafael Bridge

Translation			Rotation		
Dis-X	Dis-Y	Dis-Z	Dis-X	Dis-Y	Dis-Z
1.97E+06	-1.89E+00	-3.82E+00	2.30E+03	1.29E+08	-2.83E+04
-1.89E+00	1.99E+06	-7.61E-01	-1.87E+08	7.09E+01	-2.75E+03
-3.82E+00	-7.61E-01	2.19E+07	-7.79E+01	3.92E+02	-2.37E+03
2.30E+03	-1.87E+08	-7.79E-01	4.80E+12	-2.43E+05	1.28E+06
1.29E+08	7.09E+01	3.92E+02	-2.43E+05	1.31E+12	2.49E+06
-2.83E+04	-2.75E+03	-2.37E+03	1.28E+06	2.49E+06	5.91E+11

Note: the coordinate system used in this table is shown in Figure 3-16 where x- and y-axes are horizontal directions and z-axis is the vertical direction. Units: lb, in, rad
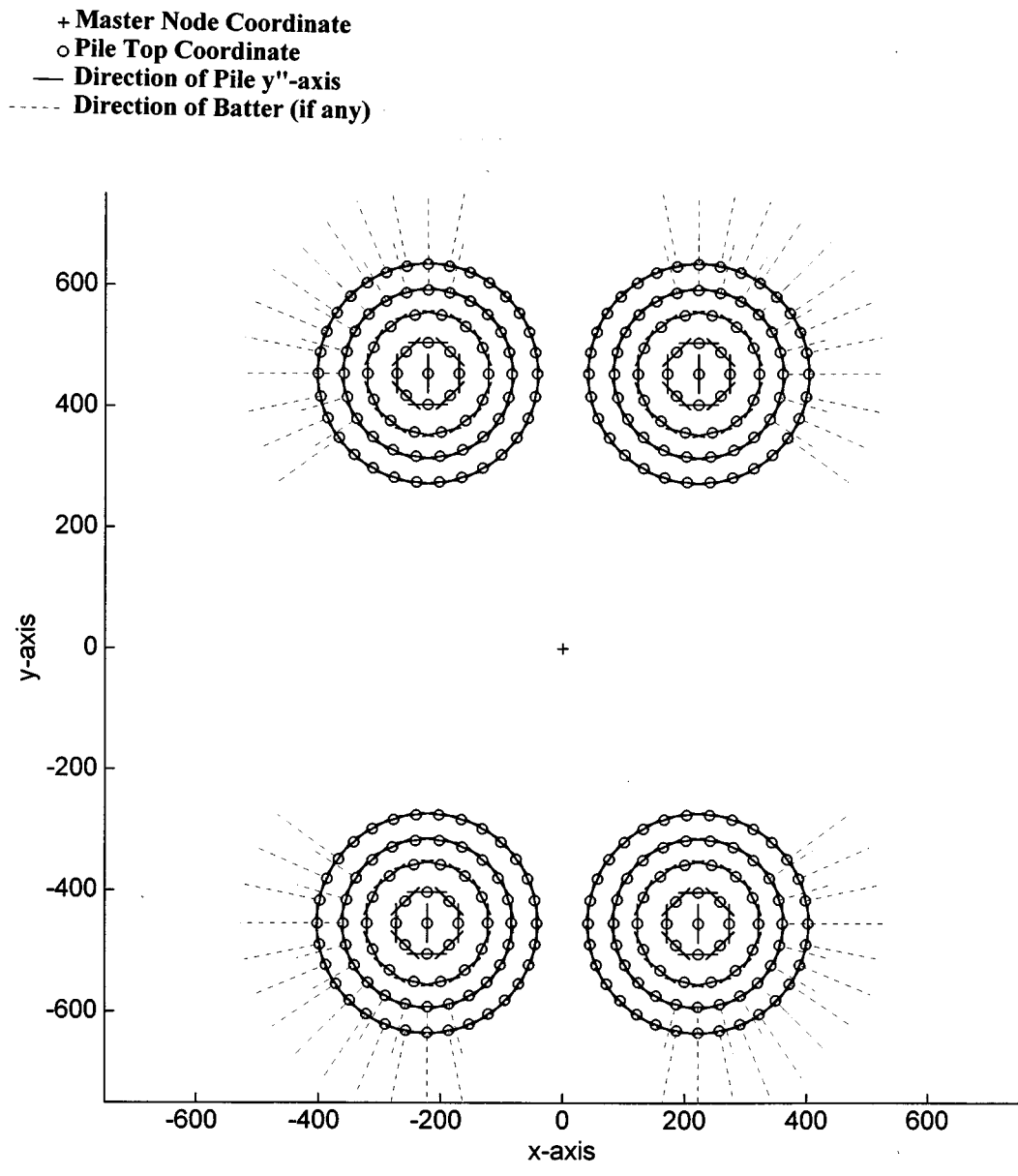
Figure 3-15   Plan view of pile group layout at Richmond-San Rafael Bridge.
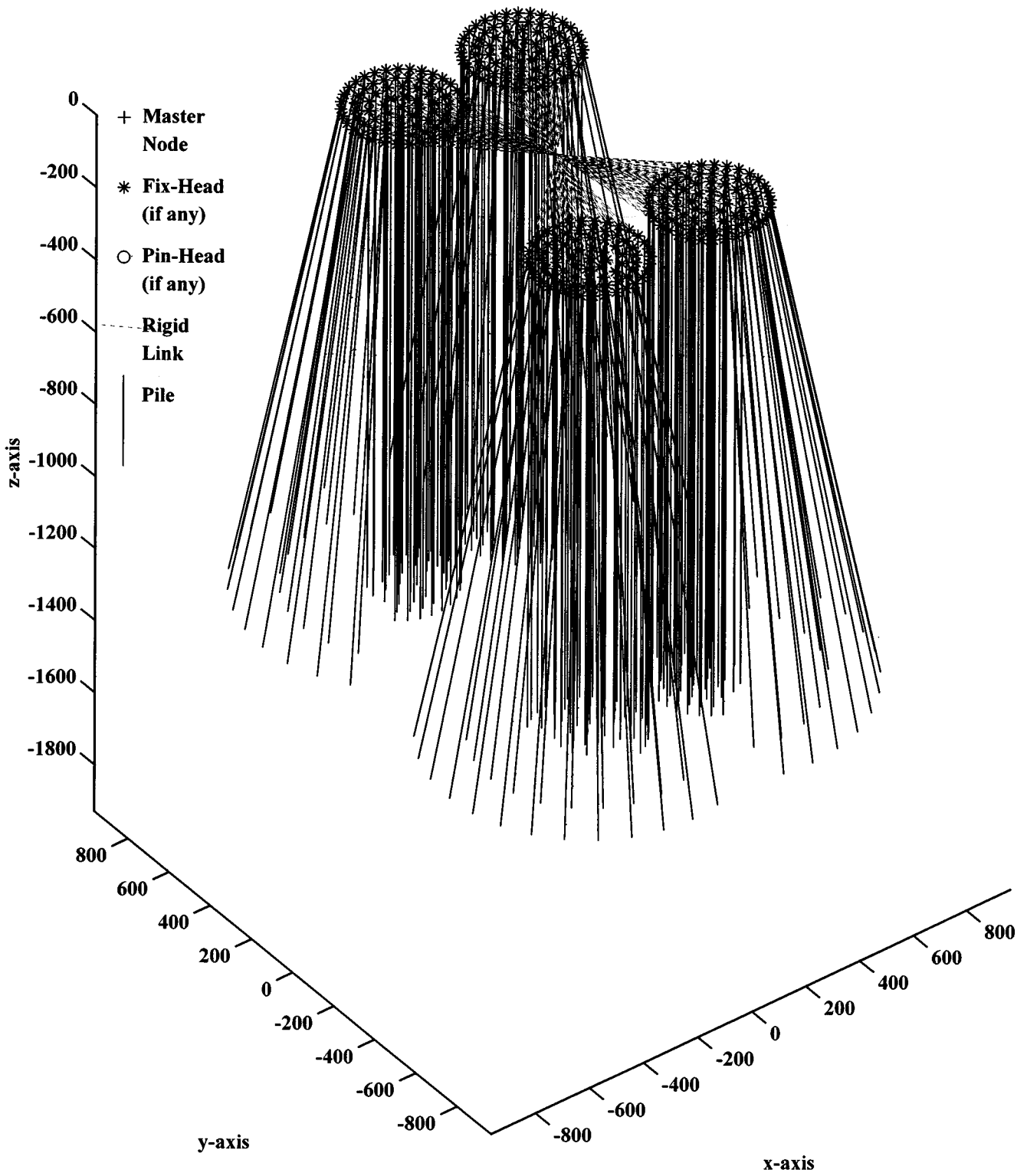
Figure 3-16 Isoparametric view of the pile group model at Richmond-San Rafael Bridge.

3.7 Foundation Damping

The conventional p-y curves developed for piles would have non-linear and inelastic behavior. When these p-y curves are implemented properly allowing for hysteretic behavior, the strain-dependent energy dissipation mechanism is automatically simulated, accounting for material damping in the pile foundation.

For additional damping associated with radiation of energy through the half space, elasto-dynamic solutions has been recommended by Gazetas et al. (1992). The classical method of solving soil-pile interaction problem involving radiation damping has been based on an elasto-dynamic approach in frequency domain (Mylonakis, et. al., 1997 and Gazetas et. al., 1992). Because of the linear superposition principle in the frequency domain, soil stiffness is usually expressed as Winkler type of linear spring which would have a unit of FL^{-2} (soil resistance per unit pile length per unit pile deflection). The radiation viscous dashpot parameter per linear length of the pile can be derived from shear wave velocity using the following equation

$$c_x = 1.6 \rho_s v_s \left(\frac{\omega d}{v_s} \right)^{-\frac{1}{4}} \qquad (3.12)$$

where c_x is the damping coefficient, ω is the angular frequency, d is the pile diameter, ρ_s is mass density and v_s is shear wave velocity. This radiation damping parameter would be frequency dependent.

One needs to be careful in mixing the conventional nonlinear p-y curves with the viscous coefficient to account for radiation damping that is based on elasto-dynamic approach. Recent centrifuge pile load tests conducted at the University of California at Davis to simulate transient earthquake loading indicated that the conventional API type of p-y curves yielded reasonable soil-pile interaction stiffness especially for clayey soils (e.g., Boulanger et al., 1999). However, viscous dashpots based on elasto-dynamic approach using small strain shear wave velocity arranged in parallel with the p-y springs resulted in exaggerated radiation damping solutions (e.g., Wang et al., 1998). Although the most common way to implement radiation dashpot is in a parallel manner for soil-pile interaction analysis, researchers at the University of California, Davis recommend that the dashpot be arranged in series with the p-y springs (see Figure 3.17 for two different arrangement of dashpots). This kind of arrangement ensure that forces acting at the viscous dashpot would be transmitted through the p-y springs; thereby reducing the effect of the viscous damper.

As in the case of pile foundation, damping for a large caisson or spread footing arises from two sources: material damping and radiation damping. The classical elasto-dynamic theory involving radiation damping makes an explicit assumption that footing bottom is in full contact with the underlying soil. When the viscous damping coefficient is derived
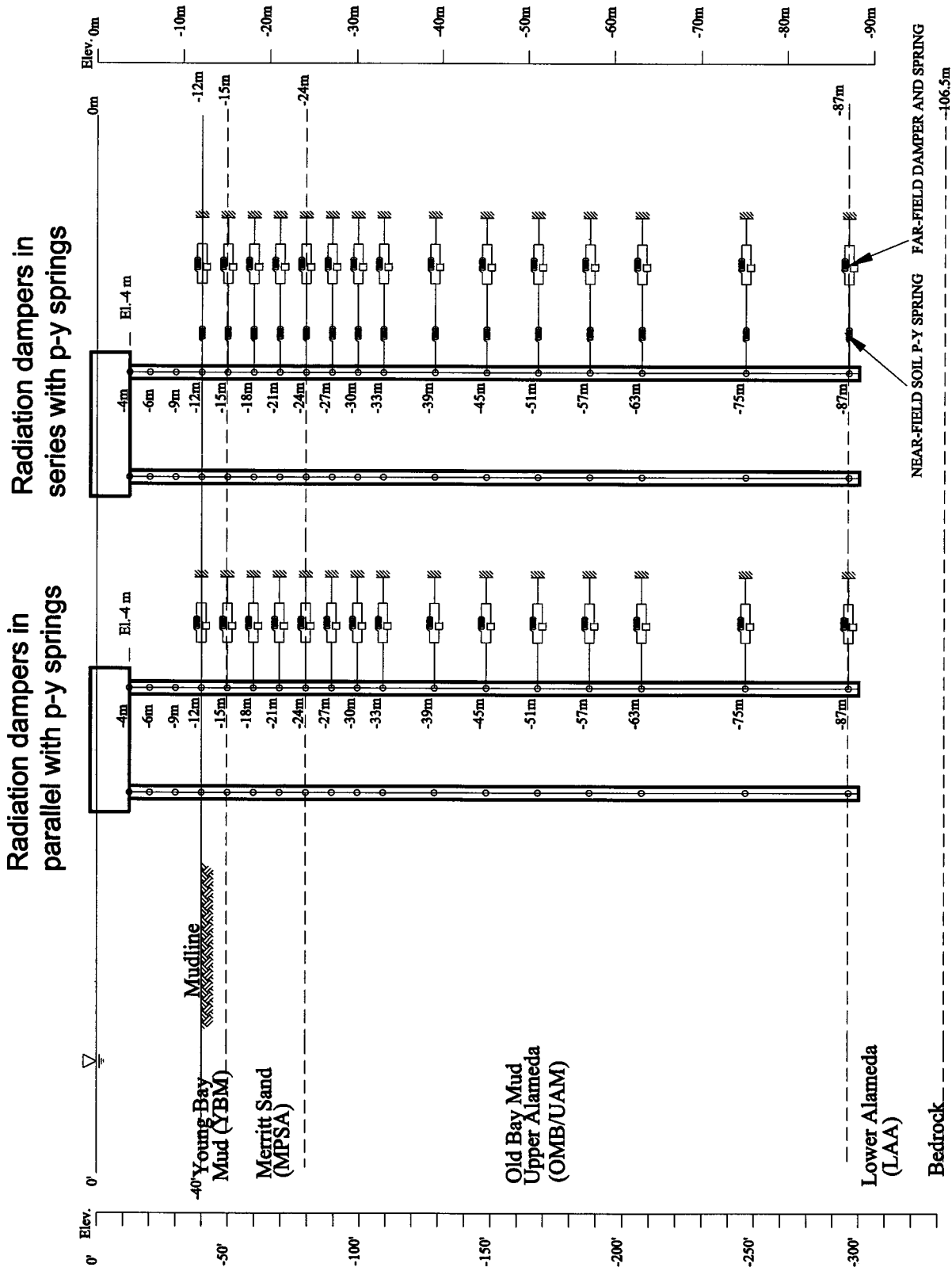
Figure 3-17 Dashpots representing radiation damping arranged in parallel and in series with the near-field nonlinear p-y springs.

63

from the linear theory, and is lumped as a damper at the center of the foundation, the model would not account for potential separation of the footing from the underlying soil. For this reason, it is generally known that the damping coefficient determined from elasto-dynamic solutions is overestimated.

To overcome the problem associated with base separation in modeling radiation damping, soil springs and dashpots can be distributed over the footprint of the foundation. The distributed vertical soil springs are nonlinear. They are calibrated to model proper foundation stiffness such as nonlinear moment-rotation characteristics to capture soil yielding and gapping phenomenon while the distributed dashpots (instead of a lumped damper) are arranged in series with the vertical soil springs to model radiation damping, as shown in Figure 3.18. The dashpots in this kind of arrangement would properly represent far-field behavior and the nonlinear soil springs represent near-field behavior. Since the nonlinear vertical soil springs would have a tension cut-off branch to simulate gapping, the dashpots that are in series in the springs would not provide any damping force as soon as base separation occurs.
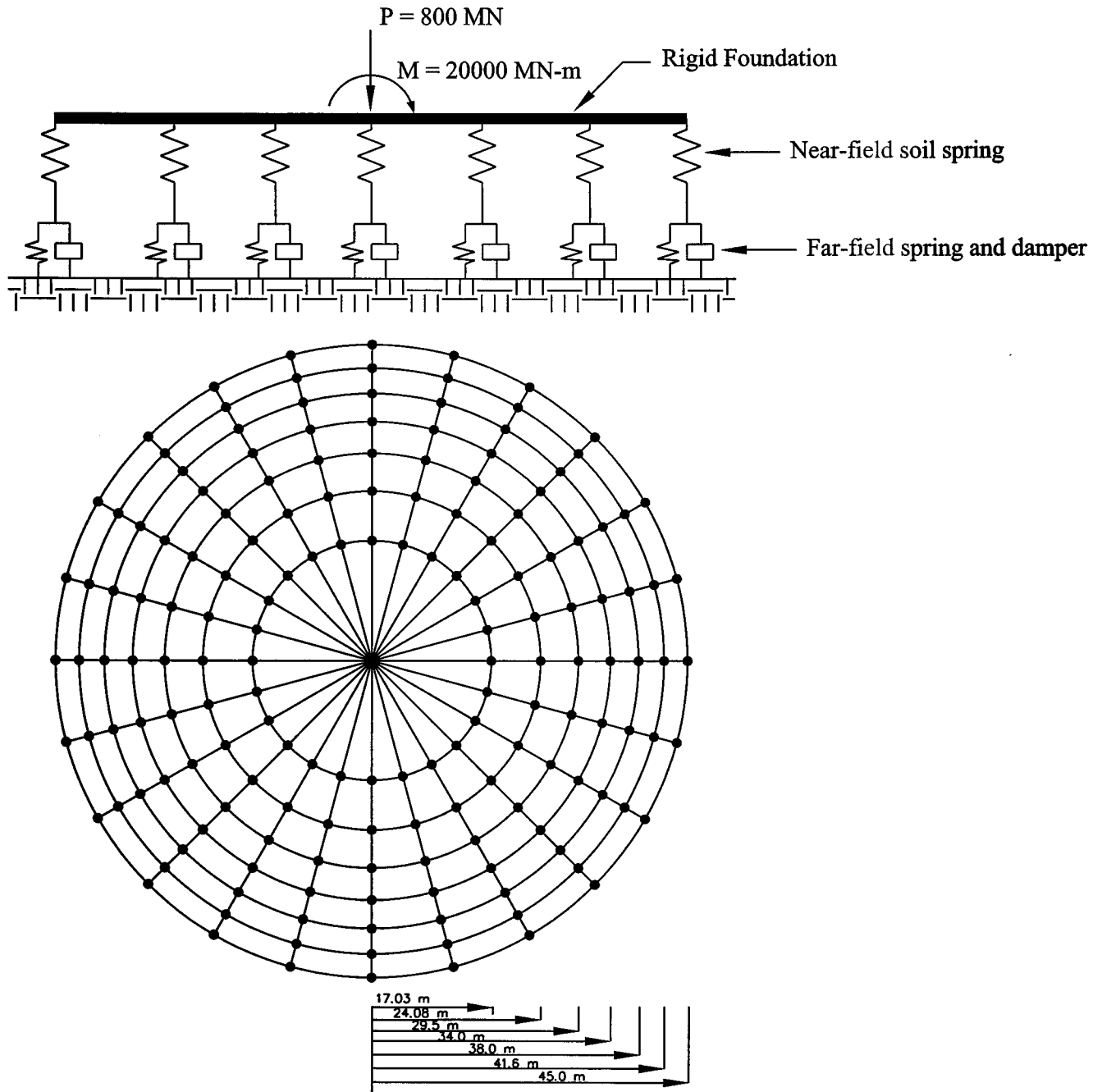
Figure 3-18 Dashpots in series with vertical springs for caisson/ spread footing.

SECTION 4
SUBSTRUCTURE METHOD USING KINEMATIC INTERACTION

4.1 Concept for Substructuring

Soil-structure interaction should be included when dealing with seismic response of bridges especially those located in poor site conditions. To evaluate dynamic response of a structure on deep foundation, it would be most desirable to create a complete analytical model of the total system including the superstructure, pile cap, and the soil-pile (foundation) system along the entire embedded pile length in a time history response analysis. Such model would account for depth varying nonlinear soil springs (p-y curves), depth varying ground motion, and inertial forces of the foundation system. However, such a model would be cumbersome and the analysis would involve a large number of degrees of freedom.

The solution for keeping model size small and reducing the number of degrees of freedom is to use the method of substructuring. The total structure can be divided into two substructures: a substructure for the foundation and a substructure for the superstructure, with a convenient interface between the two at the pile cap level. The procedure involves two steps: the first step is conducted in the foundation substructure and the second step is conducted in the bridge substructure. In the first step, the stiffness of the foundation system and the forces arising from the soil-pile interaction can be condensed at the pile cap level without prior knowledge of superstructure. Then the foundation stiffness and force vector can be used in the second step to analyze the seismic response of the bridge superstructure. Also, pile foundations are supported on multiple soil layers (soil springs) that are excited by depth-varying free-field motions of different characteristics. As explained in the next section, kinematic interaction analysis provides a rational means to develop appropriate response spectrum that retain the characteristics of the depth varying motion. Kinematic soil-structure interaction analyses provide (1) condensed stiffness matrix for the foundation system, (2) condensed forcing function arising from the foundation, and (3) response spectrum.

4.2 Theoretical Background

For a single-degree-of-freedom lumped mass system as shown in Figure 4.1(a), the equation of motion can be given as

$$m\ddot{x} + c\dot{x} + kx = -m\ddot{x}_g \tag{4.1}$$

where x_g is the absolute displacement of the support with respect to a fixed frame of reference, x is the relative displacement of the mass with respect to the ground, and m, c and k are mass, damping coefficient and stiffness coefficient, respectively. The response of this SDOF system to a specified ground acceleration may be solved by Duhamel
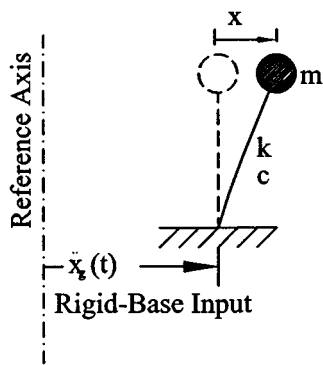
a. Single-Degree-of-Freedom System
   Rigid Base Motion
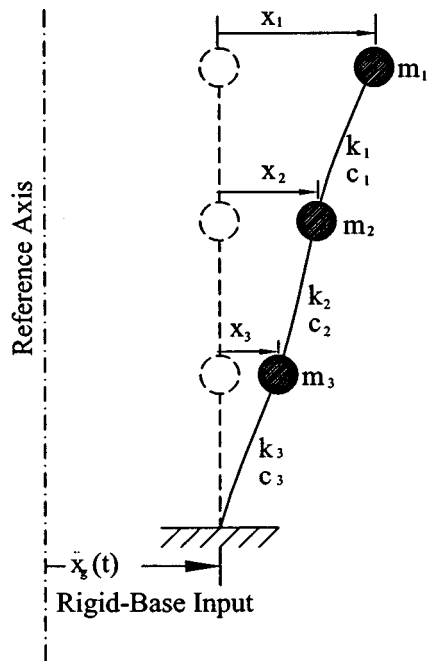
b. Multiple-Degree-of-Freedom System
   Rigid Base Motion
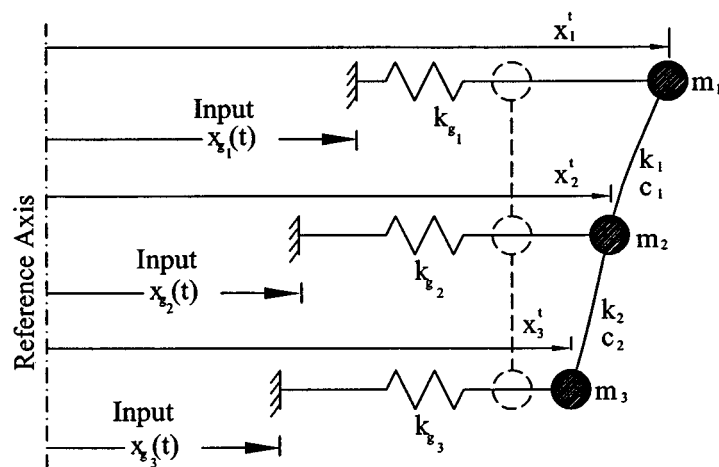
c. Multiple-Degree-of-Freedom System
   Multiple Input Motion

Figure 4-1   Lumped mass systems.

68

integral. The maximum value of the response can also be computed from the response spectrum of the ground motion (S_d), such that

$$x_{max} = \frac{1}{\omega} S_d(\zeta, T) = \frac{1}{\omega} \left[\int_0^t \ddot{x}_g(\tau) \exp[-\xi\omega(t-\tau)] \sin\omega(t-\tau)d\tau \right]_{max} \tag{4.2}$$

For the formulation of a multiple-degree-of-freedom (MDOF) lumped mass system subjected to base motion as shown in Figure 4.1(b), the solution can be obtained in a manner analogous to the SDOF system. The equations of motion for the MDOF system can be written in the matrix form as

$$[m]\{\ddot{x}\} + [c]\{\dot{x}\} + [k]\{x\} = -[m]\{1\}\ddot{x}_g(t) \tag{4.3}$$

Approximate response of the MDOF system is often obtained by carrying out the analysis for a few modes in the normal coordinate system and superimposing these responses. The transformation to normal coordinate system results in a set n uncoupled equations for n-degree of freedom system (e.g., Clough and Penzien, 1975). The equation for the nth mode can be written as

$$M_n \ddot{X}_n + C_n \dot{X}_n + K_n X_n = \lambda_n \ddot{x}_g(t) \tag{4.4}$$

where $\lambda_n = \phi_n^T [m]\{1\}$, and ϕ_n is the nth mode shape. For each individual mode of the structure, the maximum response can be obtained from the response spectrum (S_d),

$$v_{n,max} = \phi_n \frac{\lambda_n}{M_n} S_d(\xi_n, T_n) \tag{4.5}$$

where M_n, ξ_n and T_n are the modal mass, damping ratio and period of the nth mode, respectively. When a structure is supported at more than one points and has different ground motions applied at each as shown in Figure 4.1(c), the formulation of equations for this multiple-support system is expressed in terms of the total motions of the structure (including the support motion) as

$$[m]\{\ddot{x}^t\} + [c]\{\dot{x}^t\} + [k]\{x^t\} = -[k_g]\{x_g\} \tag{4.6}$$

where $[k_g]$ is the stiffness matrix expressing the force developed in the active degrees of freedom by the motions of the support, and $\{x_g(t)\}$ is a time-varying vector representing multiple input motions. Now, the question arises as to which ground motion should be used to define the response spectrum (S_d) in the earthquake-response analysis. This situation is highly relevant to pile-foundation where each pile is supported on multiple soil layers (soil springs) and the characteristics of free-field motions of those soil layers could be significantly different from each others depending on the soil conditions. The

following discussion provides a basis for developing a response spectrum for such a multiple-input multiple-degree-of-freedom system.

4.3 Development of Kinematic Motion and Condensed Stiffness Matrix

To develop a response spectrum for a multiple-input multiple-degree-of-freedom system, we consider a global structural model consisting of superstructure, pile-cap, and pile-foundation, as shown in Figure 4.2. For the purpose of discussion, we neglect the damping term and assume a lumped mass system. The equations of motion for this MDOF system due to multiple-input ground motion $\{x_g(t)\}$ are written as,

$$\begin{bmatrix} [m_s] & & \\ & [m_c] & \\ & & [m_p] \end{bmatrix} \begin{Bmatrix} \{\ddot{x}_s\} \\ \{\ddot{x}_c\} \\ \{\ddot{x}_p\} \end{Bmatrix} + \begin{bmatrix} [K_{ss}] & [K_{sc}] & \\ [K_{cs}] & [K_{cc}] & [K_{cp}] \\ & [K_{pc}] & [K_{pp}] \end{bmatrix} \begin{Bmatrix} \{x_s\} \\ \{x_c\} \\ \{x_p\} \end{Bmatrix} = \begin{Bmatrix} 0 \\ 0 \\ [K_g]\{x_g\} \end{Bmatrix} \tag{4.7}$$

where $\{x_s\}$, $\{x_c\}$ and $\{x_p\}$ are displacement of the superstructure, pile-cap, and pile degrees of freedom, respectively relative to the earth inertia reference frame (i.e, total displacements). The pile-cap would have 6 degrees of freedom (three translation, and three rotation). We assume that mass of the pile is small, and can be ignored, i.e, $[m_p]=0$. Typically this is the case because inertial forces of the piles are relatively small in relation to the more massive superstructure and therefore, neglecting the foundation inertial effect does not normally cause significant error. Then the system of equations becomes

$$\begin{bmatrix} [m_s] & & \\ & [m_c] & \\ & & [0] \end{bmatrix} \begin{Bmatrix} \{\ddot{x}_s\} \\ \{\ddot{x}_c\} \\ \{\ddot{x}_p\} \end{Bmatrix} + \begin{bmatrix} [K_{ss}] & [K_{sc}] & \\ [K_{cs}] & [K_{cc}] & [K_{cp}] \\ & [K_{pc}] & [K_{pp}] \end{bmatrix} \begin{Bmatrix} \{x_s\} \\ \{x_c\} \\ \{x_p\} \end{Bmatrix} = \begin{Bmatrix} 0 \\ 0 \\ [K_g]\{x_g\} \end{Bmatrix} \tag{4.8}$$

With the pile mass assumed to be zero, static condensation can be conducted to eliminating the pile degrees of freedom. Dynamic response analysis in time can be conducted involving only the equations involving the superstructure $\{x_s\}$ and the pile cap nodes $\{x_c\}$ from the following equation derived from the first two sets of the above equation.

$$\begin{bmatrix} [m_s] & \\ & [m_c] \end{bmatrix} \begin{Bmatrix} \{\ddot{x}_s\} \\ \{\ddot{x}_c\} \end{Bmatrix} + \begin{bmatrix} [K_{ss}] & [K_{sc}] \\ [K_{cs}] & [K] \end{bmatrix} \begin{Bmatrix} \{x_s\} \\ \{x_c\} \end{Bmatrix} = \begin{Bmatrix} 0 \\ \{f\} \end{Bmatrix} \tag{4.9}$$

where $[K]$ and $\{f\}$ in the above equation are defined as

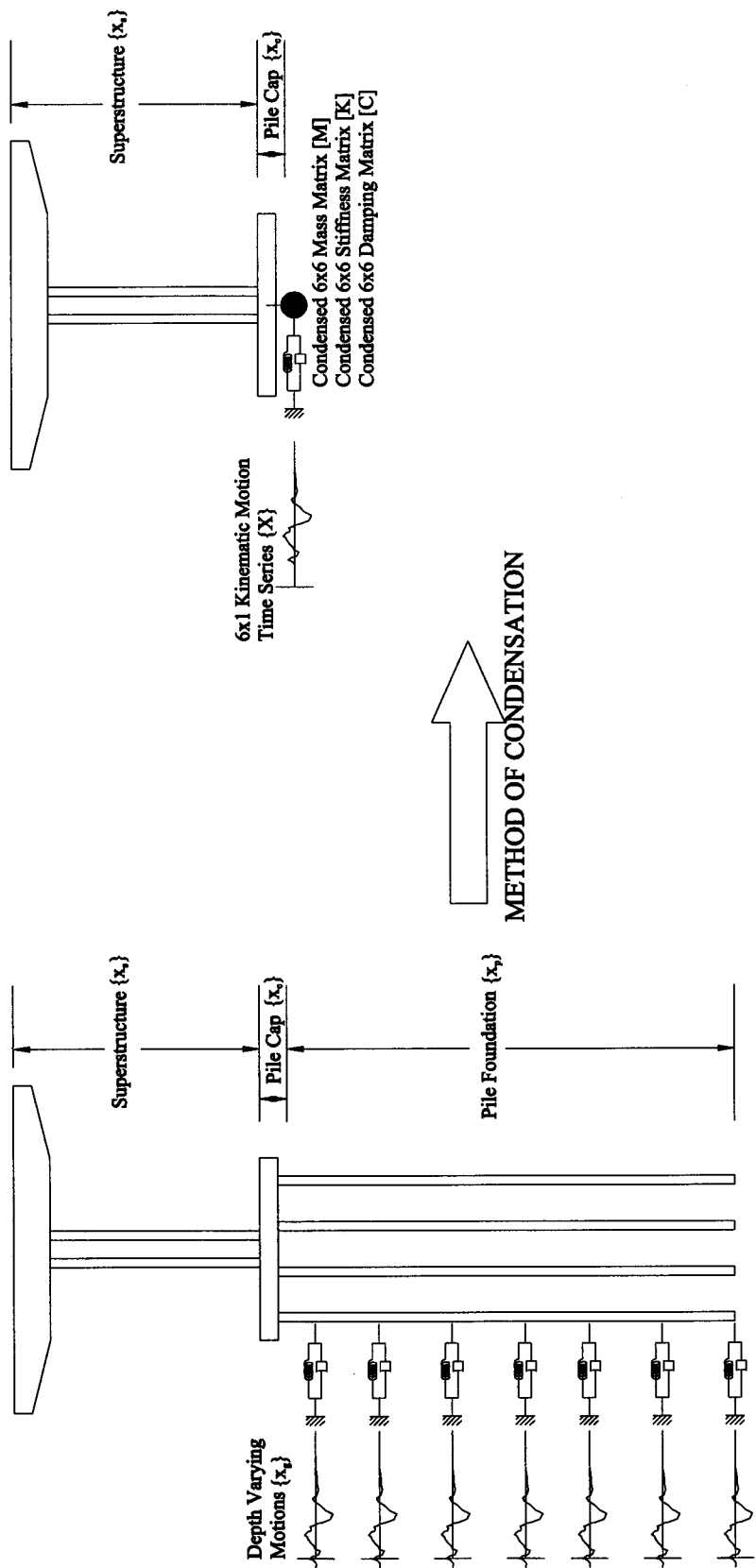$$[K] = [K_{cc}] - [K_{cp}][K_{pp}]^{-1}[K_{pc}] \tag{4.10}$$

Figure 4-2   Kinematic motion and condensed matrices.

71

$$\{f\} = -[K_{cp}][K_{pp}]^{-1}[K_g]\{x_g\} \tag{4.11}$$

It is noted that the remaining dynamic equations of motion contain only pile-cap and superstructure degrees of freedom, and in fact the solutions to these equations are what the structure engineers are seeking which represent demands for the superstructure and the pile-cap. This transformation of the original problem into a substructured system consisting only of superstructure and pile-cap is entirely based on classical static condensation (e.g., Cook, et al., 1989). The stiffness and loading of pile foundation appear in the form of 6x6 condensed stiffness matrix [K] and a 6x1 time-series forcing function {f} applied at the pile-cap. Both the stiffness matrix [K] (which is constant with time) and the forcing {f} (which is time dependent related to the time histories of the depth-varying free-field input ground motion) can be pre-calculated without knowledge of the response of the superstructure or the pile cap. Instead of using the forcing function {f} explicitly on the right hand side of the equations, we introduce a 6x1 vector {X}, such that

$$\{f\} = [K]\{X\} \tag{4.12}$$

From the above equation, it can be noted that loading from ground excitation is introduced into the overall structure as a right hand vector in a form of a displacement vector {X} times the foundation stiffness [K], and therefore {X} represent some form of rigid-base motion derived from the depth-varying freefield ground motion. This six-component motion {X} is termed "kinematic motion", and is a major element in defining ARS design criteria. This kinematic motion {X}, calculated at a single point on the pile cap implicitly contains the statically condensed forces transmitted from the ground to the superstructure along the entire embedded pile length due to both the depth-varying shaking intensity in soil motion as well as the depth-varying soil stiffnesses. The kinematic motion can been derived using a massless pile-group model, and therefore maintains the frequency contents of the original ground motion.

Theoretically, rigorous analysis of a pile foundation subjected to ground excitation would involve all six degrees of freedom kinematic motion in order to form the complete force vector {f}. In many cases, when the kinematic motion is derived at the pile-cap, the axial pile stiffness would imply a very large rotational stiffness of the pile cap leading to negligible pile-cap rotations, and therefore the rotational components can be neglected. By eliminating the rotational components, the kinematic motion represents pure translational rigid-base motion compatible with most earthquake engineering analyses involving firm ground input motions. Thus, Duhamel integral of the kinematic motion that has zero rotation (i.e., kinematic translations at pile-cap) would lead to the response spectra for the superstructure model. The three component response spectrum (involving the three translational component in ground motion) will then represents rigorously the equivalent ground shaking level felt by the superstructure. The steps involved in

developing the kinematic motion merely assumes zero pile masses and the solutions take into account all the detailed configuration of the pile group including variations with depth such as ground motion and soil and the pile properties. A zero mass assumption of the pile basically allows pre-calculation of the time dependent force vector {f} for the entire time history without the knowledge of the superstructure response. After completion of the dynamic response analyses for the second superstructure system involving both the pile cap and the superstructural nodes. The time history solution of the pile cap node can be back-substituted to the massless pile foundation to derive detailed member stresses along each of the pile.

The process of static condensation involves the property of the pile and the interaction of soil springs. The resultant kinematic motion or its response spectra from the described kinematic soil-structure interaction analysis would then become structure (foundation) specific and should only be used for the specific foundation that it is derived for. From the past experience it is observed that the resultant kinematic motion does retain the original characteristics of the free-field ground motion, but corresponds to a depth where the largest force level is transmitted from the ground to the pile affecting the response of the superstructure. Typically, for a uniform soft clay site, the freefield motion at about 3 pile diameters would be a better indicator of the effective motion felt by the superstructure than the freefield mudline motion. However, this rule of thumb can change, especially for soft soil sites which have stiffer surficial soil (e.g. sand) layers. Also, rigorously speaking the depth to effective input motion would be frequency dependent.

Figure 4.3 shows an example of development of kinematic motions for a battered pile group supporting the east pier for the main suspension structure of the New San Francisco – Oakland Bay Bridge (EMI, 2000). The piles are 2.5 meters diameter steel pipe piles and are about 70 meters long driven in young bay mud followed by old bay mud. Free-field site response analyses were first conducted at the site using the design rock motion consistent with a 1500 year event. The free-field motions computed along the pile length served as multiple-input ground motions, $\{x_g(t)\}$, as discussed previously. Following the above-mentioned mathematical formulation, a set of kinematic motion, {X}, was obtained using a dedicated computer code, KIPS (EMI, 1998). The resultant kinematic motion is compared with the freefield motions for the longitudinal direction (y-direction) in Figures 4.4 and 4.5. The comparison is given in both time history and response spectra. Similar comparison is presented in Figures 4.6 and 4.7 for the acceleration and displacement in the y-direction.

4.4 Treatment of Mass and Damping

The substructuring approach using static condensation, as mentioned above, provides rigorous solutions for massless piles. However for piles with some limited mass, the method is only approximate and the error depends on the relative magnitude of the pile mass to the superstructure mass. The solution can be greatly improved by implementing a condensed mass in the foundation substructure. This is to maintain the fundamental
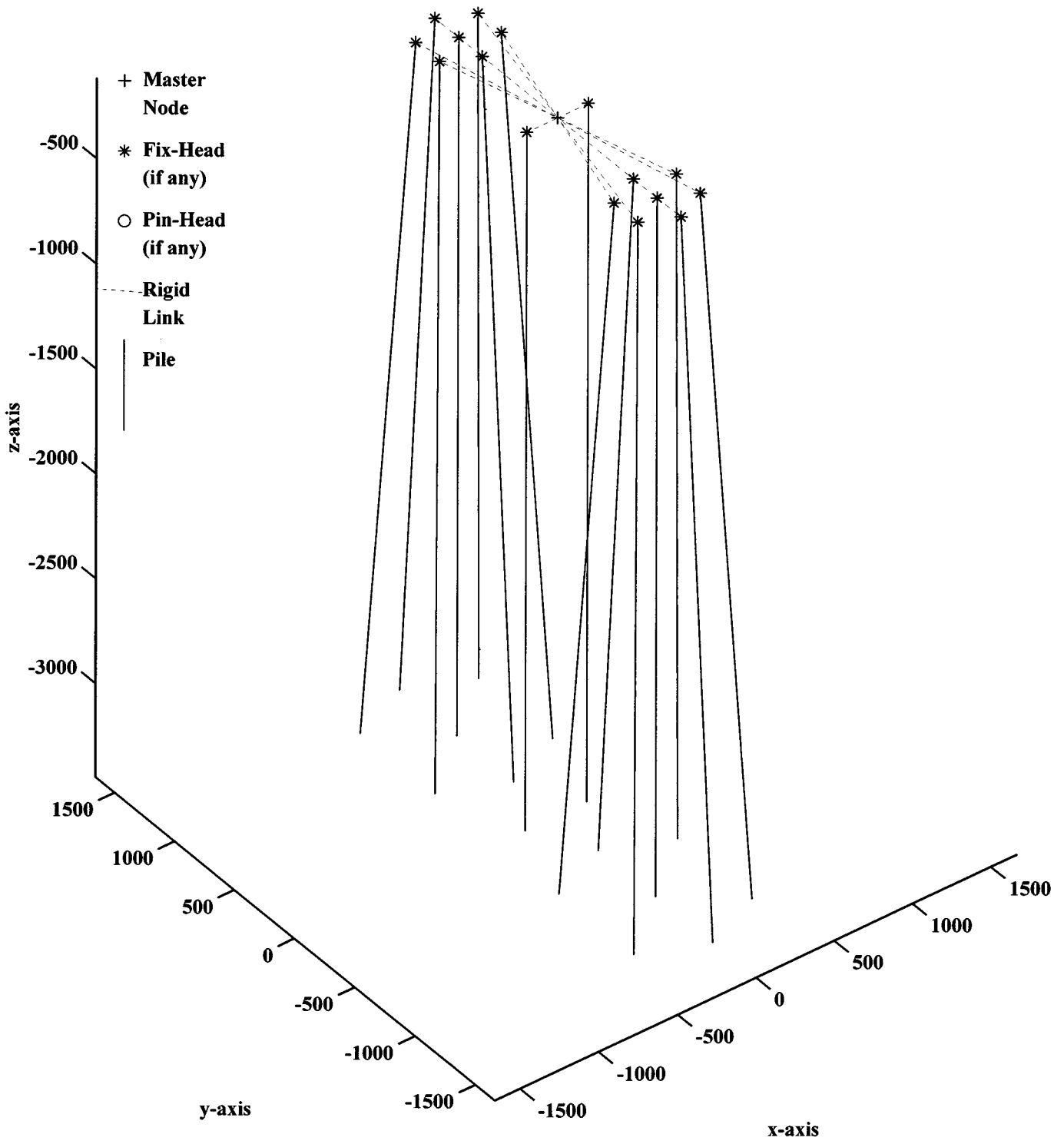
Figure 4-3   A battered pile group in Bay Mud.

Vert. Scale
┌─2 g
│
└─0 g

Hori. Scale
0 s   10 s

Kinematic
El. -3 m
El. -6 m
El. -9 m
El. -12.5 m
El. -16.2 m
El. -19.5 m
El. -23.2 m
El. -26.8 m
El. -30.2 m
El. -36.6 m
El. -42.1 m
El. -47.6 m
El. -53.1 m
El. -61.6 m

Vert. Scale
┌─20 in
│
└─0 in

Hori Scale
0 s   10 s

Kinematic
El. -3 m
El. -6 m
El. -9 m
El. -12.5 m
El. -16.2 m
El. -19.5 m
El. -23.2 m
El. -26.8 m
El. -30.2 m
El. -36.6 m
El. -42.1 m
El. -47.6 m
El. -53.1 m
El. -61.6 m

Figure 4-4   Comparison of kinematic motion and free-field motion time histories, in x- direction.

75

X-COMPONENT

Figure 4-5 Comparison of kinematic motion and free-field motion in response spectra, in x- direction.
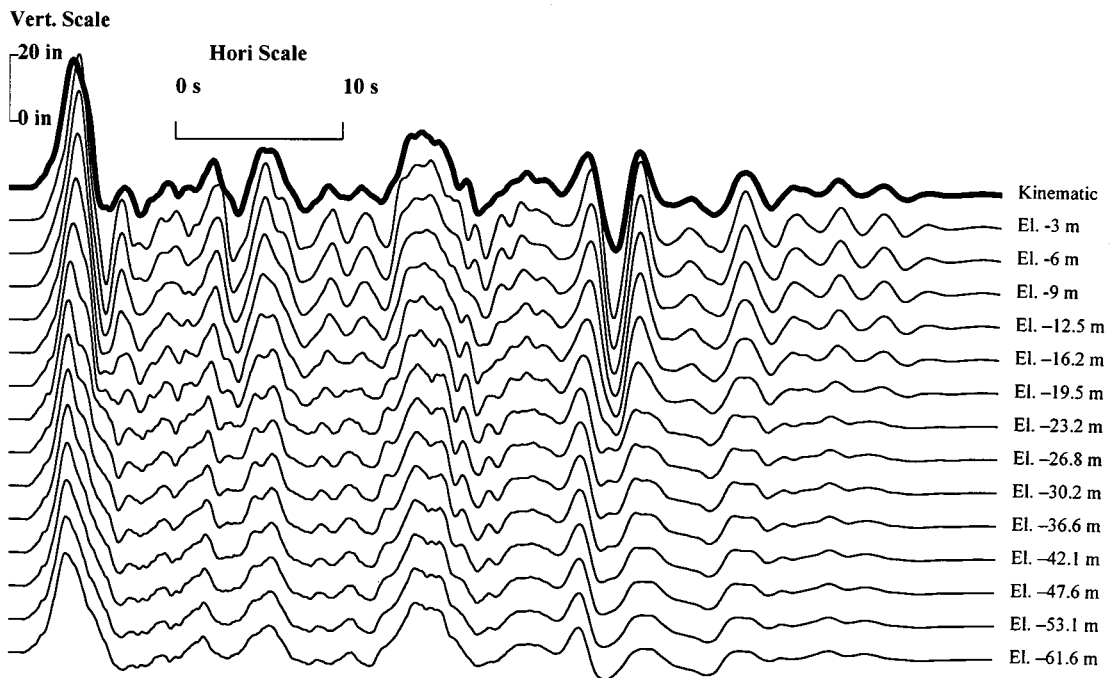
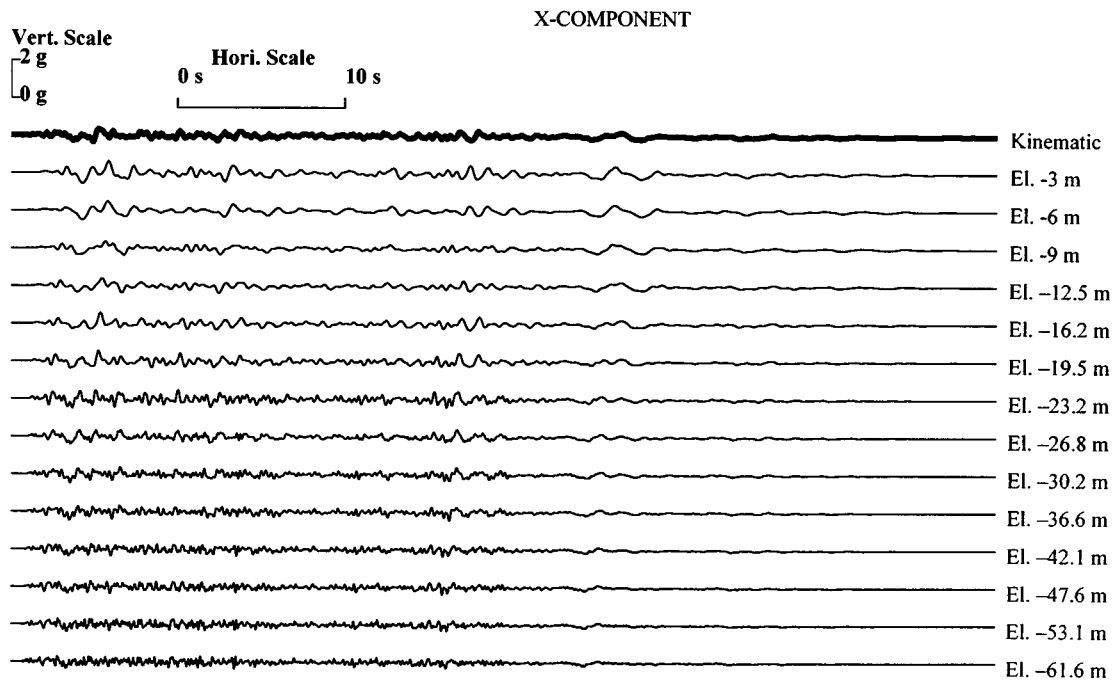Y-COMPONENT

Figure 4-6   Comparison of kinematic motion and free-field motion time histories, in y- direction.
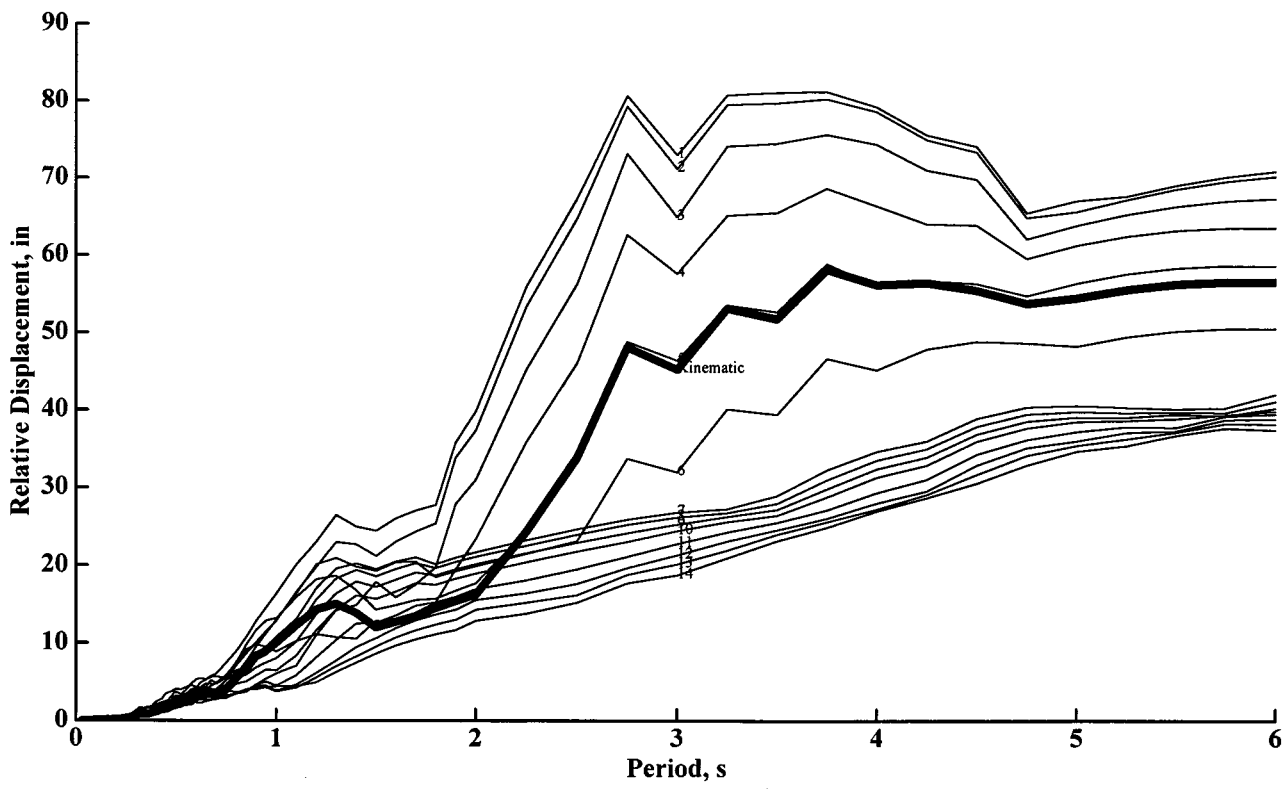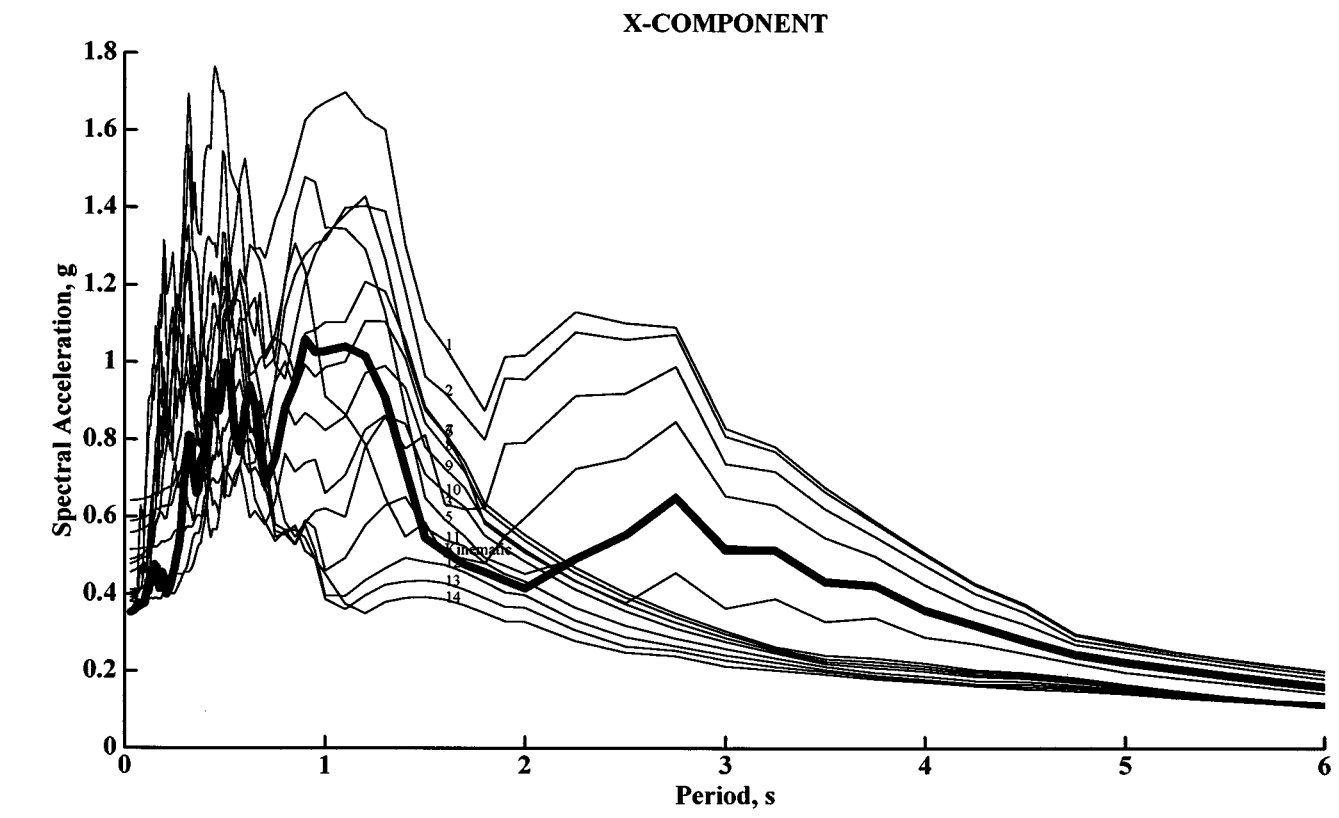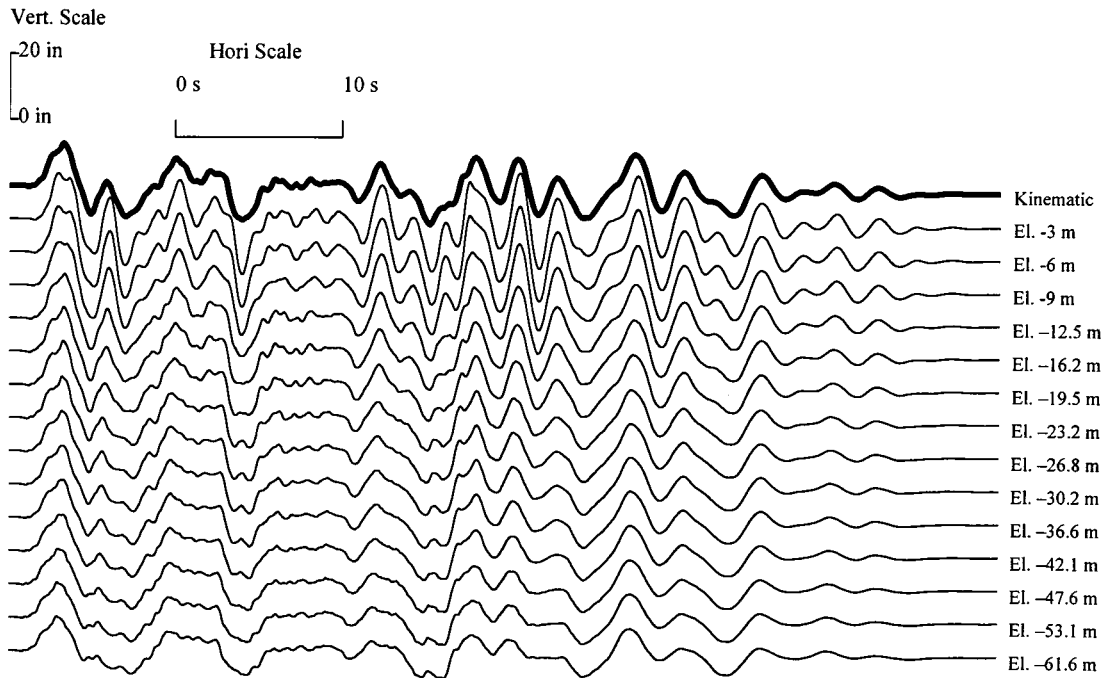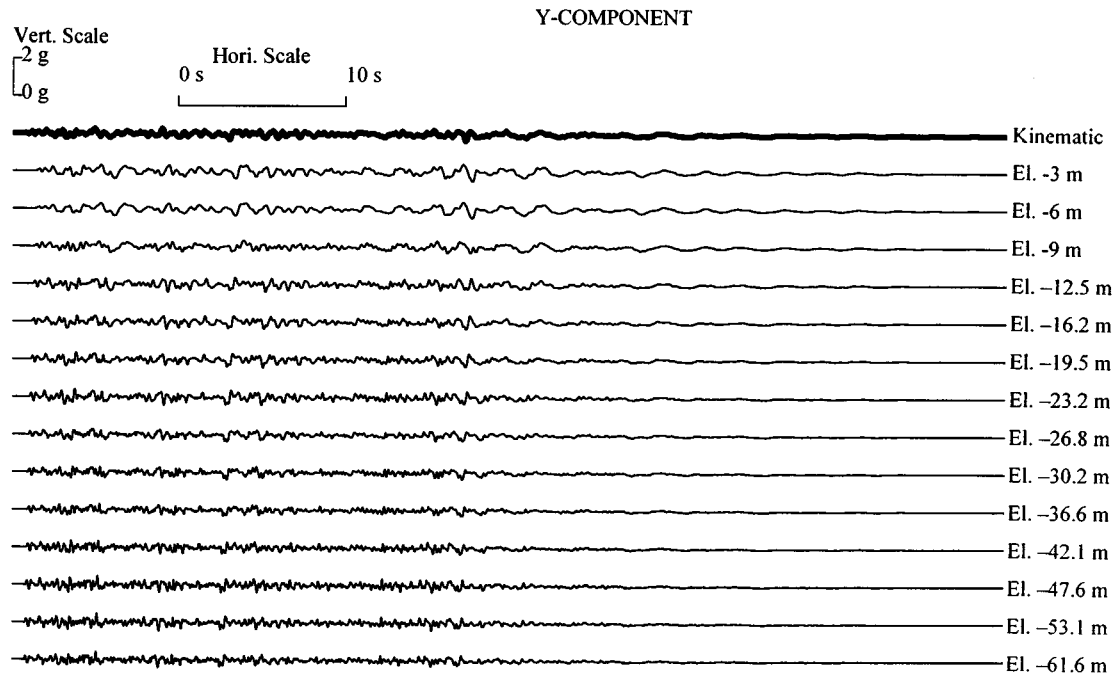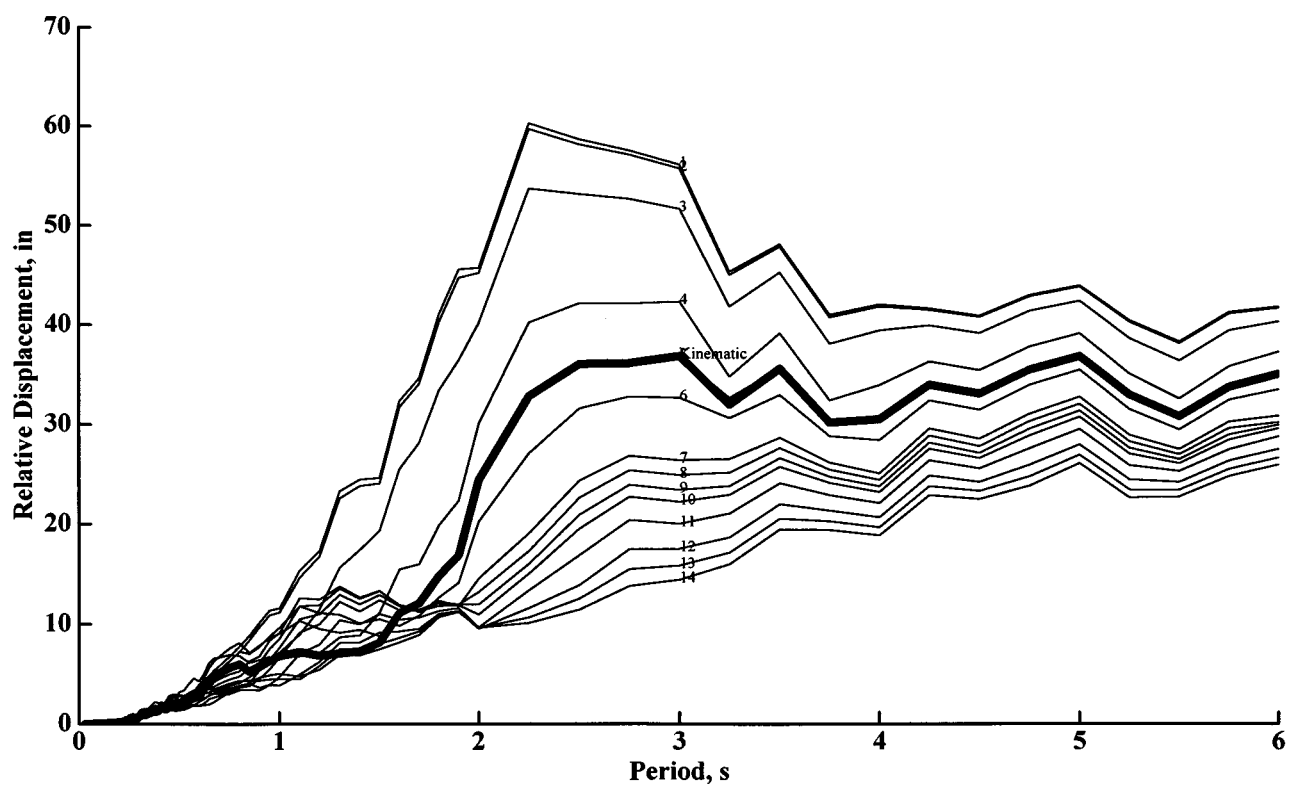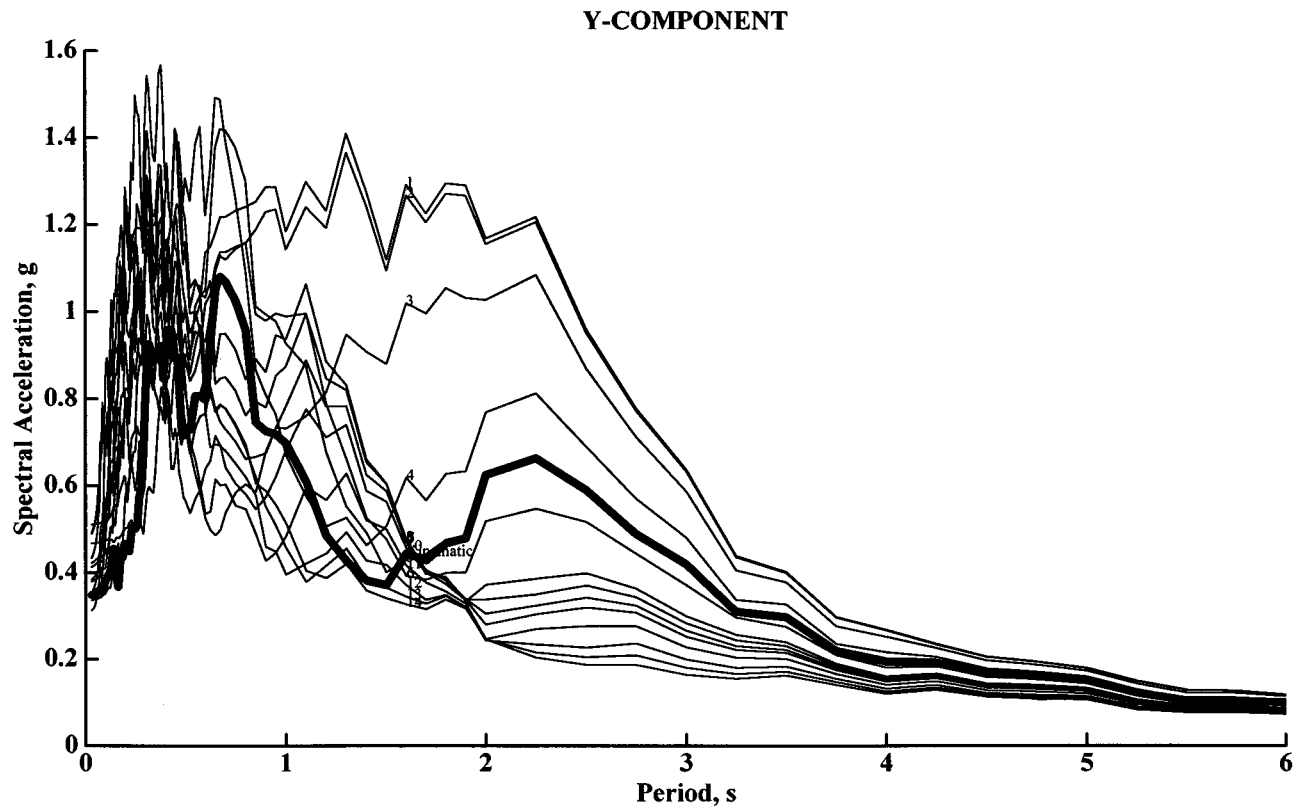
Y-COMPONENT

Figure 4-7   Comparison of kinematic motion and free-field motion in response spectra, in y- direction.

78

mode of vibration of the entire foundation system in the condensed substructure which consists of 6 degrees of freedom (3 translation and 3 rotational modes) at the pile cap. One approach would be based on computation of eigenvalues for the soil-pile system representing the entire foundation. The condensed mass, [M], can be approximated by

$$[M] = \frac{1}{\omega^2}[K] \tag{4.13}$$

where [K] is the condensed stiffness matrix (6x6) obtained from static condensation and ω is an angular frequency. The value for ω is often chosen as the fundamental frequency (1st mode) for each of the six axes (3 translation and 3 rotation) of the entire foundation. By doing so, the condensed model consisting of 6x6 mass matrix [M] and 6x6 stiffness matrix [K] would reproduce the same 6 fundamental modes of vibration as the original foundation prior to adding the superstructure.

In many cases, however, computation of natural frequencies and mode shapes for a large pile group can be difficult. A method similar to static condensation can be employed to reduce the number of degrees of freedom for a dynamic system which reduces the expense of computing eigenvalue and eigenvector. This condensation algorithm is known in the literature as Guyan reduction, mass condensation, dynamic condensation, or eigenvalue economization. In the context of pile foundation, free vibration characteristics of the pile-cap/pile system can be expressed as,

$$\left(\begin{bmatrix} [K_{cc}] & [K_{cp}] \\ [K_{pc}] & [K_{pp}] \end{bmatrix} - \omega^2 \begin{bmatrix} [m_c] & \\ & [m_p] \end{bmatrix} \right) \begin{Bmatrix} \{x_c\} \\ \{x_p\} \end{Bmatrix} = \begin{Bmatrix} 0 \\ 0 \end{Bmatrix} \tag{4.14}$$

where the subscript c denotes the pile-cap d.o.f and the subscript p denotes the pile d.o.f. In order to obtain a relation between x_c and x_p, we temporarily ignore all the mass and the above equation reduces to

$$\begin{Bmatrix} \{x_c\} \\ \{x_p\} \end{Bmatrix} = [T]\{x_c\} \tag{4.15}$$

where

$$[T] = \begin{bmatrix} I \\ -[K_{pp}]^{-1}[K_{pc}]^T \end{bmatrix} \tag{4.16}$$

Substituting the above equation into the free-vibration eigenvalue equation and pre-multiplying by $[T]^T$ yields the condensed eigenproblem as follows

$$([K] - \omega^2[M])\{x_c\} = \{0\} \tag{4.17}$$

where the reduced stiffness and mass matrices are symmetric and are given by

$$[K] = [T]^T \begin{bmatrix} [K_{cc}] & [K_{cp}] \\ [K_{pc}] & [K_{pp}] \end{bmatrix} [T] \tag{4.18}$$

and

$$[M] = [T]^T \begin{bmatrix} [m_c] & \\ & [m_p] \end{bmatrix} [T] \tag{4.19}$$

It can be seen that [T] plays a similar role as Ritz vectors in the Raleigh-Ritz method. Furthermore, it is noted the condensed mass [M] is banded and is a combination of both mass and stiffness coefficients. If the piles carry no mass, then [K] is the same matrix as produced by static condensation. If damping matrix appears in the equation of motion, the same principle can be employed to obtain a condensed damping matrix [C] as

$$[C] = [T]^T \begin{bmatrix} [C_{cc}] & [C_{cp}] \\ [C_{pc}] & [C_{pp}] \end{bmatrix} [T] \tag{4.20}$$

However, in typical seismic response analysis of global bridge foundation damping is not used explicitly. Global damping parameters such as those based on Raleigh damping coefficients are generally used.

SECTION 5
SUBSTRUCTURE METHOD USING INERTIA INTERACTION

5.1   Inertia Interaction

The substructure method that considers foundation mass during substructuring of the foundation is based on a procedure using inertia interaction. In this method, the forcing function derived for the bridge substructure as a right hand vector includes consideration of foundation mass. The most rigorous solution is obtained in frequency domain approach both in foundation substructure and bridge substructure. This poses as severe limitations for bridge response analyses because nonlinear behavior cannot be implemented. For example, plastic hinging and geometric nonlinearity at expansion joints cannot be accounted for in this type of analysis.

Some attempts have been made to overcome the limitations by developing a hybrid frequency-time domain approach (Tseng and Penzien, 1999). Because time domain analysis would be conducted for the bridge substructure to incorporate structural nonlinear behavior, frequency-independent mass, stiffness, and damping matrices are needed for foundation. In this approach, frequency domain procedure is used to develop frequency-dependent foundation impedance, which has two components; real part and imaginary part. The real part of foundation impedance is related for foundation stiffness and foundation mass while the imaginary part is related to foundation damping.

Approximation is carried out to estimate frequency-independent mass and stiffness matrices from the real component of the foundation impedance function. Frequency-independent damping matrix is obtained from the imaginary component of the foundation impedance. Furthermore, the forcing function on the right hand side of the equation for the bridge substructure is composed of three terms; inertia force, viscous force, and elastic restoring force from the foundation.

5.2   Frequency Domain Inertia Interaction

The substructure method using kinematic interaction offers reasonable solutions for most bridge problems. If foundation mass is to be accounted for rigorously in the superstructure and substructure, the solution process would be best conducted in frequency domain using inertia interaction. The equations of motion for a total bridge system consisting of depth varying input ground motion $\{x_g(t)\}$ are written as,

$$\begin{bmatrix} [m_s] & & \\ & [m_c] & \\ & & [m_p] \end{bmatrix} \begin{Bmatrix} \{\ddot{x}_s\} \\ \{\ddot{x}_c\} \\ \{\ddot{x}_p\} \end{Bmatrix} + \begin{bmatrix} [K_{ss}] & [K_{sc}] & \\ [K_{cs}] & [K_{cc}] & [K_{cp}] \\ & [K_{pc}] & [K_{pp}] \end{bmatrix} \begin{Bmatrix} \{x_s\} \\ \{x_c\} \\ \{x_p\} \end{Bmatrix} = \begin{Bmatrix} 0 \\ 0 \\ [K_g]\{x_g\} \end{Bmatrix} \qquad (5.1)$$

where $\{x_s\}$, $\{x_c\}$ and $\{x_p\}$ are total displacement of the superstructure, pile-cap, and pile/soil degrees of freedom, respectively relative to the fixed reference. The pile-cap

would have 6 degrees of freedom (three translation, and three rotation). The frequency response of the overall system can be obtained by considering the input ground motion $\{x_g(t)\}$ as linear superposition of harmonic motions $e^{i\omega t}$ at each angular frequency ω, such that

$$\{x_g(t)\} = \{X_g(\omega)\}e^{i\omega t} \tag{5.2}$$

where $\{X_g(\omega)\}$ is the amplitude of input ground motion vector at each frequency which can be obtained by performing Fourier Transform of the input depth-varying motions. The response of the degrees of freedom for superstructure, pile-cap, and pile/soil can be expressed in complex notations. To simplify the equations, the notation of (ω) is dropped as follows

$$
\begin{Bmatrix} \{x_s\} \\ \{x_c\} \\ \{x_p\} \end{Bmatrix} = \begin{Bmatrix} \{X_s\} \\ \{X_c\} \\ \{X_p\} \end{Bmatrix} e^{i\omega t} \tag{5.3}
$$

and

$$
\begin{Bmatrix} \{\ddot{x}_s\} \\ \{\ddot{x}_c\} \\ \{\ddot{x}_p\} \end{Bmatrix} = \begin{Bmatrix} \{\ddot{X}_s\} \\ \{\ddot{X}_c\} \\ \{\ddot{X}_p\} \end{Bmatrix} e^{i\omega t} = -\begin{Bmatrix} \{X_s\} \\ \{X_c\} \\ \{X_p\} \end{Bmatrix} \omega^2 e^{i\omega t} \tag{5.4}
$$

where $\{X_s\}$, $\{X_c\}$ and $\{X_p\}$ are amplitudes of the frequency response at each frequency. For each harmonic frequency, the equations of motion can be written in the following expression in frequency domain

$$
\begin{bmatrix} [D_{ss}(\omega)] & [D_{sc}(\omega)] & \\ [D_{cs}(\omega)] & [D_{cc}(\omega)] & [D_{cp}(\omega)] \\ & [D_{pc}(\omega)] & [D_{pp}(\omega)] \end{bmatrix} \begin{Bmatrix} \{X_s\} \\ \{X_c\} \\ \{X_p\} \end{Bmatrix} = \begin{Bmatrix} 0 \\ 0 \\ [K_g]\{X_g\} \end{Bmatrix} \tag{5.5}
$$

in which each impedance matrix $[D_{ij}(\omega)]$ is related to mass matrix and stiffness matrix as shown

$$[D_{ij}(\omega)] = [K_{ij}] - \omega^2[m_{ij}] \qquad i,j = s,c,p, \quad \text{where } m_{ij} = 0 \text{ for } i \neq j \tag{5.6}$$

Static condensation is performed to eliminate the degrees of freedom $\{X_p\}$ to reduce the system of equations. The reduced set of equations of motion consists only of the superstructure and pile-cap degrees of freedom. In the following, (ω) is dropped for clarity

$$\begin{bmatrix} [D_{ss}] & [D_{sc}] \\ [D_{cs}] & [D_{cc}]+[G_{cc}] \end{bmatrix} \begin{Bmatrix} \{X_s\} \\ \{X_c\} \end{Bmatrix} = \begin{Bmatrix} 0 \\ \{F_c\} \end{Bmatrix} \tag{5.7}$$

where $[G_{cc}]$ and $\{F\}$ are frequency dependent foundation impedance matrix and forcing function vector, respectively, and are defined as

$$[G_{cc}] = -[D_{cp}][D_{pp}]^{-1}[D_{pc}] \tag{5.8}$$

$$\{F_c\} = -[D_{cp}][D_{pp}]^{-1}[K_g]\{X_g\} \tag{5.9}$$

In the bridge substructure, the reduced equations of motion discussed above can be solved easily in frequency domain. It can be seen that the procedure would lead to rigorous solutions for the superstructure without needing to include the pile/soil degrees of freedom. However, one needs to pre-calculate the foundation impedance $[G_{cc}]$ and the forcing function vector $\{F_c\}$ accurately, which can be accomplished in the foundation substructure without knowledge of the superstructure. As evident in the equations for $[G_{cc}]$ and $\{F_c\}$, no prior knowledge of superstructure is needed in the foundation substructure.

5.3 Hybrid Frequency-Time Domain Inertia Interaction

Despite rigorousness of the substructuring technique entirely in frequency domain, it has limited application for bridge design due to requirement of linear behavior in all bridge and foundation components. Advances have been made to improve the technique so that the bridge substructure can be analyzed in time domain to implement nonlinearity of structural components. Because formulation of foundation impedance is achieved in the context of frequency domain in the foundation substructure, this substructuring technique can be regarded as a hybrid frequency-time domain approach.

As defined previously, the matrix $[G_{cc}]$ and vector $\{F_c\}$ are the foundation impedance matrix and its associated foundation driving force vector for each frequency, respectively. A foundation motion vector $\{\overline{X}_c\}$ is computed as

$$\{\overline{X}_c\} = [G_{cc}]^{-1}\{F_c\} \tag{5.10}$$

which is referred to as inertia interacted motion. When this inertia interacted motion is multiplied by the foundation impedance matrix $[G_{cc}]$, the result would yield foundation driving force vector $\{F_c\}$. The effects of depth-varying free-field motions are contained in $\{\overline{X}_c\}$.

Considering the bridge structure consisting only of superstructure and pile-cap degrees of freedom, the reduced matrix of equations of motion as derived previously from the frequency domain approach are rewritten as

$$\begin{bmatrix} [D_{ss}] & [D_{sc}] \\ [D_{cs}] & [D_{cc}]+[G_{cc}] \end{bmatrix} \begin{Bmatrix} \{X_s\} \\ \{X_c\} \end{Bmatrix} = \begin{Bmatrix} 0 \\ \{F_c\} \end{Bmatrix} \qquad (5.11)$$

Definition of the matrices $[D_{ss}]$, $[D_{sc}]$, $[D_{cs}]$, $[D_{cc}]$ and $[G_{cc}]$ have been given earlier. The vector $\{X_s\}$ and $\{X_c\}$ are the frequency dependent displacement amplitudes (total) of the superstructure and pile cap degrees of freedom. If the vector in the right hand side of the equation is replaced by $\{F_c\} = [G_{cc}]\{\overline{X}_c\}$, the equations of motion become

$$\begin{bmatrix} [D_{ss}] & [D_{sc}] \\ [D_{cs}] & [D_{cc}] \end{bmatrix} \begin{Bmatrix} \{X_s\} \\ \{X_c\} \end{Bmatrix} = \begin{Bmatrix} 0 \\ [G_{cc}](\{\overline{X}_c\}-\{X_c\}) \end{Bmatrix} \qquad (5.12)$$

In order to express this set of equations in time domain, frequency independent stiffness, mass, and damping matrices are needed. They are approximated from frequency dependent impedance matrix $[G_{cc}]$ such that

$$([\overline{K}_{cc}]-\omega^2[\overline{M}_{cc}]) \approx \mathrm{Real}([G_{cc}]) \qquad (5.13)$$

$$\omega[\overline{C}_{cc}] \approx \mathrm{Imaginary}([G_{cc}]) \qquad (5.14)$$

where the real constants in matrices $[K_{cc}]$, $[M_{cc}]$, and $[C_{cc}]$ are assigned numerical values to provide best fits to the individual frequency-dependent impedance matrix over the frequency range of interest. Then the equations of motion in frequency domain can be converted to time domain in the following format

$$\begin{bmatrix} [m_s] & \\ & [m_c]+[\overline{M}_{cc}] \end{bmatrix} \begin{Bmatrix} \{\ddot{x}_s\} \\ \{\ddot{x}_c\} \end{Bmatrix} + \begin{bmatrix} [K_{ss}] & [K_{sc}] \\ [K_{cs}] & [K_{cc}]+[\overline{K}_{cc}] \end{bmatrix} \begin{Bmatrix} \{x_s\} \\ \{x_c\} \end{Bmatrix} = \begin{Bmatrix} 0 \\ [\overline{M}_{cc}]\{\ddot{\overline{x}}_c\}+[\overline{C}_{cc}]\{\dot{\overline{x}}_c\}+[\overline{K}_{cc}]\{\overline{x}_c\} \end{Bmatrix}$$
$$(5.15)$$

Typical foundation consists of many piles representing multiple degrees of freedom, and the technique would indeed reduce the number of degrees of freedom in the global bridge substructure by not including the degrees of freedom below the interface. It can also be seen that there is a higher order term (e.g, inertia interacted acceleration) in the right hand vector in addition to the term related to the inertia interacted displacement. Clearly, the inertia interacted motion is not a form of ground motion and must be used to form the

force vector in the bridge substructure. Therefore, a response spectrum derived from the inertia interaction analysis is meaningless and misleading. On the basis of comparatively small pile mass in relationship to the superstructure, one might be inclined to neglect the acceleration term in the right hand vector to treat the inertia interacted motion as a ground motion in attempt to generate a response spectrum. Unfortunately, this can result in serious error as filtering action takes place during the inertia interaction analysis which could lead to unusually large pseudo acceleration in the response spectrum especially at the resonance frequency of the foundation substructure.

If the results from the inertia interaction analysis are properly implemented in the bridge substructure, i.e, forming a correct right hand vector by including all appropriate terms, the final solutions would be similar to the solutions based on kinematic substructuring method. In fact, the inertia interaction analysis is expected to be more accurate in the situation where the inertial effects of the foundation system dominate the overall bridge behavior. An any case, it is clear that the inertia interacted motion is not a typical ground motion, and must be implemented with caution.

A group of four piles, as shown in Figure 5.1 has been selected as an example of inertia interaction analysis. The piles are 0.61-m diameter concrete piles embedded in soil with a uniform subgrade reaction modulus of 8300 kN/m^2. Five percent damping was chosen to form a damping matrix using Raleigh relation. Free-field motions along the pile length were computed using 1-D site response analysis which were then implemented in the inertia interacted soil structure analysis. The purpose for this type of analysis is to produce frequency dependent impedance functions of the foundation substructure. These functions are then used in seismic response studies of the superstructure without having to model all the foundation elements, because the impedance functions effectively represent foundation behavior and thereby reduce the number of degrees of freedom in the global model. The impedance functions as computed from the inertia interaction analysis are shown in Figures 5.2 through 5.6. The foundation impedance functions consist of 6 components: 3 translation, 3 rotation, and the functions are shown in Figures 5.2 and 5.3. It can be noted that each function is frequency dependent and the impedance at zero frequency is directly related to the static compliance matrix (inverse of stiffness matrix). Figures 5.5 and 5.6 present impedance interacted motions for the two components, which can be used to form forcing functions in the right-hand side of the equation of motions for the global bridge model.
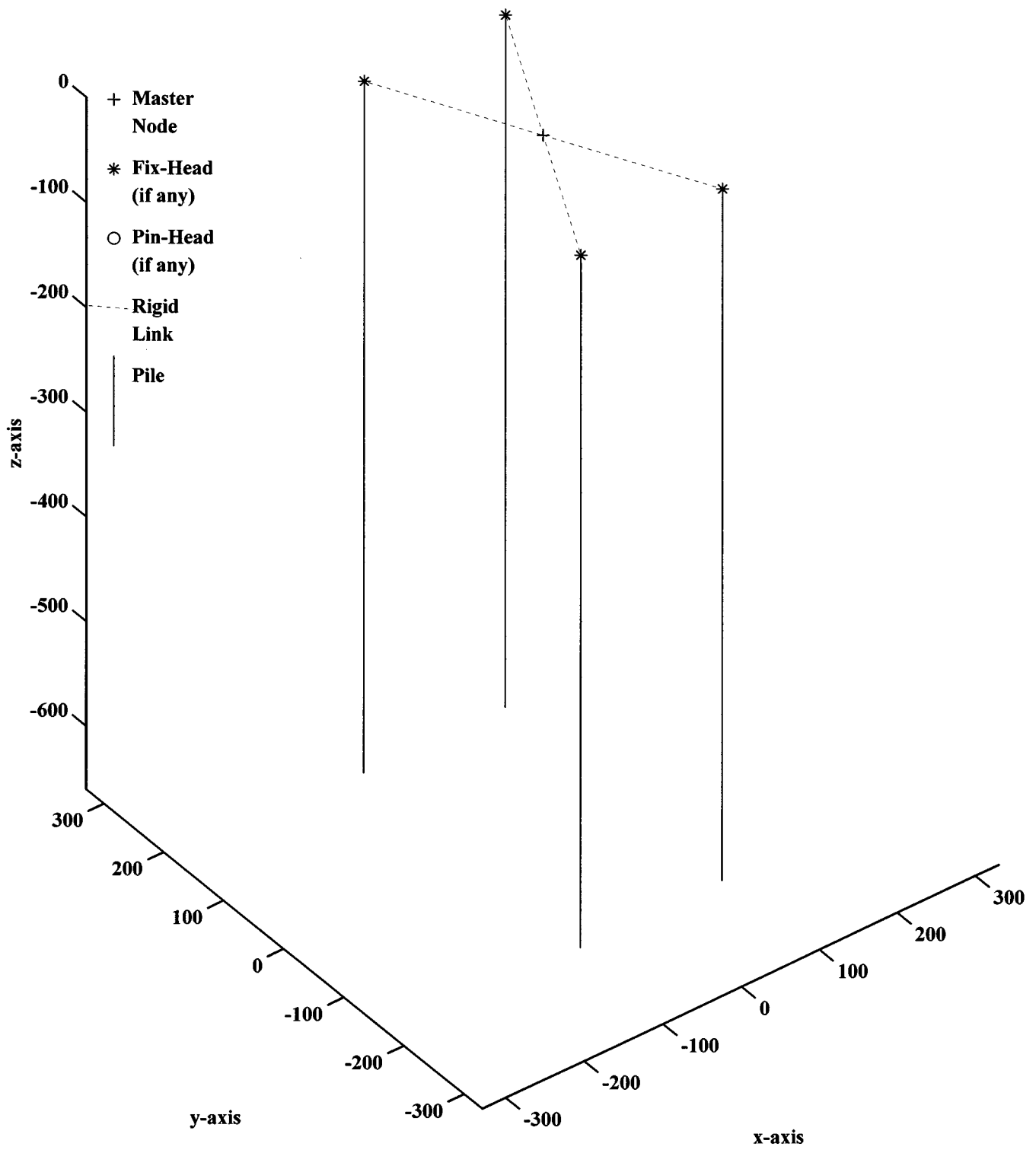
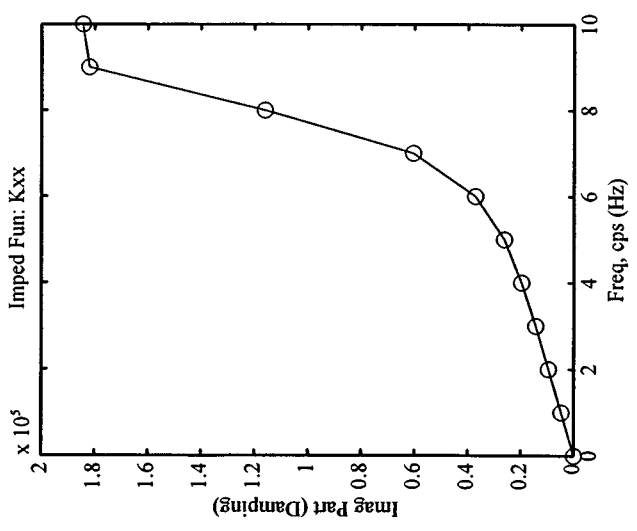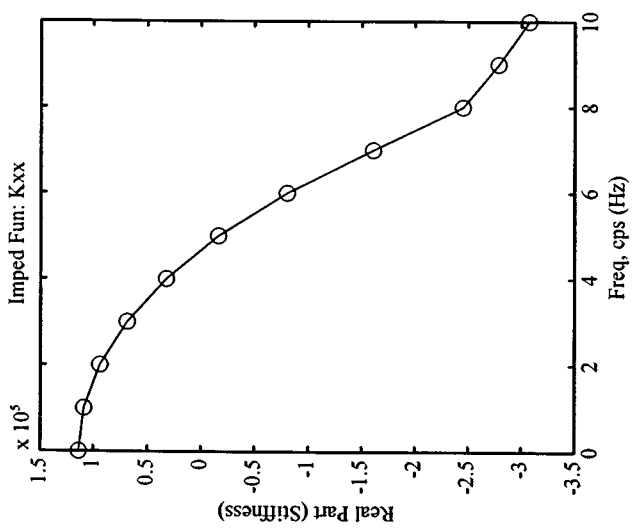**Figure 5-1**   Vertical pile group for inertial interaction analysis.

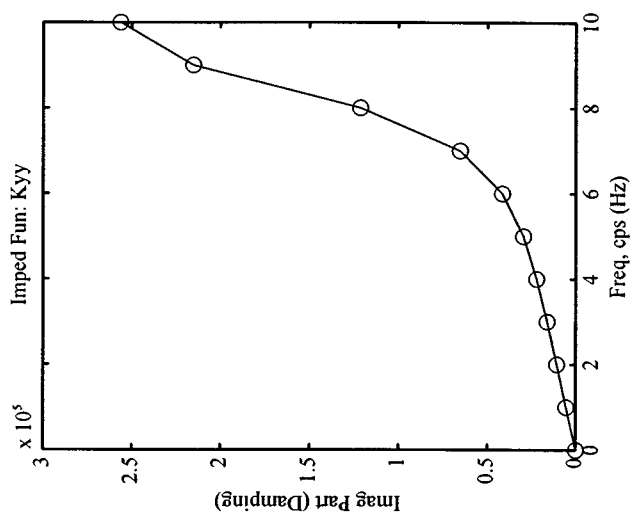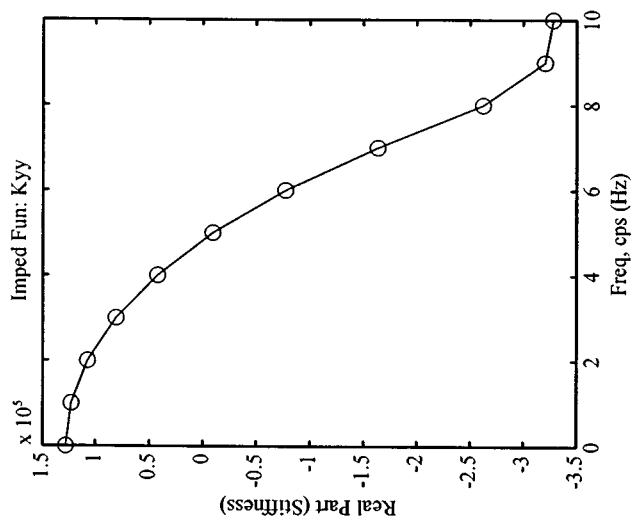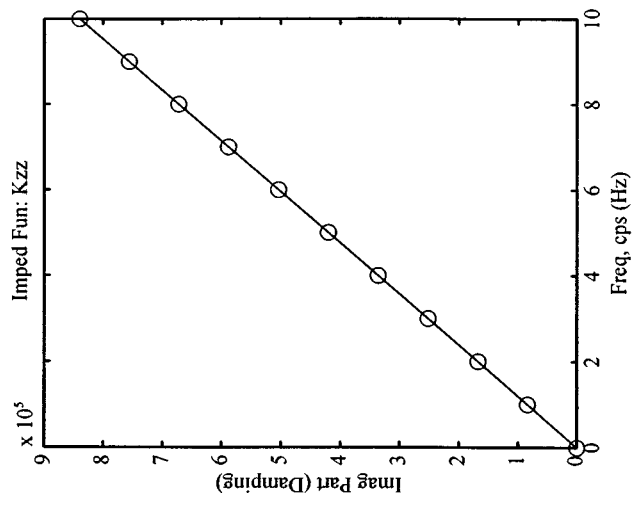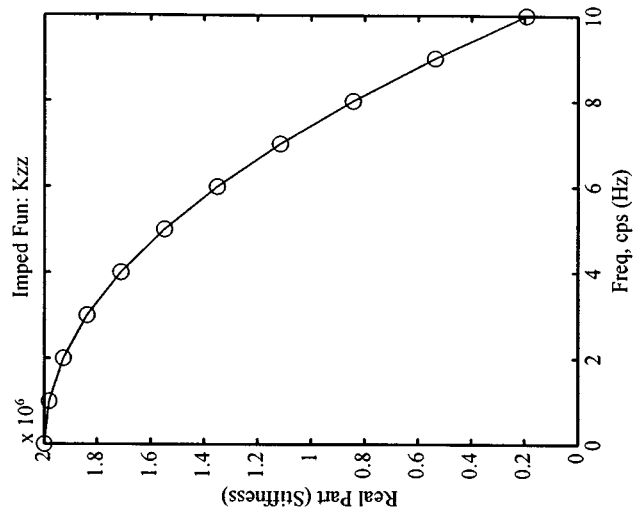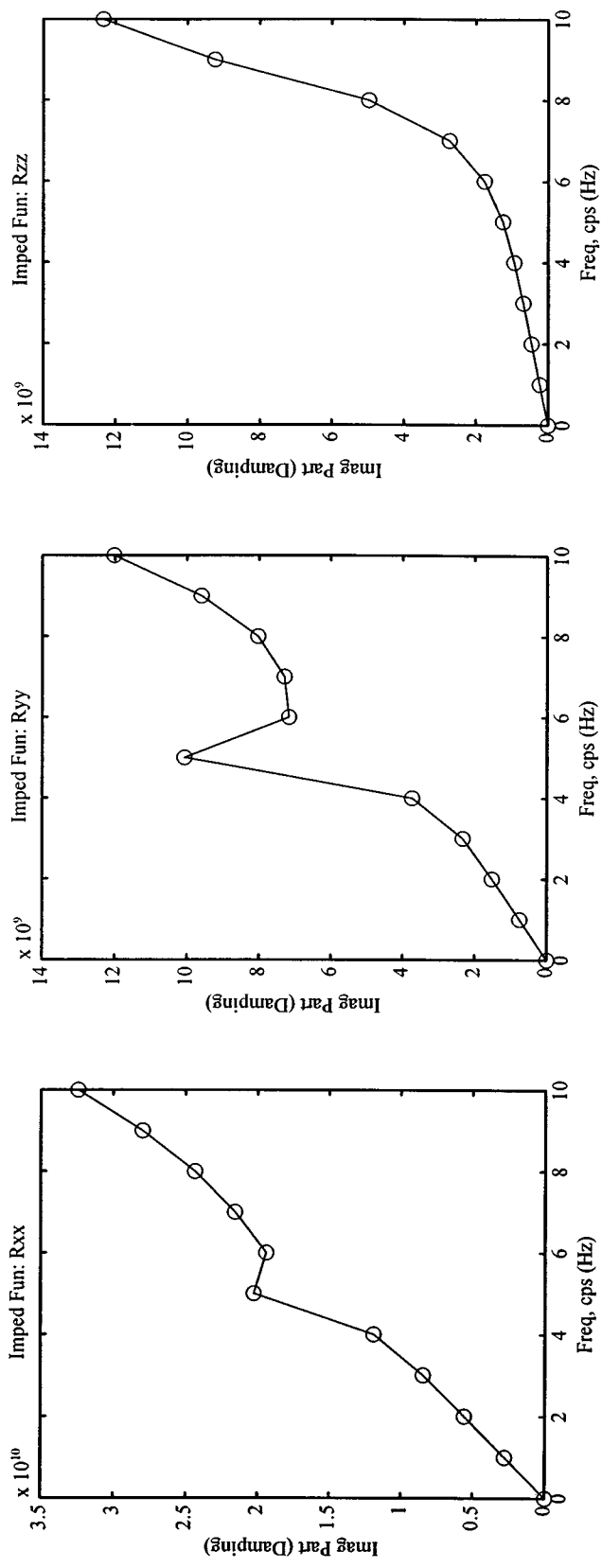Figure 5-2   Impedance functions for three translational components.
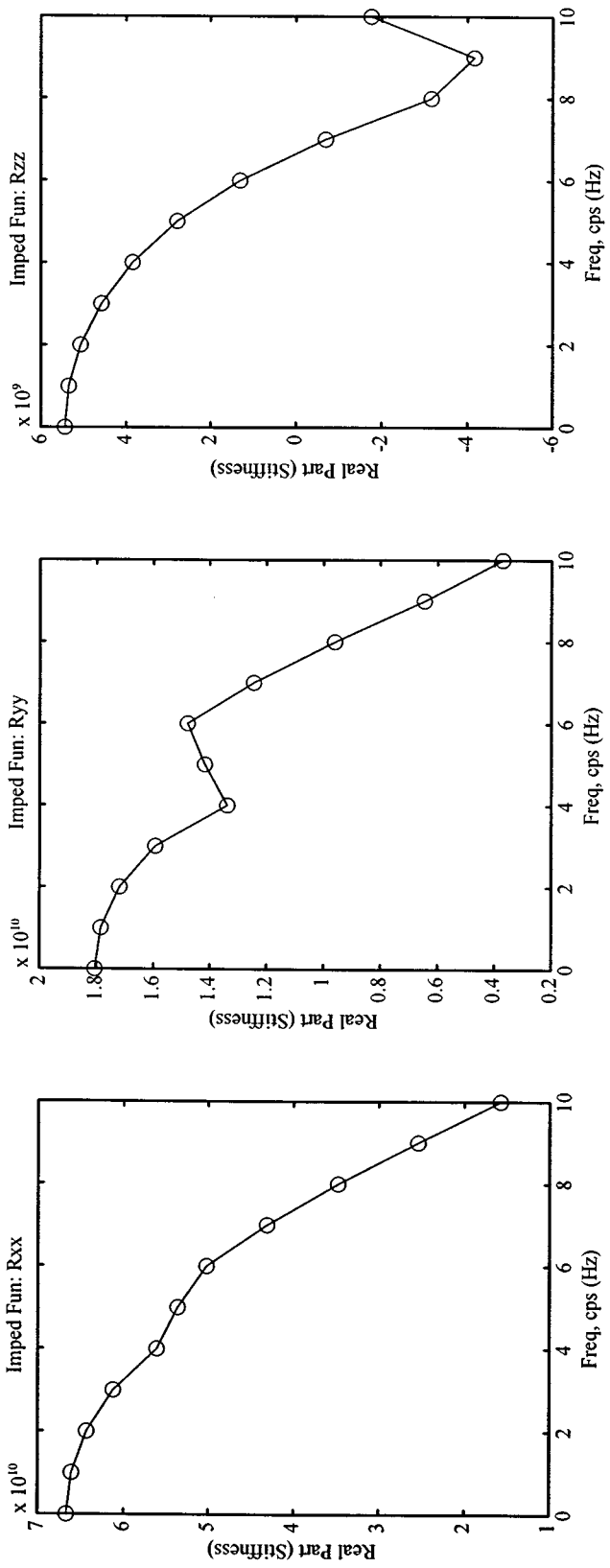
87

Figure 5-3   Impedance functions for three rotational components.

88

INERTIA INTERACTED MOTION: X-COMPONENT
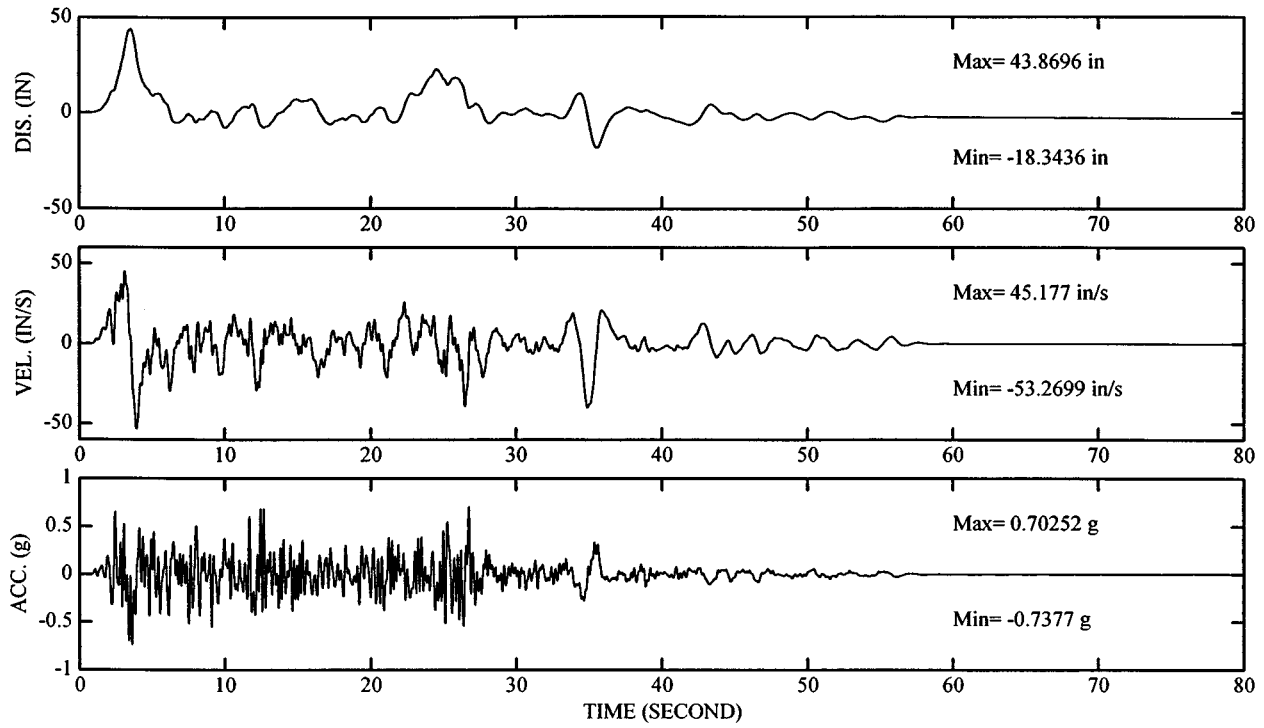

Figure 5-4   Inertia interacted motion in x- direction.
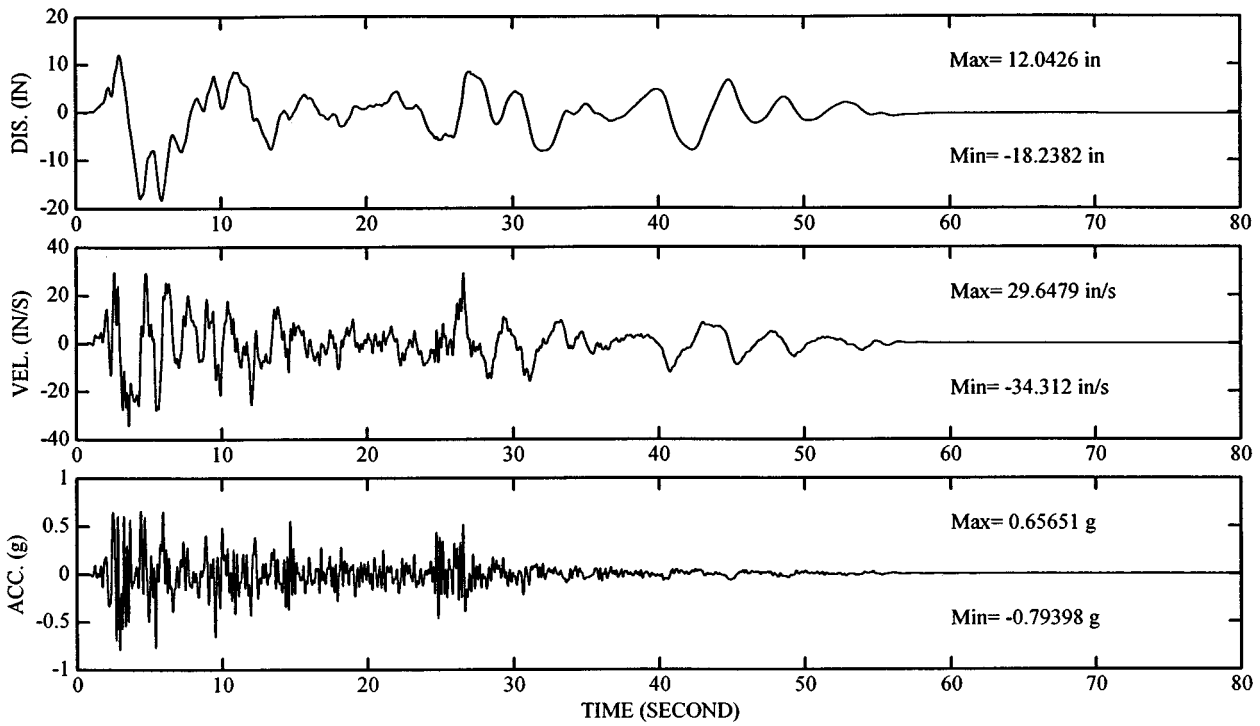
Figure 5-5   Inertia interacted motion in y- direction.

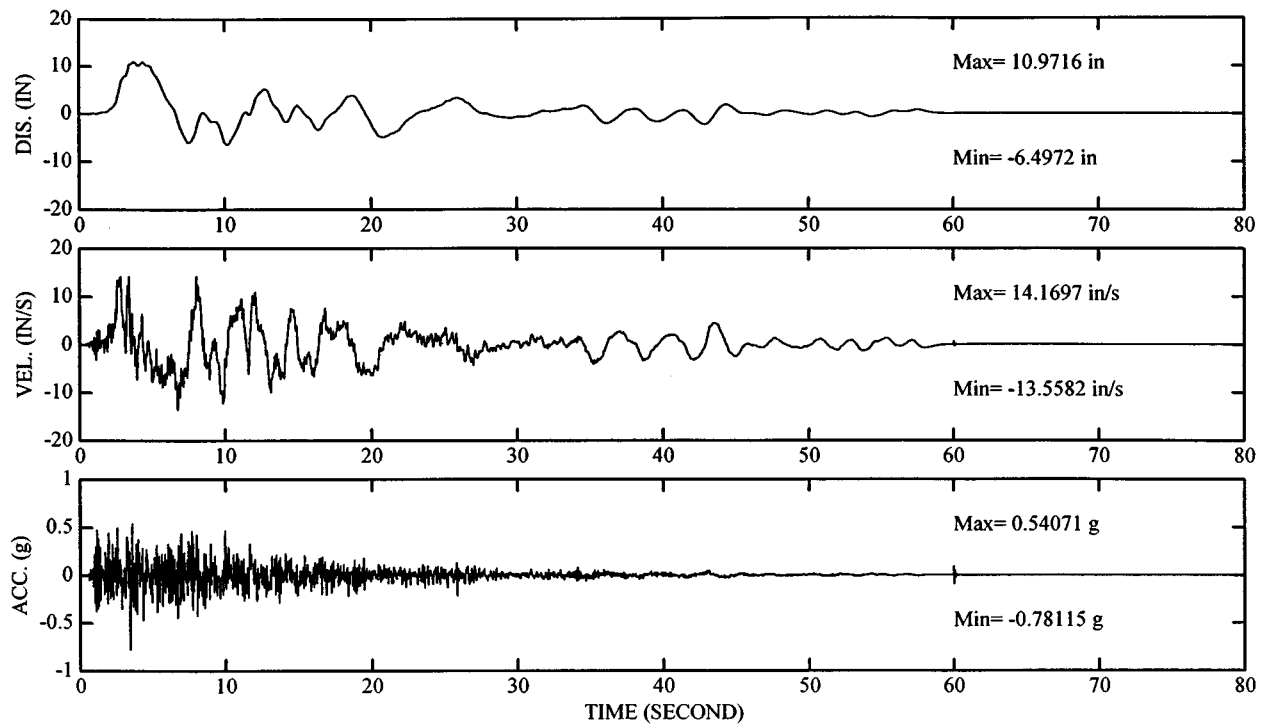INERTIA INTERACTED MOTION: Z-COMPONENT

Figure 5-6   Inertia interacted motion in z- direction.

SECTION 6
SUMMARY AND CONCLUSIONS

Seismic response analyses of bridges today consider the effects of soil-structure interaction because the fixed-base design approach used in the past has been found to be inadequate and can lead to erroneous results. While development of ground motion plays a major role in seismic response analyses, interaction between soil, foundation and superstructure requires careful examination of each component to determine how each one is affected by loading mechanisms and boundary conditions.

Various ground motion issues that are relevant to current design practice in bridge engineering are discussed in this report. Seismic hazard analyses and the development of design ground motion rely heavily on the characterization of strong motions that have been recorded from past earthquakes. The various ground motion parameters chosen for design are therefore empirical in nature with large bands of uncertainties. The goal of ground motion studies is to develop effective loading parameters or forcing functions at the foundation level of the bridge structure appropriate for design. The process involves prediction of rock motion for certain fault rupture scenarios including attenuation and spatial variation of seismic waves, conducting site response analyses to consider wave propagation through the soil deposit, performing soil-pile interaction analyses to arrive at effective loading mechanisms on foundations, and incorporating uncertainties into the entire process.

Soil-structure interaction is a broad topic. As the structural engineers are shifting to strength and ductility based design approaches from the conventional strength based design approach, accurate descriptions of foundation behavior is needed that include interaction of structure components of the foundation and the supporting soil. The core of soil-structure interaction problems is related to nonlinear soil behavior and gapping phenomenon. Both yielding of soil when it is severely loaded and separation between soil and structure would lead to gradual reduction in foundation stiffness, causing nonlinear foundation behavior.

Inelastic characteristics of soil, which can be described as a permanent set of deformation when load is removed, is a source of hysteretic dissipation of energy. The foundation damping is related to the hysteretic behavior and radiation of energy into semi infinite half space. It has been found from experience that the radiation damping parameters as derived from the elasto-dynamic theory overestimate the damping force because potential gapping behavior is not considered. Generally, the radiation damping is not very significant compared to the material damping associated with the hysteretic behavior of the soil. Nonetheless, it is possible to model the radiation dashpot in series with near-field soil spring to reduce large damping force. Depending on the type of foundation, other modeling techniques and soil-structure interaction aspects of typical foundations are thoroughly discussed in the context of seismic response analyses for the bridge structure.

Two types of substructuring approach are presented; kinematic interaction and inertia interaction. Both methods are aimed at reducing a total number of degrees of freedom in the modeling of a bridge structure by representing the foundation with a reduced number degree of freedom. Usually, the condensed number of degrees of freedom for a foundation is six; three for translation and another three for rotation.

The inertia interaction analysis considers pile mass, as opposed to the kinematic approach. Both the kinematic and hybrid frequency-time domain inertia interaction approaches involve approximations and there are relative merits in both approaches. In general, when the foundation mass becomes significant as in the case of large caissons, the inertia interacted substructuring approach would be more preferable to the kinematic approach. Of course, if feasible, a total system consisting of all foundation and superstructure components would be the best solutions in cases where geomatric nonlinearity can be properly accounted in the foundation.

It must be pointed out that the inertia interacted motion is not a form of base ground motion and should be used to form the force vector in the bridge substructure using three terms. Therefore, a response spectrum derived from the inertia interaction analysis is misleading. On the other hand, the kinematic motion can be used as a base ground motion because the right-hand side of the equation in the bridge substructure consists only of one term, kinematic displacement multiplied by foundation stiffness matrix. The kinematic based soil-structure interaction analyses would thus provide a rational means of developing a design spectrum incorporation depth-varying free-field motion, foundation type, and soil-pile interaction. In fact, response spectra of the kinematic motions have been used successfully to develop site specific design criteria in many toll bridge projects.

SECTION 7
REFERENCES

Abrahamson, N.A. (1992), "Generation of Spatially Incoherent Strong Motion Time Histories", Proc. Tenth World Conf. Earthquake Engineering, Madrid, Spain, 845-850.

Abrahamson, N.A. and Silva, W.J. (1997), "Empirical Response Spectra Attenuation Relations for Shallow Crustal Earthquakes", Seismological Research Letters, Volume 68, No. 1, January/February.

API Recommended Practice and Planning (1993), Designing, and Constructing Fixed Offshore Platforms, American Petroleum Institute, Washington, D.C.

Applied Technology Council, ATC-32 (1996), Improved Seismic Design Criteria for California Bridges, Provisional Recommendations

Ashford, S., and Rollins, K. (1999), "Full-Scale Behavior of Laterally Loaded Deep Foundations in Liquefied Sand," Preliminary Test Results, Department of Structural Engineering, University of California, San Diego

Bogard, D. and Matlock, M. (1983), "Procedure for the Analysis of Laterally Loaded Pile Groups in Soft Clay," Proceeding of Specialty Conference on Geotechnical Engineering in Offshore Practice, ASCE, April, pp 499-535

Boulanger, R. W., Curras, C. J., Kutter, B. L., Wilson, D. W., and Abghari, A. (1999), "Seismic Soil- Pile-Structure Interaction Experiments and Analyses", Journal of Geotechnical and Geoenvironmental Engineering, Vol. 125, No. 9, pp. 750-759.

Brown, D., Morrison, C., and Reese, L. (1988), "Lateral Load Behavior of Pile Group in Sand," Journal of Geotechnical Engineering, Vol. 114, No. 11, November.

Brown, D., Reese, L., and O'Niell, M. (1987), "Cyclic Lateral Loading of A Large-Scale Pile," Journal of Geotechnical Engineering, Vol. 113, No. 11, November.

Clough, R. W. and Penzien, J (1975), Dynamics of Structures, McGraw-Hill

Cook, R. D, Malkus, D.S., and Plesha, M.E. (1989), Concepts and Application of Finite Element Analysis, John Wiley & Sons

Cornell, C.A. (1968), "Engineering Seismic Risk Analysis," Bulletin of the Seismological Society of America, 58, 1583-1606

EMI, Earth Mechanics, Inc. (1997a), Geotechnical Report on Seismic Retrofit of San Diego-Coronado Bridge, Submitted to Caltrans, Contract 59X478

EMI, Earth Mechanics, Inc. (1997b), Soil-Structure Interaction, Carquinez Strait Bridge Seismic Retrofit Program, Submitted to Caltrans, Contract 59X476

EMI, Earth Mechanics, Inc. (1998), KIPS – Kinematic Interaction for Pile and Soil: In house computer program for seismic design

EMI, Earth Mechanics, Inc. (1999), Multiple Input Ground Motion; Richmond-San Rafael Bridge Seismic Retrofit Project, Submitted to Caltrans, Contract 59X475

EMI, Earth Mechanics, Inc. (2000), Seismic Ground Motion Report for East Span Replacement Project of San Francisco- Oakland Bay Bridge, Submitted to Caltrans, Contract 59-A0053

Gazetas, G; Fan, K; Tazoh, T., Shimizu, K.; Kavvadas, M.; and Makris, N. (1992), "Seismic Pile- Group-Structure Interaction", ASCE Geotechnical Special Publication No. 34, Piles Under Dynamic Loads, Edited by Shamsher Prakash.

Kaul, M. K. (1978), "Spectrum-Consistent Time-History Generation," ASCE Journal of Engineering Mechanics, EM4, 781-788

Kramer, S. L. (1996), Geotechnical Earthquake Engineering, Prentice Hall

Lam, I. P. and Law, H (1996), "Soil-Foundation-Structure Interaction-Analytical Considerations by Empirical p-y Method", Proc. 4th Caltrans Seismic Research Workshop, Sacramento, July 9-11

Lam, I. P, and Martin, G. R. (1986), "Seismic Design of Highway Bridge Foundation", Vol 2, Report No. FHWA/RD-86/102, FHWA, McLean, Virginia

Lam, I. P, Martin, G. R. and Imbsen, R (1991), "Modeling Bridge Foundations for Seismic Design and Retrofitting", Transportation Research Record 1290

Lam, I. P., Kapuskar, M. and Chaudhuri, D (1998), "Modeling of Pile Footings and Drilled Shafts for Seismic Design", Report MCEER-98-0018, Multidisciplinary Center for Earthquake Engineering Research

Lilhanand, K. and Tseng, W.S. (1987), "Generation of Synthetic Time Histories Compatible with Multiple-Damping Response Spectra", SMIRT-9, Lausanne, K2/10

Lilhanand, K. and Tseng, W.S. (1988), "Development and Application of Realistic Earthquake Time Histories Compatible with Multiple-Damping Response Spectra", Ninth World Conference on Earthquake Engineering, Tokyo, Japan, Vol II, 819-824

Matlock, H. (1970), "Correlation for Design of Laterally Loaded Piles in Soft Clay," 2nd Annual Offshore Technology Conference, Paper No 1204, May.

McVay, M., Casper, R., and Shang, T. (1995), "Lateral Response of Three-Row Groups in Loose to Dense Sands at 3D and 5D Spacing," Journal of Geotechnical Engineering, Vol. 121, No. 5, May.

Mylonakis, G., Nikolaou, A., and Gazetas, G. (1997), "Soil-Pile-Bridge Seismic Interaction: Kinematic and Inertial Effects. Part I: Soft Soil," Earthquake Engineering and Structural Dynamics, Vol. 26, pp. 337-359.

Newmark, N. M and Hall, W.J. (1973), "Procedure and Criteria for Earthquake-Resistant Design," Report NUREG/CR-0098, Nuclear Regulatory Commission, Washington, DC

Pender, M. J. (1993), "Aseismic Pile Foundation Design and Analysis", Bulletin of the New Zealand National Society for Earthquake Engineering, Vol 26, No. 1, 49-160

Reese, L., Cox, W., and Koop, R. (1974), "Analysis of Laterally Load Piles in Sand," 6th Annual Offshore Technology Conference, Paper No. 2080, May.

Reiter, L (1990), Earthquake Hazard Analysis; Issues and Insights, Columbia University Press, NY

Seed, H. B. and Idriss, I. M. (1976), Ground Motions and Soil Liquefaction During Earthquakes, EERI Monograph

Seed, R. B.Dickenson, S. E., Reimer, M. F., Bray, J. D., Sitar, N., Mitchell, J. K., Idriss, I.M., Kayen, R.E., Kropp, A., Harder, L. F. and Power, M. S (1990), "Preliminary Report on the Principal Geotechnical Aspects of the October 17, 1989 Loma Prieta Earthquake," Report UCB/EERC 90/05, University of California, Berkeley

Stevens J. B. and Audibert, J. M. E., "Re-Examination of P-y Curve Formulations", 11th Annual Offshore Technology Conference, Houston

Tseng, W.S and Penzien, J (1999), "Soil-Foundation-Structure Interaction", Bridge Engineering Handbook, Edited by Chen and Duan

Terzaghi, K. (1955), "Evaluation of Coefficients of Subgrade Reaction", Geotechnique, Vol 5, No 4, 297-326

Wang, S., Kutter, B.L., Chacko, J.M., Wilson, D.W., Boulanger, R.W. and Abghari, A. (1998), "Nonlinear Seismic Soil-Pile-Interaction", Earthquake Spectra, EERI, Oakland, CA, 14(2).